DOCTORAL THESIS

Mass spectrometry-based metabolomics study on KRAS-mutant colorectal cancer and rheumatoid arthritis

Li, Xiaona

Date of Award:
2018

HONG KONG BAPTIST UNIVERSITY

Doctor of Philosophy

THESIS ACCEPTANCE

DATE: July 17, 2018
STUDENT'S NAME: LI Xiaona

THESIS TITLE: Mass Spectrometry-based Metabolomics Study on KRAS-mutant Colorectal Cancer and Rheumatoid Arthritis

This is to certify that the above student's thesis has been examined by the following panel members and has received full approval for acceptance in partial fulfillment of the requirements for the
degree of Doctor of Philosophy.

Chairman:	Prof Mak Nai Ki Professor, Department of Biology, HKBU (Designated by Dean of Faculty of Science)
Internal Members:	Dr Cheng Yuen Kit Associate Professor, Department of Chemistry, HKBU (Designated by Head of Department of Chemistry) Dr Ren Kangning Assistant Professor, Department of Chemistry, HKBU
External Members:	Prof Li Liang Professor Department of Chemistry University of Alberta Canada Dr Yao Zhongping Associate Professor Department of Applied Biology & Chemical Technology The Hong Kong Polytechnic University HONG KONG
Proxy:	Dr Leung Ken C F Associate Professor, Department of Chemistry, HKBU
In-attendance:	Prof Cai Zongwei Chair Professor, Department of Chemistry, HKBU

Issued by Graduate School, HKBU

Mass Spectrometry-based Metabolomics Study on KRAS-mutant Colorectal Cancer and Rheumatoid Arthritis

LI Xiaona

A thesis submitted in partial fulfillment of the requirements

for the degree of

Doctor of Philosophy

Principal Supervisor:

Prof. CAI Zongwei (Hong Kong Baptist University)

Dr. LI Hungwing (Hong Kong Baptist University)

July 2018

Declaration

I hereby declare that this thesis represents my own work which has been done after registration for the degree of PhD at Hong Kong Baptist University, and has not been previously included in a thesis or dissertation submitted to this or any other institution for a degree, diploma or other qualifications.

I have read the University's current research ethics guidelines, and accept responsibility for the conduct of the procedures in accordance with the University's Committee on the Use of Human & Animal Subjects in Teaching and Research (HASC). I have attempted to identify all the risks related to this research that may arise in conducting this research, obtained the relevant ethical and/or safety approval (where applicable), and acknowledged my obligations and the rights of the participants.

Signature: Li Xiaona

Date: July 2018

Abstract

Ample studies have shown that perturbation of metabolic phenotype is correlated with gene mutation and pathogenesis of colorectal cancer (CRC) and rheumatoid arthritis (RA). Mass spectrometry (MS)-based metabolomics as a powerful and stable approach is widely applied to bridge the gap from genotype/metabolites to phenotype.

In CRC suffers, *KRAS* mutation accounts for 35%-45%. In previous study, SLC25A22 that encodes the mitochondrial glutamate transporter was found to be overexpressed in CRC tumor and thus to be essential for the proliferation of CRC cells harboring *KRAS* mutations. However, the role of SLC25A22 on metabolic regulation in *KRAS*-mutant CRC cells has not been comprehensively characterized. We performed non-targeted metabolomics, targeted metabolomics and isotope kinetic analysis of *KRAS*-mutant DLD1 cells with or without SLC25A22 knockdown using ultra-high performance liquid chromatography (UHPLC) coupled to Orbitrap MS and tandem MS (MS/MS). In global metabolomics analysis, 35 differentially regulated metabolites were identified, which were primarily involved in alanine, aspartate and glutamate metabolism, urea cycle and polyamine metabolism. Then targeted metabolomics analysis on intracellular metabolites, including tricarboxylic acid (TCA) cycle intermediates, amino acids and polyamines, was established by using LC-MS/MS coupled with an Amide BEH column. Targeted metabolomics analysis revealed that most TCA cycle intermediates, aspartate (Asp)-derived asparagine, alanine and ornithine (Orn)-derived polyamines were strongly down-regulated in

SLC25A22 knockdown cells. Moreover, the targeted kinetic isotope analysis using [U-$^{13}C_5$]-glutamine as isotope tracer showed that most of the ^{13}C-labeled TCA cycle intermediates were down-regulated in SLC25A22-silencing cells. Orn-derived polyamines were significantly decreased in SLC25A22 knockdown cells and culture medium. Meanwhile, accumulation of Asp in knockdown of GOT1 cells indicated that oxaloacetate (OAA) was majorly converted from Asp through GOT1. Exogenous addition of polyamines could significantly promote cell proliferation in DLD1 cells, highlighting their potential role as oncogenic metabolites that function downstream of SLC25A22-mediated glutamine metabolism. SLC25A22 acts as an essential metabolic regulator during CRC progression as promotes the synthesis of TCA cycle intermediates, Asp-derived amino acids and polyamines in *KRAS*-mutant CRC cells. Moreover, OAA and polyamine could promote KRAS-mutant CRC cell growth and survival.

Rheumatoid arthritis (RA) is a chronic, inflammatory and symmetric autoimmune disease and a major cause of disability. However, there is insufficient pathological evidence in term of metabolic signatures of rheumatoid arthritis, especially the metabolic perturbation associated with gut microbiota (GM). Based on consistent criteria without special diet and therapeutic intervention to GM, we enrolled 50 RA patients and 50 healthy controls. On basis of the platform of UHPLC-MS and GC-MS, were performed for the non-targeted metabolomics to investigate alterations of endogenous metabolites in response to RA inflammation and

interaction with GM. 32 and 34 significantly changed metabolites were identified in urine and serum of patients with RA, respectively. The altered metabolites were identified by HMDB, METLIN database or authentic standards, and mostly metabolites were attributed into tryptophan and phenylalanine metabolism, valine, leucine and isoleucine biosynthesis, aminoacyl-tRNA biosynthesis and citrate cycle. To obtain alterations of more components in tryptophan and phenylalanine metabolism, we developed and validated a targeted metabolomics method of 19 metabolites by using LC-QqQ MS. Combining the results of targeted metabolomics with global metabolomics, significantly up-regulated kynurenine (KYN), anthranilic acid (AA) and 5-hydroxylindoleacetic acid (HIAA) simultaneously in urine and serum was found to implicate the activation of tryptophan metabolism under the condition of RA, which acted pro-inflammatory roles in inflammation and was closely correlated with GM. IDO/TDO functioned as a pro-inflammation mediator was overexpressed in RA patients. Urinary kynurenic acid and serum serotonin that have impacts on anti-inflammation in immune system were down-regulated in RA patients. The levels of phenylacetic acid and phenyllactic acid serving as a pro-inflammatory and an anti-inflammatory agent, respectively, increased in serum of patients with RA. Moreover, certain essential amino acids (EAAs), and mostly conditional EAAs were decreased in RA patients, which have been reported to inhibit cell proliferation of immune cells. In particular, deficiency of branched chain amino acids (BCAAs, valine and isoleucine) was observed in serum of patients with RA, which may lead to muscle

loss and cartilage damage. The specificity of all altered metabolites resulted from RA was considerably contributed through the GM-derived metabolites. The findings revealed that GM-modulated RA inflammation was mainly resulted from tryptophan and phenylalanine metabolism, and amino acid biosynthesis, which may provide more information for better understanding the RA mechanism.

Key words: Metabolomics, mass spectrometry, colorectal cancer cell, rheumatoid arthritis, gut microbiome

Acknowledgements

First and foremost, I would like to express my great gratitude to my supervisor, Prof. Zongwei CAI for his invaluable advice, encouragement and supports in the study. Prof. Cai provides me a lot of opportunities to explore and develop my potentials in scientific inquiry, not only inspiring me to enhance logical thinking ways and solid experimental skills, but also making me a conscious effort on strengthen my ability of expression, communication and leadership, which are beneficial for my future work.

The members of Prof. Cai group provided considerable help and advice to my personal and profession time in BU. Great thanks to Dr. Arthur C K CHUNG, Dr. Yanjun HONG and my co-supervisor Dr. Hungwing LI, for their sincere help, patience and encouragement. I also would like to express my great thanks to Mr. David T.W. CHIK and Mr. Fox Lin ZHU for their friendly supports in technology. I also would like to thank all the former and present groupmates, for their precious experiences, kindly help and discussion.

Moreover, I greatly thanks to our collaborators, Prof. Jun YU, Dr. Chichung WONG in CUHK and Prof. Aiping LU, Prof. Ge ZHANG, Mr. Xiaohao WU in BU (School of Chinese Medicine, SCM), as well as Prof. Lianbo XIAO and Dr Hui FENG in Shanghai Guanghua hospital of integrated traditional Chinese and western medicine, Mainland China. Their supports of sample and efforts on the project inspired me going ahead.

I appreciate the financial supports from the IRMS. I am particularly grateful to the Hong Kong PhD Fellowship Scheme from Hong Kong Research Grant Council to support my PhD study.

Finally and importantly, I would like to express my deepest gratitude to my family for their love, understanding and encouragement. Thank you!

Xiaona Li

Hong Kong Baptist University

Kowloon Tong

Hong Kong SAR, China

Table of Contents

List of Tables

List of Figures

List of Abbreviations

AA	anthranilic acid
Ac-Asp	N^1-acetyl-aspartic acid
ACN	acetonitrile
ACPA	anti–citrullinated protein antibody
Ac-Put	N^1-acetylputrescine
ACR	American College of Rheumatology
Ac-Spd	N^1-acetylspermidine
AGC	automated gain control
AICAR	5-aminoimidazole-4-carboxyamide ribonucleoside
Ala	alanine
AOA	amino-oxyacetic acid
Asn	asparagine
Asp	aspartate
ATCC	American Type Culture Collection
AUC	area under the curve
BCAAs	branched chain amino acids
CIA	collagen-induced arthritis
CID	collision-induced dissociation
Cit	citrate
CRC	colorectal cancer

CRP	C reactive protein
DAS	Disease Activity Score
DAS	N^1, N^{12}-diacetylsmpermine
DMEM	Dulbecco's modified eagle's medium
EAAs	essential amino acids
EI	electron impact
ESR	erythrocyte sedimentation rate
ETC	electron transport chain
FA	formic acid
FBS	fetal bovine serum
FC	fold change
FT-IT	Fourier transform-ion trap
Fum	fumarate
GC	gas chromatography
Gln	glutamine
GLS	glutaminase
Glu	glutamate
GM	gut microbiota
GPNA	L-γ-glutamyl-*p*-nitroanilie
HESI	heated electrospray ionization
HFBA	heptaflurobutyric acid
HIAA	5-hydroxylindoleacetic acid

HILIC	hydrophilic interaction chromatography
HMDB	human metabolome database
HR	high resolution
HRMSA	high resolution MS analyzer
HSS	high-strength silica
IC	ion chromatography
IL	Interleukin
iNOS	inducible nitric oxide synthase
IPA	indolepropionic acid
IPC	ion pair chromatography
IS	internal standard
Isocit	isocitrate
KYN	kynurenine
LAB	*lactic acid bacteria*
LC	liquid chromatography
LTQ-OT	linear trap quadrupole -Orbitrap
ME	malic enzyme
MeOH	methanol
MS	mass spectrometry
NEAAs	nonessential amino acids
NK	natural killer
NK	natural killer

NMDA	*N*-methyl-D-aspartate
NMR	nuclear magnetic resonance
NP	normal phase
NSAI	non-steroidal anti-inflammatory inhibitors
OAA	oxaloacetate
ODC	ornithine decarboxylase
OPLS-DA	orthogonal partial least squares discriminant analysis
Orn	ornithine
PCA	principle component analysis
PI3K	phosphoinositide 3-kinase
PLS-DA	partial lease squares-discriminant analysis
Put	putrescine
QC	quality control
QqQ	Triple quadrupole
Q-TOF	quadrupole time-of-flight
RA	rheumatoid arthritis
RF	rheumatoid factor
RP	reversed-phase
RPLC	reversed-phase liquid chromatography
RSLC	rapid separation liquid chromatography
RT	retention time
S-1-P	sphingosine 1-phosphate

SAM	S-adenosylmethionine
SCFAs	short chain fatty acids
SDS-PAGE	sodium dodecyl sulfate polyacrylamide gel electrophoresis
SF	synovial fluid
Spd	spermidine
Spm	spermine
SRM	selected reaction monitoring
SAT	spermidine/spermine N^1-acetyltransferase
Suc	succinate
TBA	tributylamine
TCA	tricarboxylic acid
TEA	trimethylamine
TIC	total ion chromatography
TNF	tumor-necrosis factor
Trp	tryptophan
UHPLC	ultra-high performance liquid chromatography
VIP	variable importance for the projection
ZIC-pHILIC	zwitterionic hydrophilic interaction chromatography
α-KG	α-ketoglutarate

Chapter 1 Introduction

1.1 Metabolomics: bridging from small molecules to human health

The first metabolomics study was traced back to 1971, when Pauling conducted the study “quantitative analysis of urine vapor and breath by gas-liquid partition chromatography” [1]. The term of “metabolomics” was first used by Oliver in 1998 , and defined the object as “metabolome” [2]. In the same study, the technique is to denote the group of metabolites consisting mostly small molecule metabolites, which amplify the product of upstream molecular changes in the transcriptome and the proteome (shown in Figure 1.1). In practice, terms of “metabolomics” and “metabonomics” have been interchangeable [3].

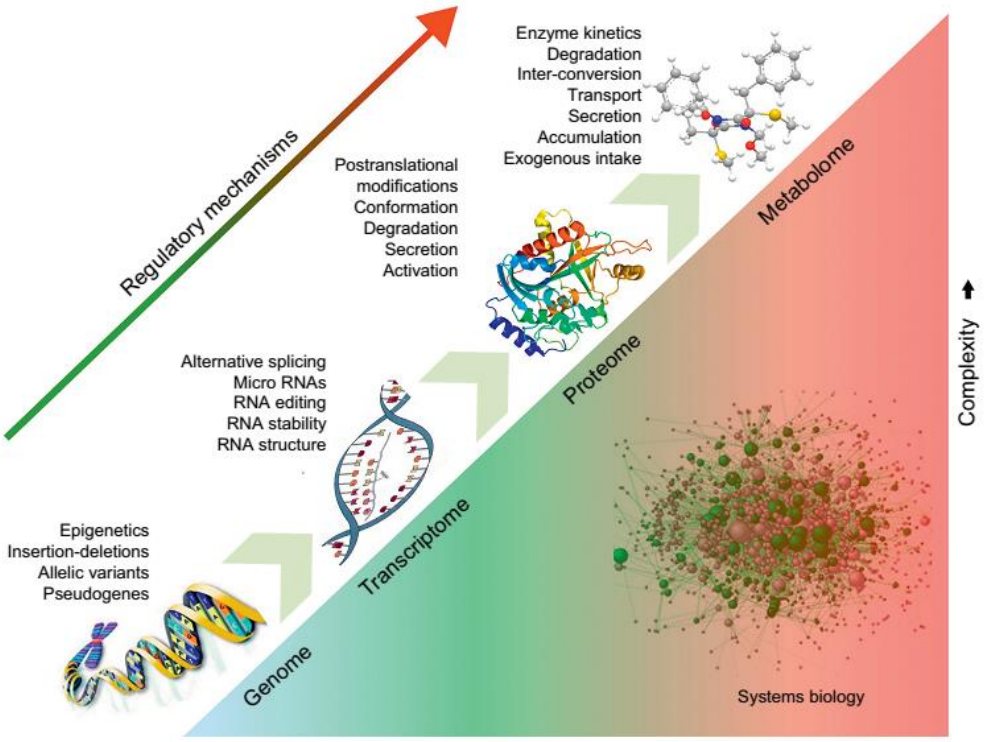

Figure 1.1 Metabolomics and system biology (reproduced with permission from [4]). Systems biology aims to discover interactions based on levels of DNAs, RNAs, proteins and metabolites, and provides views of biological process and pathological differences on human diseases.

Specifically speaking, metabolomics is the quantitative and systematic analysis of all metabolites. Metabolome changes are perturbed responding to inherent genetics (monogenetic or multigenetic) mutant or external stimulus (microbiomes, disease, drug, diet or physical activity) in biological cell, tissue, organ or organism [5]. Metabolomics has been proved to be an acceptable and reproducible technology.

Components of endogenous metabolites may vary diverse compound classes with molecular weight less than 1000 Da or 1500 Da, *e.g*. lipids, peptides, steroids, alkaloids, nucleic acids, organic acids, amino acids, carbohydrates, vitamins, and so on, presenting with different polarity and dynamic ranges. Because metabolites are closely correlated with the phenotype of organism or human homeostasis, metabolomics study has attracted extensive attention on bridging the gap between human genotypes and phenotypes through small molecules (Figure 1.2) [6], and on providing integrated evidences of key molecular signatures and characteristics for diseases diagnosis and progression at different stages [7].

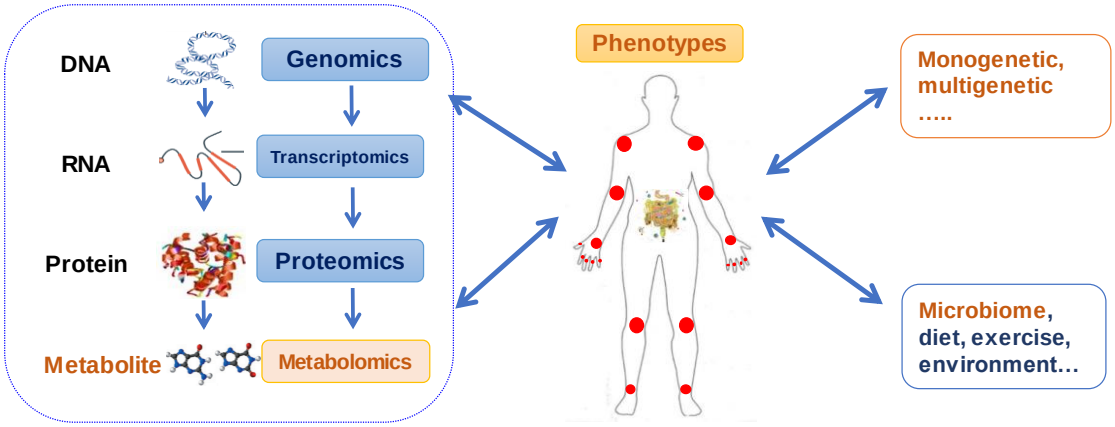

Figure 1.2 Metabolomics is a powerful tool to bridge the gap from genotype/stimulus to phenotypes. Metabolite as the downstream product of DNA, RNA and protein, is the subject of metabolomics, which can reflect abnormal phenotypes responding to perturbations of genetics or exogenous stimulus.

There are four approaches to investigate the metabolome [6, 8]: (1) metabolomics: quantification of "all" metabolites at a defined time under specific environmental conditions; (2) metabolite profiling: quantification of a group of related compounds or metabolites in a specific pathway; (3) metabolic fingerprinting: pattern recognition to classify samples by shifts in "global" metabolite composition; (4) targeted metabolomics: quantification of a number of known metabolites in clusters with similar chemical structures.

It is clear that as a branch of interdisciplinary scientific field [9, 10], metabolomics relies on novel, stable and powerful platforms for data acquisition, bioinformatics and network interpretation. In clinical research, metabolome is potential to become biomarkers for early diagnosis, prognosis and therapeutic assessment of cancer [11-14], cardiovascular biomarker discovery [15, 16], drug monitoring and assessment [7, 17], autoimmune disorders [18-20], *etc*. Therefore, metabolomics study links laboratory to clinic. In this introduction, we summarized the approaches of global metabolomics and targeted metabolomics analysis, and their applications in CRC cells and RA.

1.1.1 Nontargeted metabolomics

Non-targeted metabolomics study aims for quantification of all or as many as metabolites, making contributions to reveal gene function and to discover potential biomarkers for disease diagnosis, prognosis, progression or therapeutic intervention. There is no single technology that enables to cover the whole complex metabolome. Mass spectrometry (MS) and nuclear magnetic resonance (NMR) are two major approaches for metabolomics study. The workflow of MS-based metabolic profiling analysis is shown in Figure 1.3 [21-24]. After collection of biological samples (urine, plasma, serum, feces, cells or others), sample extraction is performed with different organic solvents for liquid chromatography (LC) and/or derivatization for gas

chromatography (GC) analysis. Subsequently, data acquisition is conducted using UHPLC-high resolution (HR) MS (both in positive and negative ion modes) and/or GC-MS. Of note, data processing and metabolites identification are the time-consuming steps. Data processing involves assessment of data quality, peak picking, alignment, normalization and retention time correlation, aiming to extract all real metabolic features from biological sample. Multivariate analysis includes principal component analysis (PCA), partial least squares discriminant analysis (PLS-DA) or orthogonal partial least squares discriminant analysis (OPLS-DA) after mean-centering and scaling [25], aiming to find out significant features. Identification of metabolites is performed by comparing retention time, MS/MS fragmentation and isotope pattern of biological sample generated by HR MS with those of authentic standard or database, the result of which can be further used for pathway analysis, correlation analysis, *etc*. Eventually, investigations of dysregulated endogenous metabolites and their roles in mechanism could lead us to a better understanding of the gene function or diagnosis, progression of disease.

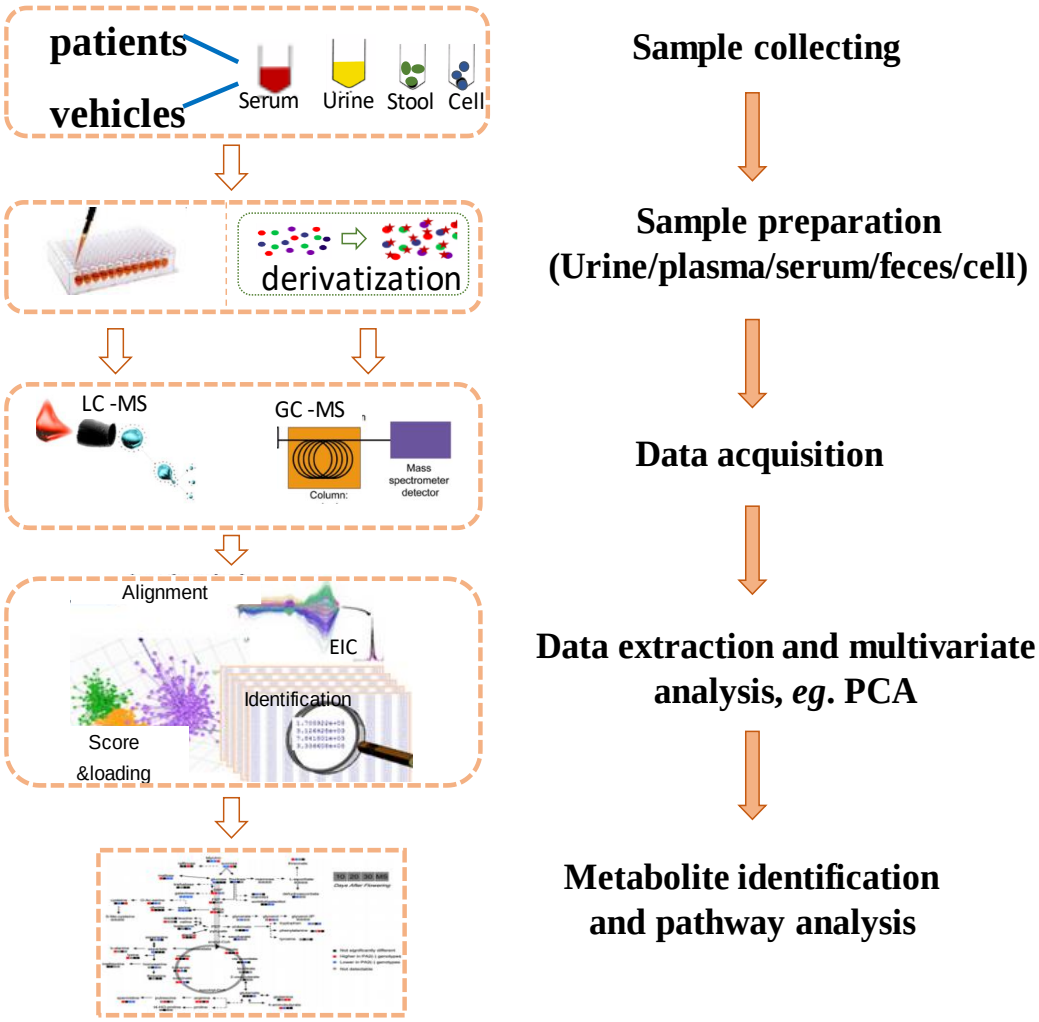

Figure 1.3 Workflow of MS-based non-targeted metabolomics study in biological samples.

Qualified sample is a prerequisite for discovering reliable potential biomarkers and significant metabolic pathway [26]. Sample preparation method is essential to non-targeted metabolomics since it can directly affect metabolite contents. However, this step is sometimes overlooked in metabolomics study. The choice of sample pretreatment method depends on purpose of analytical platform. Generally speaking,

characteristics of a good sample preparation for global metabolomics are as follows [27]: (1) wide coverage of metabolites; (2) simple and fast operation for preventing the loss or degradation of unstable metabolites and insuring high-throughput; (3) good reproducibility; (4) simultaneous accomplishment metabolites extraction and quenching for cells or microbes.

Moreover, there are some concerns in biological sample pretreatment. Yin *et al* [28] evaluated factors which could affect the sample quality in pre-analytical phase, and recommended the following tips for human biological sample, in particular for blood sample. (1) Test quality of biofluid collection tube before use, considering EDTA plasma tube was recommended for blood collecting but not suitable for NMR analysis; (2) remove hemolyzed samples; (3) kept samples at -80 ℃ by multi-aliquots of biobank to reduce metabolites differences due to over 3 times of freeze-thawing cycles; (4) place blood immediately in ice blocks after collection until further processing (for a fixed time; ideally not longer than 2 h) ; (5) weigh and exclude unqualified blood samples using sphingosine 1-phosphate (S-1-P) as a pre-analytical biomarker. Based on LC-MS platform, suggested common pretreatment of biological samples are shown in Figure 1.4.

For data acquisition, NMR and MS with chromatographic separation are two widespread complementary approaches for metabolic profiling study [5, 22]. Each

technique possesses its advantages and disadvantages (shown in Table 1.1). NMR is based on the magnetic properties of specific atomic nuclei, such as ^{1}H, ^{13}C or ^{31}P, which could provide chemical structure and abundance of metabolites in biological samples (biofluids and tissues) [15]. Due to broad dynamic ranges, simple sample pretreatment and capacity of structure elucidation, NMR is extensively applied for metabolic profiling of biological samples, such as screening molecular toxicity, biomarker discovery [34, 35], assessment of diagnostic [36, 37], disease stage [38], treatment [39], *etc*. However, NMR is limited application due to its lower sensitivity in comparison with MS, which could be coupled to GC or UHPLC for metabolite separation.

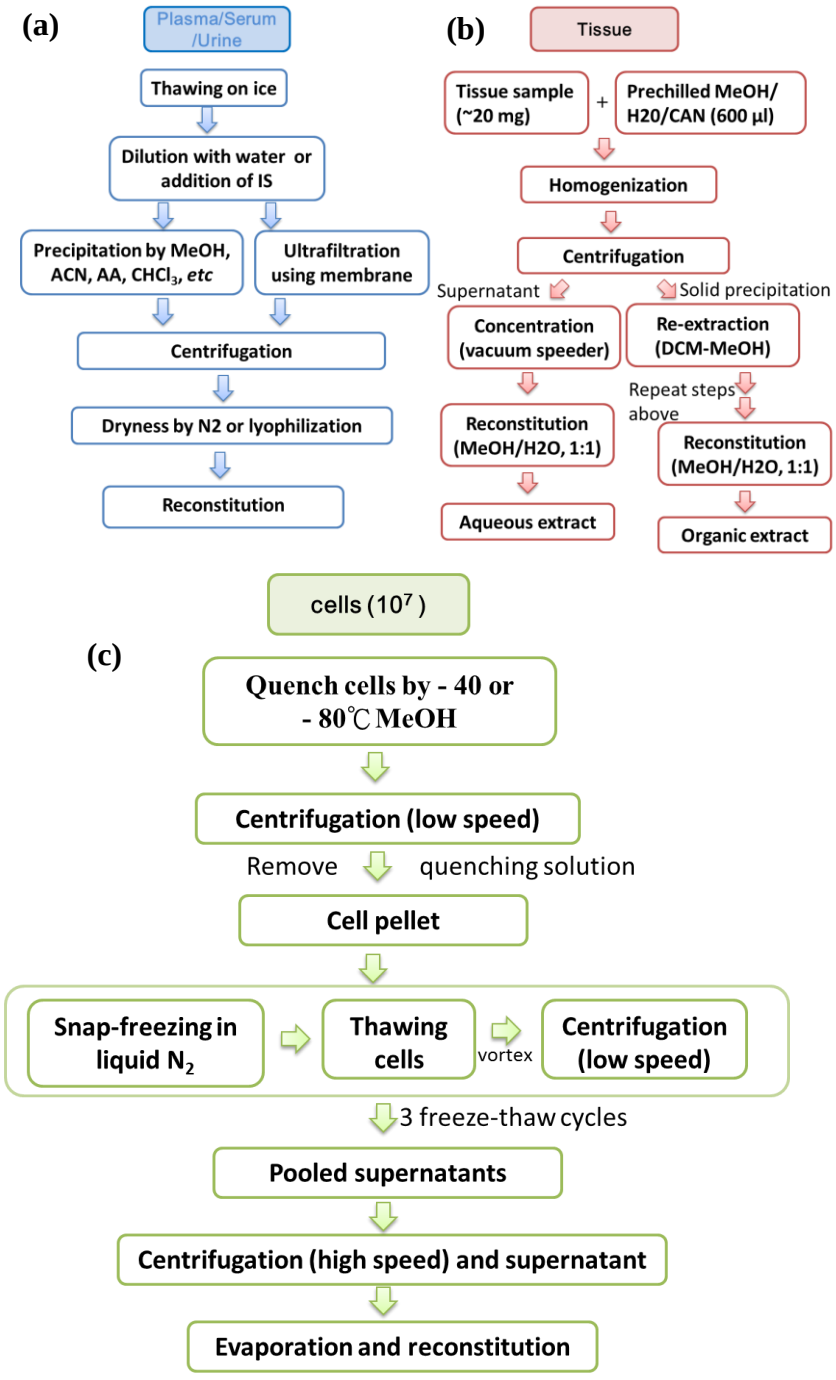

Figure 1.4 Suggested pretreatment of (a)plasma/serum/urine [22, 29-31], (b) tissue [21, 30] and (c) cell [24, 32, 33].

IS: internal standard, ACN: acetonitrile, $CHCl_3$: trichloromethane, AA: acetic acid, DCM: dichloromethane.

Table 1.1 Pros and cons of NMR and MS (GC-MS and LC-MS) in metabolomics study.

Technique	Pros	Cons
NMR [3, 36, 40, 41]	Non-invasion Simple sample preparation Capable of detect metabolites of intact tissues Provide structure information	Poor sensitivity Spectral deconvolution
MS * [5, 41]	Good sensitivity Selectivity from high resolution Excellent separation Less sample size	Sample destruction Component bias
GC-MS [42-44]	Good sensitivity Identical database for metabolite identification Less samples size Good separation	Component bias Sample destructive Laborious and time-consuming
LC-MS [21, 22, 29, 40]	Excellent sensitivity Multiple and flexible choice of separation Minimize sample size	Component bias Sample destructive No shared database

Notes:

*represents characteristics of MS compared to NMR, then the pros and cons of GC-MS and LC-MS are respectively listed.

Regarding mass spectrometry, outstanding analyzer integrated with excellent ability of separation exerts good sensitivity, selectivity and reproducibility for metabolome study with diverse physio-chemical properties and large dynamic range in complicated biological matrix [22]. GC-MS is an useful analytical platform for metabolomics study due to its high sensitivity, good peak resolution and good reproducibility [45]. GC-MS is applied to detect volatile, thermally stable and nonpolar compounds. In addition, it is suitable for detecting polar compounds after derivatization, including amino acids, organic acids, nuclear acids, carbohydrates, amines and alcohols [42-44]. Unlike the electrospray ionization coupled with LC, electron impact (EI) can provide stable and reproducible spectrum for metabolites identification and is also less prone to matrix effects [42]. Moreover, better separation ability of multi-dimensional capillary column coupled to (hybrid) high resolution quadrupole time-of-flight (Q-TOF) MS perform broaden the coverage of metabolome due to excellent ability of qualification and quantification [46, 47]. However, the chemical derivatization of biological sample for improving the non-polarity, volatility and thermostability, including silylation, alkylation and acylation, is a laborious and time-consuming procedure [42]. Particularly, most silylation reagents are sensitive to moisture or trace amount of water [45].

Comparing with NMR and GC-MS, LC-MS performs better sensitivity (10-100 fold) and selectivity on nontargeted metabolomics, due to multiple choice of chromatography separations and high resolution MS (HRMS) analyzer. Currently, widely applied chromatography separations include reversed-phase liquid chromatography (RPLC), hydrophilic interaction chromatography (HILIC) [48], ion pair chromatography (IPC) [49], and so on. Reversed-phase column, like traditionally C18 column, coupled with HILIC column (*e.g.* amide, amino propyl), enhances separation ability of semi-polar and polar compounds, respectively. Additionally, hybrid mass spectrometers, such as Q-TOF, linear trap quadrupole-Orbitrap (LTQ-OT), Fourier transform-ion trap (FT-IT) mass spectrometry plays extraordinary performance on metabolite identification, owing to their high resolution and mass accuracy (< 5 ppm) [29]. Moreover, integrating different mechanism of separation [40] (like RP×HILIC) with HR MS contributes to the increase of peak capacity and coverage of biological samples. Nevertheless, LC-MS doesn't have strong informative libraries like GC-MS based on collision-induced dissociation (CID) mass spectra, cause diverse LC column and MS construction result in different performances [22, 50]. With regards to metabolite identification based on MS data, three approaches were recommended: (1) spectral matching. Under the specific condition of LC-MS equipment and column, comparing MS/MS or MS^n fragments in

hand with open or commercial accessed, in- or out-house data libraries, *e.g*. HMDB and METLIN [23]. (2) Parent ion matching. Super accurate parent ions are obtained by employing HR MS, *e.g.* orbitrap MS using MALDI as ionization method [51]. (3) Standard matching. Retention time, accurate mass ion and MS/MS fragmentation of sample are extremely similar to those of authentic standards.

The selectivity and the dynamic linear range of LC-MS (~ 10^6) does not satisfy the requirement of biological samples coverage (over 10^{12}) [41]. Nowadays, integrated GC-MS and LC-MS, the two complementary techniques, sometimes in combination with NMR, is more likely to provide changes of metabolites with both low-molecule-weight and medium-to-high-molecule-weight, which is critical for mapping complex metabolic pathways correlated with the phenotype of human [7, 52].

Due to less sample size and excellent separation of column prior to detection, LC-MS can facilitate metabolites identification and quantitation. Taken together, development of separation techniques including HPLC/UPLC [50, 53, 54], GC [40, 52], and capillary electrophoresis (CE) [55], as well as parameter optimization of MS analyzer [41], could improve ability of qualification and quantification of metabolome.

1.1.2 Targeted metabolomics based on LC-MS/MS

Non-targeted and targeted metabolomics study focus on global comprehensive metabolome and specific interested metabolome, respectively [56]. Significantly perturbed metabolites discovered in non-targeted metabolomics analysis are attributed into significant pathways for diagnosis and progression of diseases or gene function, which also provide insights into targeted metabolomics analysis [57]. Targeted quantification of metabolomics includes relative quantification and absolute quantification. Due to diverse physiochemical properties of endogenous metabolites, a robust, sensitive and reproducible platform is necessary for targeted metabolic analysis. On basis of LC-MS platform, the triple quadrupole mass spectrometer using selected reaction monitoring (SRM) mode coupled to UPLC with different columns is widely applied.

Triple quadrupole (QqQ) detector is used to acquire MS/MS data by using SRM transitions with unit resolution. Precursor ions are set to be selected in Q1 after the pre-scanning of m/z range, then generate fragmentation by collision gas (argon or helium) in Q2. Finally product ions are detected in Q3 [22]. Additionally, HRMS as an alternative choice for targeted metabolomics analysis, can not only provide sensitive and selective response for metabolic features quantitation in complex bio-mixture, but also provide high accurate ions for metabolites quantification [58].

However, good separation behavior of metabolites is the prerequisite to sensitive and selective detection in MS analyzer.

Generally, liquid chromatography system is suited to analyze polar and semi-polar metabolites. Reversed-phase LC, using conventional C18-bonded silica and high-strength silica (HSS) column, is commonly used for detecting medium-polar and non-polar analytes, but not for polar metabolites due to poor retention behavior of analyte in stationary phase [22]. Hence, HILIC has been emerged as a complementary routine to elute polar and ionic metabolites such as carbohydrates, organic acids, amino acids, bioamines, *etc.* with increasing percentage of aqueous mobile phase. The approach has the advantage of avoiding void volume [48, 59, 60]. Mechanism of HILIC is that analytes are retained by their hydrophilic interactions, cationic/anionic interactions and hydrogen bridges with stationary phase [61]. HILIC stationary phase is divided into three types: neutral (no electrostatic interactions), charged (strong electrostatic interactions) and zwitterionic (weak electrostatic interactions). Among them, Zwitterionic stationary is suited for metabolic profiling, while in targeted analysis appropriate stationary phase should be chosen based on expected analytes. pH, additive and mobile phase play important roles in retention behavior of metabolites [62]. For example, alkaline mobile phase is recommended when using polymer-based zwitterionic hydrophilic interaction chromatography (ZIC-pHILIC)

column to capture metabolites in cells, including amino acids, nucleotides, organic acids, phosphates, *etc* [63]. Owing to higher proportion of organic solvent, HILIC coupled with MS showed better ionization efficiency and sensitivity [60]. However, HILIC column is not robust enough as RP column, representing as poor reproducibility of retention time and short column lifespan.

Ion-pair reversed phase chromatography is an alternative method for determining ionic and polar molecules in biological mixtures. Ion-pairing chromatography lies in the addition of ion-pairing reagents with opposite charge to targeted analytes. Mobile phases of ion-pairing chromatography are meant to improve ion pairs with ionic components and to format hydrophobic region to help enhancing the retention. Tributylamine (TBA) and trimethylamine (TEA) are popularly used in anionic metabolites, such as phosphorylated carbohydrates [64, 65], nucleotides [66], and carboxylic acids [64]; while heptafluorobutyric acid (HFBA) is suitable for cationic analytes, like polyamines [67], amino acids [68], vitamins [69], *etc*. Ion-pairing chromatography have relative good reproducibility, resolution, metabolite coverage and sensitivity in light of good peak shape [65]. Comparing with HILIC approach, ion-pairing chromatography showed better separation ability, especially for co-eluted biological isomers [65]. However, IPC has a disadvantage of ion suppression to MS

detector, which requires a long-time cleaning cycle when switching between positive and negative ion modes.

HILIC or IPC technology coupled to mass spectrometer are widely used to quantify intracellular metabolites [64, 65, 70, 71], such as TCA cycle intermediates, amino acids, nucleotides, *etc*. The approach avoids the derivatization of polar metabolites [72]. In addition, targeted quantification of nonpolar and polar metabolites could be carried out by using RP and HILIC or IPC combined separations coupled to tandem mass spectrometry [73].

1.2 Applications of targeted/non-targeted metabolomics in diseases

Metabolomics is a powerful platform to comprehensively investigate altered metabolic components responding to human (patho-) phenotypes simulated by gene mutation or diseases [74]. Series of analytical platforms (LC-MS, GC-MS and NMR) are capable of monitoring alteration of small molecules in biological samples, which help with discovering biomarkers of disease diagnosis [75-77], severity and risk assessment [78, 79] and therapeutic or prognosticate effect [13, 74].

1.2.1 Metabolomics study on colorectal cancer (CRC)

Colorectal cancer (CRC) is the third prevalent cancer worldwide and second cause of cancer death in developed countries with poor diagnostic rate at early stage [80]. In the previous serum metabolomics study, 2-hydroxybutyrate, aspartic acid and

kynurenine were discovered to establish prediction model for early stage diagnostic efficiently [77]. In metabolic profiling studies of CRC tumor and matched normal tissue and biofluids (serum, urine) by using NMR, GC-MS and UPLC-MS, enhancing ability of tissue hypoxia, biosynthesis of glycolysis, nucleotide, amino acid and lipid occurred in CRC biological samples, which provide insights into stage discriminating and prognostic [13, 79] and help to understand the mechanism of CRC [81-84].

Targeted metabolomics analysis of small molecules is an important approach to uncover CRC patho-mechanism. There are many reports revealed sorts of important metabolites by comparing biological samples (tissue, plasma) of colorectal cancer and those of healthy volunteers. Quantitative metabolites analysis of colon cancer cells indicated enhanced glycolysis activity representing as low glucose, high lactate and glycolytic intermediates, which is in consistent with Warburg effect. In contrast, most amino acids accumulation in cancer cells might be ascribed to autophagy degradation of proteins and activation of glutaminolysis [85]. Additionally, Bener *et al.* [86] found that essential amino acids apart from histidine and arginine showed higher levels in plasma of colorectal cancer patients without significant differences except threonine (p <0.012) and methionine (p <0.0001); whereas nonessential amino acids (NEAAs) include ornithine, glutamic acid, taurine, proline, serine, glycine, and alanine showed higher levels in the cancer patients with significant differences (p <0.0001).

1.2.2 Metabolites and pathways related to CRC

Otto Warburg [87, 88] showed that most cancer cells primarily produce energy through a high rate of glycolysis (to generate pyruvate) and by fermenting lactate in cytoplasm, which is different from normal cells via low rate of glycolysis followed by oxidative phosphorylation of pyruvate in mitochondria, which known as Warburg effect (showed in Figure 1.5).

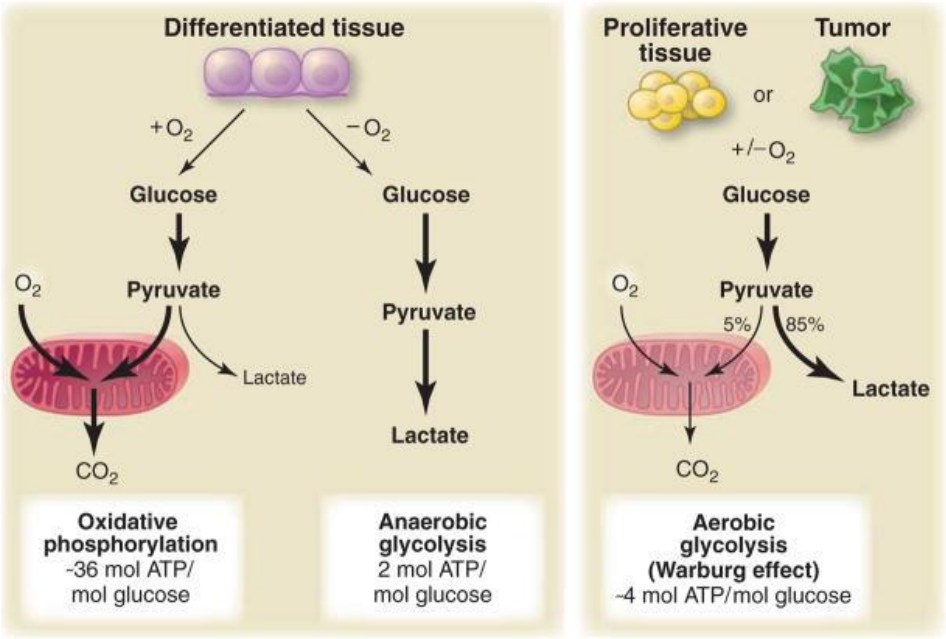

Figure 1.5 Schematic of oxidative phosphorylation, anaerobic glycolysis and aerobic glycolysis (Warburg effect or Warburg hypothesis) (reproduced with permission from [88]).

Glutamine metabolism consists of glutaminolysis (oxidative carboxylation) and reductive carboxylation, beginning with transformation of glutamine (Gln) to glutamate (Glu) and the conversion of glutamate into α-ketoglutarate (α-KG) [89]. In glutaminolysis pathway, α-KG is oxidized into tricarboxylic acid cycle (TCA) intermediates in mitochondria and decarboxylated to pyruvate; while in reductive reactions, α-KG is metabolized into isocitrate by reduction, finally generate lipids, which also named *de novo* lipogenesis.

On basis of Otto Warburg, cancer cells tend to consume more glucose and produce more lactic acid in comparison with normal cells or tissues. Warburg effect is caused by oncogenic activation of glucose uptake, such as phosphoinositide 3-kinase (PI3K). However, these tumor cells are also replying on exogenous glutamine for survival [90]. Glutamine could donate its amide (γ-nitrogen) and converts into glutamate in the purine and pyrimidine synthesis, and glutamine-derived glutamate supports nitrogen for non-essential amino acids [90, 91], the latter reaction is shown in Figure 1.6. Compounds showed in red, containing carbon, not nitrogen; while metabolites showed in blue containing carbon and nitrogen originated from glutamine and/or glutamate. Glutamic acid is transferred the amine group (original from glutamine's α-nitrogen) to α-ketoacids, namely carbon catabolites of glucose and glutamine, such as pyruvate, 3-phosphoglycerate, oxaloacetate, and glutamic acid

gamma-semialdehyde, which generate NEAAs (alanine, serine, aspartate, and ornithine). Glycine and cysteine are biosynthesized from serine, while asparagine generated from aspartate with amide group donating by glutamate. Of note, tyrosine as one NEAA, is not metabolized from glucose or glutamine, but from phenylalanine of EAA.

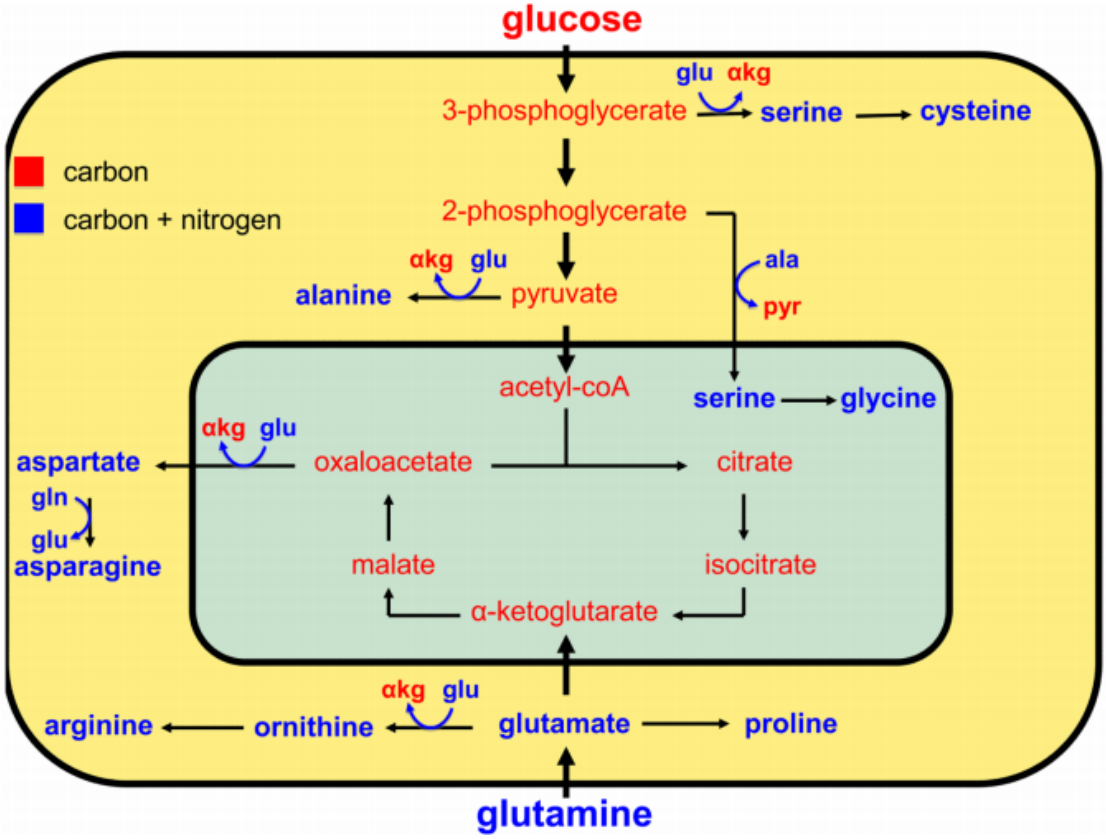

Figure 1.6 Glucose and glutamine can support the synthesis of the nonessential amino acids as carbon and nitrogen sources (reproduced with permission from [90]).

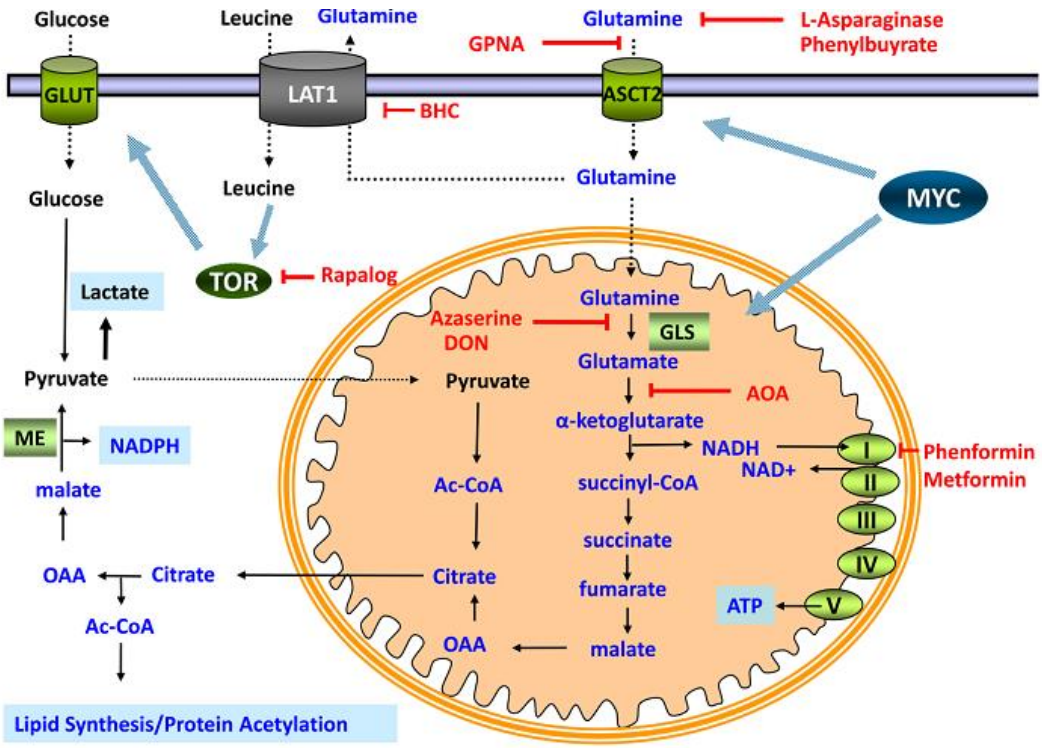

Figure 1.7 Pharmacologic targets in glutamine metabolism (reproduced with permission from [90]). The compounds in red are medicines that enable to affect glutamine metabolism.

Figure 1.7 showed the relation between glutamine and critical kinase, genes and metabolites. The transcription factor c-Myc [92] could increase glutamine uptake from extracellular via the up-regulation of SLC1A5 or ASCT2 encoding glutamate importer and direct target and high affinity of the Myc oncoprotein. On the other hand, Myc converts glutamine into glutamic acid when glutaminase (GLS) up-regulated. However, glutamine uptake could be decreased by depleting extracellular glutamine

with L-asparaginase and phenylbutyrate or via inhibiting ASCT2-dependent uptake with L-γ-glutamyl-p-nitroanilie (GPNA). Glutamine participates into glutaminolysis to generate NADPH or is exported to promote TOR kinase activation after glutamine enters cells. In addition, conversion of glutamic acid into *α*-ketoglutarate would be inhibited by amino-oxyacetic acid (AOA). Then less *α*-KG produces down-regulated citrate and its product of oxaloacetate (OAA) in mitochondrial. So that the reduction of OAA which is converted into malate, results in less pyruvate and NADPH by the oxidation of malate to pyruvate via malic enzyme (ME). OAA can be replenished by high rate of glutamine metabolism when sufficient glutamine is provided (NAD^+ would be generated). Biguanides, phenformin and metformin can inhibit the process. Thus, activities of amino acid exchanger LAT1 and TOR using glutamine as substrate are also suppressed by some medicine.

Recent years, metabolic flux analysis studies of cancer cells *esp.* with ^{13}C-labeled glucose and ^{13}C-glutamine are emerging to attract extensive attentions. The findings revealed dysregulation of proposed pathway under specific conditions or treatment, such as hypoxia or mitochondria dysfunction caused by gene mutation. Figure 1.8 showed the metabolic flux analysis of cancer cells under hypoxia and mitochondrial dysfunction, using ^{13}C-glucose (marked in red) and ^{13}C-glutamine (marked in green) as isotope tracers. According to the schematic, carbon skeleton of

glycolysis and TCA cycle intermediates would be labeled with different numbers of ^{13}C-carbon in glycolysis or glutamine metabolism (both oxidative reaction and reductive reaction). Besides, cancer cells conduct a metabolic flux of lipid synthesis (*de novo* lipogenesis) (marked in yellow), that five carbons labeled glutamine generate ^{13}C-lipid acids via $^{13}C_4$-*α*-ketoglutarate.

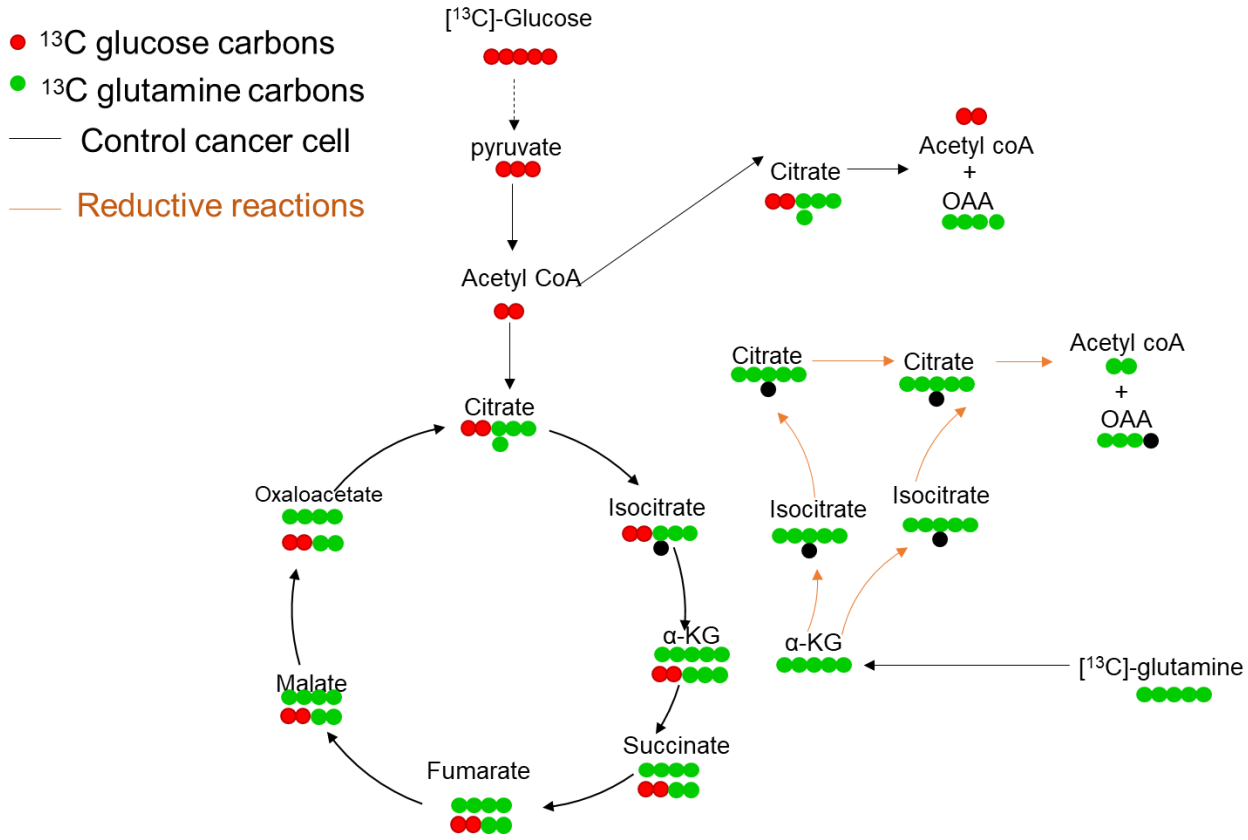

Figure 1.8 Overview of metabolic flux analysis of cancer cell metabolism with ^{13}C-glucose (marked in red) and ^{13}C-glutamine (marked in green) as isotope tracers (adapted from Figure 2 in reference [87]).

1.2.3 Metabolomics study on rheumatoid arthritis (RA)

Rheumatoid arthritis is a chronic, inflammatory, systemic autoimmune disease mainly presenting in 30-50 years population and leads to painful swelling, irreversible joint destruction and even disability [93]. According to incidence and prevalence study, about 0.5-1% of adult suffers from RA worldwide [94, 95]. RA is predicted as a major cause of chronic disability in the following 10-20 years. Of note, about 79 % of RA patients are female [96]. Moreover, RA is affected by complicated interplay of multigenetic (HLA-DR4 alleles, PTPN22, STAT4, CTLA4, cytokines, *etc.*) and environmental factors (*i.e*. smoking, microorganisms, stress, *etc.*) [95, 97]. As shown in Figure 1.9, individuals with genetic susceptibility environmental factors may activate immunological response, which is associated with the progression of disease [93, 97]. Generally, the American College of Rheumatology criteria (1987) is used for diagnosis of rheumatoid arthritis, which is a patient who meets at least 4 in 7 criteria might suffer rheumatoid arthritis. So far, a single test is unable to confirm diagnosis of RA. In laboratory, some parameters including blood cell count, rheumatoid factor (RF), erythrocyte sedimentation rate (ESR), C-reactive protein (CRP) and anticyclic citrullinated peptide antibody are helpful for diagnosis of RA. However, the accurate diagnosis of RA is difficult at early course, since its onset is insidious [98].

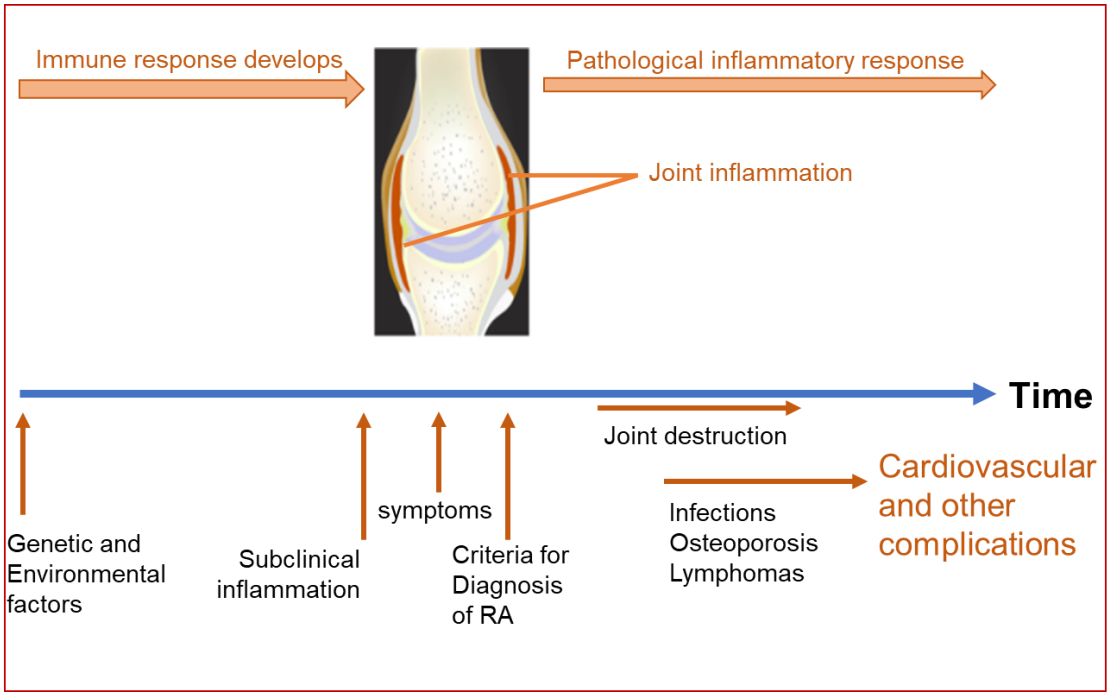

Figure 1.9 Longitudinal course of RA (adapted from Figure in reference [98]).

Metabolomics study is useful to help to understand the metabolome variation and antirheumatic drug responding to progression and/or therapeutic effect of RA. As reported, comparing urinary or serum metabolic profiling of RA patients or RA model animals with healthy controls, perturbed metabolites included TCA cycle intermediates (*e.g.* succinic acid, citric acid), amino acids or derivatives (*e.g.* histidine, phenylalanine, phenylacetylglycine), vitamins (*e.g.* pantothenic acid), carnitines, *etc.*, which are attributed to TCA cycle, tryptophan metabolism, phenylalanine and tyrosine metabolism, biosynthesis of carnitines, bile acids and fatty acids metabolism [19, 99, 100]. TCA cycle activity could be perturbed by damaged cartilage or chondrocytes. Some amino acids, such as tryptophan and histidine, could scavenge free radicals [101]. Branch-amino acid (BCAA) levels were decreased in

collagen-induced arthritis (CIA) rats which might be resulted from increased oxidation [102]. Traditional Chinese Medicine (TCM) treatment of rheumatoid arthritis have been reported that TCM could restore arthritis syndrome to some extent, such as Huang-Lian-Jie-Du-Tang and Wu-tou decoction [99, 100]. Additionally, anti-tumor necrosis factor (TNF) is usually used to control RA activity and suppress joint damage. Metabolic profiling approach is able to separate the good responders to anti-TNF treatment after 6 months from non-responders [103].

Previous findings via high throughput microbial DNA sequencing advanced our understanding of the interaction between microbes and hosts, which provide novel evidence into that the microbiomes participate into the pathogenesis of RA. Microbiomes presenting as ten-fold of human cells and sharing our spaces [104], serve the physiological, metabolic and immune capacities of host through exchanging nutrients from human body [105]. Micro-organisms dysfunction in hosts could trigger autoimmune disorders or diseases, such as obesity, stroke and cardiovascular disease [106, 107]. Particularly, despite of progress on the molecular pathogenesis of RA, its etiology is still unclear. Recent reports have shown that the presence and species of microbiomes were perturbed in RA animal model [108, 109] and patients [110, 111]. Moreover, the oral and gut bacteria could be restored after RA treatment [111]. Intriguingly, some abnormal metabolites and pathways associated with gut microbiome have been discovered in RA-suffered hosts [99, 112, 113]. Further studies focusing on metabolites alteration in RA patients are required.

1.3 The aims of project

Based on the above summarization, MS metabolomics is a powerful tool to broadly applied in elucidation of gene function and mechanism of CRC and RA. In our previous study, it is first time to discover that SLC25A22 gene is overexpressed in CRC patients with *KRAS* mutation. However, the metabolic effects of SLC25A22 gene on *KRAS*-mutant CRC cells is unclear. Considering RA as an autoimmune disease, there are insufficient evidence of metabolites perturbation in urine and serum responding to RA inflammation. Moreover, in view of metabolome, quite a few of study focused on the correlations of RA with GM. Therefore, my thesis aimed to the following four concerns.

(1) Based on the MS platform of global metabolomics, we aimed to investigate the metabolic effect of SLC25A22 gene on the KRAS mutant CRC cells, and to discover the importantly perturbed pathways.

(2) Based on the MS platform, we aimed to establish reliable targeted metabolomics method to characterize the altered polar intracellular metabolites in CRC cells by using LC-QqQ MS. In further, we aimed to quantify the abnormal metabolites and trace the metabolite fates by comparing knockdown of SLC25A22 CRC cells with controlled CRC cells with *KRAS* mutant, which further provided insights into the pathogenesis of CRC with *KRAS* mutation.

(3) Based on the platform of global and targeted metabolomics, we aimed to discover the urinary and serum metabolic features alteration in RA patients by comparing with health volunteers.

(4) Based on abnormal urinary and serum metabolites in patients with RA, we aimed to reveal the correlation of metabolic dysfunction with arthritis phenotype, particularly the relationship of GM with RA, which could further uncover the roles of abnormal small molecules associated with GM in RA.

Chapter 2 Non-targeted Metabolomics Revealed SLC25A22 as Essential Regulator in KRAS-mutant Colorectal Cancer

2.1 Introduction

Colorectal cancer (CRC) is the third most common cancer worldwide [114]. *KRAS* oncogene, mutated in approximately 30 % - 50 % of CRC patients [115, 116], presents both as a prognostic and predictive marker for targeted therapy of CRC [117, 118], and mutations in *KRAS* results in non-response to anti-EGFR inhibitors [118-120]. In our previous study, we identified SLC25A22 is overexpression in CRC tumor with KRAS mutation. SLC25A22, which as one member of mitochondrial transporter family (SLC25) and encodes a mitochondrial glutamate transporter, is a novel oncogene essential for the viability of CRC cell lines with simultaneous mutations in *APC* or *CTNNB1* and *KRAS* [121]. Apart from its role in CRC tumorigenesis, SLC25A22 has also been found to be mutated in encephalopathies, which frequently involved in altering the highly conversed amino acids that will completely abolish glutamate carrier activity [122, 123]. However, the full spectrum of metabolic effects of SLC25A22 on *KRAS*-mutant CRC cell lines not yet comprehensively characterized.

Metabolomics analysis plays a crucial role in the discovery of potential metabolic biomarkers during the development of drug and diagnosis, as well as in revealing gene function during the cell metabolism [120, 125-127]. Global and targeted metabolomics, which respectively aims to profile the entire and specific components of the metabolome, providing signatures for various metabolic phenotype and aids in the understanding of the mechanism

of action of drugs or genes in biological systems at the level of metabolites. Nuclear magnetic resonance (NMR) or mass spectrometry (MS) coupled to gas chromatography (GC) or liquid chromatography (LC) are widely used to identify and quantify the metabolome on a global scale [128, 129]. Therefore, metabolomics has become promising strategy to further elucidate metabolic pathways regulated by SLC25A22 in *KRAS*-mutant CRC and provide insights into the therapy of CRC with *KRAS* mutation.

In the study, global metabolomics based on UHPLC-MS was utilized to evaluate the effects of SLC25A22 on cellular metabolism in *KRAS*-mutant CRC cells. Global metabolome profiles of control (pLKO) and SLC25A22 knockdown DLD1 cells (shSLC25A22) were obtained by using UHPLC-Orbitrap-MS. The workflow was shown in Figure 2.1. Our analyses unrevealed alanine, aspartate and glutamate metabolism and nitrogen metabolism were perturbed significantly due to knockdown of SLC25A22 in *KRAS* mutant CRC cell.

2.2 Materials and methods

2.2.1 Chemicals and reagents

Pure water was prepared by Milli-Q system (Millipore, USA). Methanol (MeOH), acetonitrile (ACN) and formic acid (FA) were of LC grade. All authentic standards were obtained from Sigma (St. Louis, US).

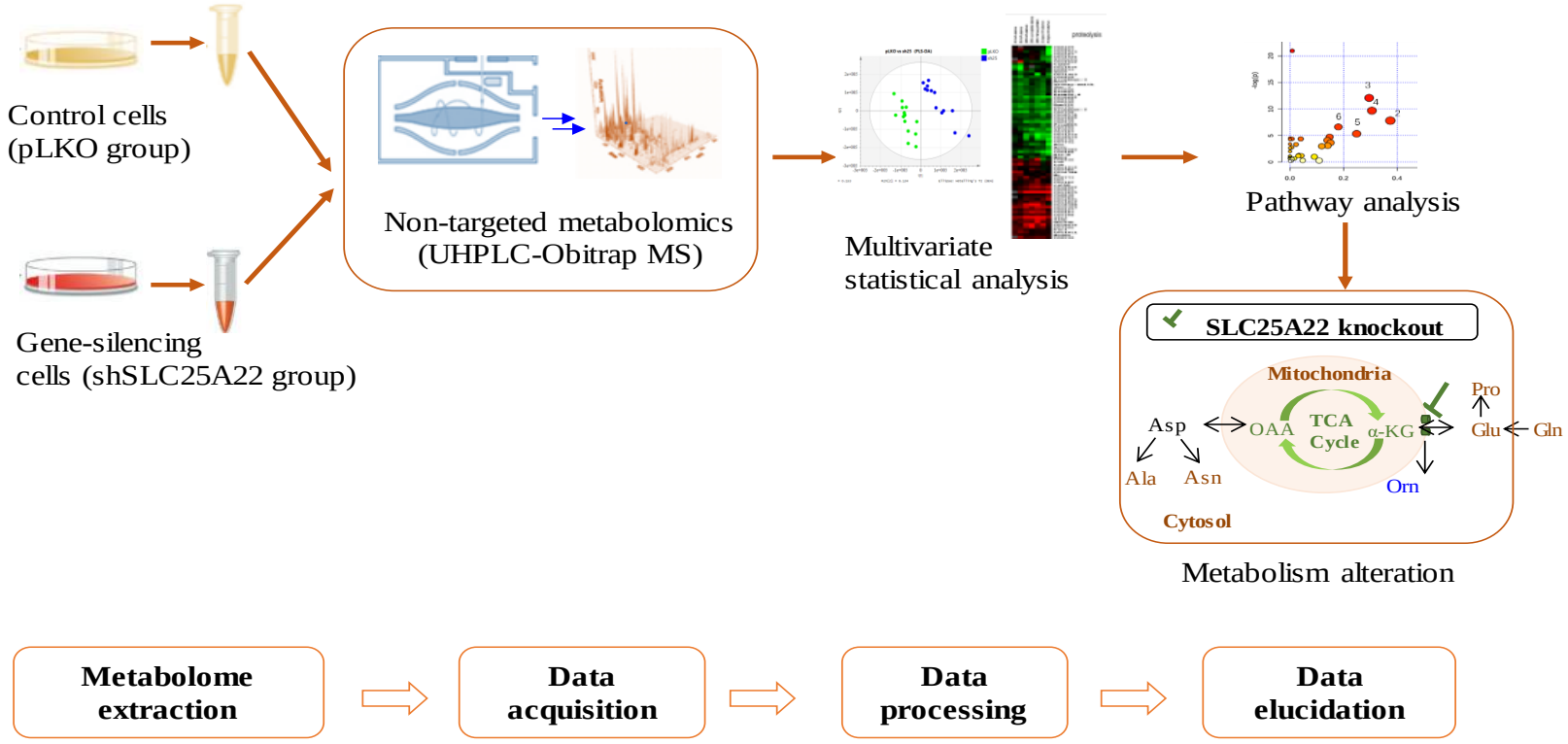

Figure 2.1 The workflow of global metabolomics analysis.

2.2.2 Cell culture

DLD1, HCT116 and SW1116 cell line was obtained from American Type Culture Collection (ATCC, Rockville, MD). All cells were routinely cultured in the Dulbecco's modified eagle's medium (DMEM) medium supplemented with 10 % fetal bovine serum (FBS) and 100 unit/mL penicillin-streptomycin. DLD1 cells stably expressing pLKO (control, n=15) and shSLC25A22 (SLC25A22 knockdown, n=13) were cultured in the presence of puromycin (2 μg/mL). Cells were seeded at 5×10^6 per 10 cm dish for 24 h prior to global metabolomics analysis and targeted metabolomics analysis (in the chapter 3). In the glutamine (Gln)-dependent experiment, different concentrations of glutamine were added into the cell medium.

2.2.3 shRNA-mediated knockdown, colony formation and apoptosis

SLC25A22 shRNA lentiviral vector was obtained from the RNAi Consortium (TRC) shRNA library (Open Biosystems, Huntsville, AL). The clone ID was TRCN0000044569 and the antisense sequence was 5'-GTGGTGTACTTCCCGC TCTTT-3'.

Cells were plated in 24-well plates at 100-500 cells per well in 0.5 mL of complete media. At the end point, cells were stained with 0.1% crystal violet and

number of colonies was counted. Cell growth curves were obtained using the xCelligence system (ACEA Biosciences, San Diego, CA).

Apoptosis was conducted using the Annexin-PE/7-aminoactinomycin D (7-AAD) staining kit (BD Biosciences, CA). The part of work was conducted by collaborators in Chinese University of Hong Kong (CUHK).

2.2.4 Sample preparation

Culture medium was aspirated and the cells were washed twice in ice-cold PBS and once in pure water. The cells were extracted by adding 1 mL chilled methanol and H_2O (v/v, 8:2) containing 0.1 μg/mL 4-chloro-phenylalanine as the internal standard (IS). The cells were then incubated at -80 ^{o}C for 60 min, scraped and transferred into Eppendorf tubes. Cell extracts were subjected to three freeze-thaw cycles using liquid nitrogen and ice. The supernatant was transferred into a new tube after centrifugation for 10 min at 16000 *g*, 4 ^{o}C. The residues were then extracted by 0.5 mL methanol, and the supernatants were pooled for lyophilization. The residues were stored at -80 ^{o}C until analysis prior to analyses.

Samples were reconstituted in 200 μL MeOH: H_2O (v/v, 85:15); 100 μL was diluted to 50 % MeOH (v/v) in water for non-targeted metabolomics study, followed by 30 μL pooled together from each participant as a quality

control (QC) sample; and the other 100 μL for targeted metabolomics. All samples were detected within 24 h after reconstitution.

2.2.5 Data acquisition of global metabolomics

The data was acquired from Ultimate 3000 rapid separation liquid chromatography (RSLC) coupled with Q Exactive Focus MS (Thermo Scientific, USA) for global metabolomics analysis. Acquity UPLC HSS T3 (2.1 × 100 mm, 1.8 μm, Waters) was used to separate metabolites at 30 °C. The mobile phases were water (A) and ACN (B), both with 0.1 % FA (formic acid, v/v). The injection volume was 10 μL. The LC gradient program was as follows: 0 min, 2 % B; 1 min, 2 % B; 19 min, 100 % B; 21 min, 100 % B; 21.1 min, 2 % B; 25 min, 2 % B. The flow rate was 0.3 mL/ min. The QE Focus MS was equipped with a heated electrospray ionization (HESI) source. The MS parameters were as follows. The spray voltages were 3.5 kV for positive ion mode and 3 kV for negative ion mode, respectively. The pressure of sheath and auxiliary gas was set at 45 arb and 10 arb, respectively. The temperatures of capillary and auxiliary gas were both 320 °C. The S-lens RF level was 60%. The scan range was 70-1000 (*m/z*). The resolution was 35,000. The maximum inject time (max IT) was 100 ms. Automated gain control (AGC) was set at $1\times e^6$ ions.

Data was acquired both in positive and negative ion mode. Cell samples were

analyzed at random, and the sequence was performed in a “3 samples-1 QC” order after 5 QC sample injections. The QC samples were applied for analytical quality assurance and signal correlation [130].

2.2.6 Data processing and metabolites identification of global metabolomics

The raw data of metabolic profiling acquired in UHPLC-Orbitrap-MS was firstly converted into CDF data format by using Xcalibur workstation (Thermo Scientific, USA), and metabolic features were extracted by running XCMS package under R version 3.2.2 with chromatographic alignment and matching [131]. The noise level of global metabolomics data of XCMS parameters was set at 50,000 in positive and 20,000 in negative ion mode, respectively. Subsequently, a three-dimensional csv-format document involving *m/z*, retention time (RT) and peak intensity was obtained. Next, data was filtered using “80% rule” [132], and normalized by the IS (4-chlorophenylalanine) and protein content. Finally, the data was subjected to multivariate statistical analysis by SIMCA-P 13.0 (Umetrics, Sweden) after mean-centering and scaling to the standard deviation.

The potential biomarkers were identified by comparing exact *m/z*, retention time and MS/MS pattern of samples with those of authentic standards or those in database, such as Metlin (https://metlin.scripps.edu) and

human metabolome database (HMDB, http://www.hmdb.ca) [133]. We applied 10 ppm as mass error and ± 6 s as retention time error for feature grouping and matching. Moreover, MS/MS pattern of potential biomarkers were collected at the resolution of 70,000, the isolation width of 0.6 amu, IT of 100 ms and the collision energies of 10, 20 and 30 eV. Pathway and enrichment analysis were conducted by MetaboAnalyst (http://www.metaboanalyst.ca/) [134].

2.2.7 Statistical analysis

In the global metabolomics analysis, differential metabolites between DLD1-pLKO cells and DLD1-shSLC25A22 cells were chosen by VIP (Variable importance for the projection) over than 1 in the PLS-DA (partial lease squares-discriminant analysis) model, coupled with fold change (FC) of shSLC25A22/pLKO more than 1.1 or less than 0.8 with significant differences ($p < 0.05$) in Student's *t-test*.

2.3 Results and discussion

2.3.1 *KRAS* mutant CRC cells addicted on glutamine

Because SLC25A22-encoding transporter functions as glutamate (Glu) uptake into mitochondrial, we proposed that SLC25A22 affects the mitochondrial tricarboxylic acid (TCA) cycle which is resulted from glutamate flux malfunction. It needs to confirm that whether *KRAS* mutant CRC cells are dependent on Gln.

Figure 2.2 A showed that *KRAS* mutant cells (DLD1, HCT116 and SW1116) were inhibited obviously by glutamine deprivation, while *KRAS* wild-type cells, showed relatively resistant to Gln deprivation, indicating that *KRAS* mutant cells were addicted in glutamine. Moreover, glutamate (2 mM) supplementation could partially rescue cell proliferation (upper in Figure 2.2B) and suppress apoptosis (lower in Figure 2.2 B) of *KRAS* mutant cells in the Gln-free medium. Whereas, glutamate could restore cell growth in control cells without glutamine, but not in SLC25A22-silenced cells, suggesting that SLC25A22 is required for pro-survival effect of glutamate (Figure 2.2 C).

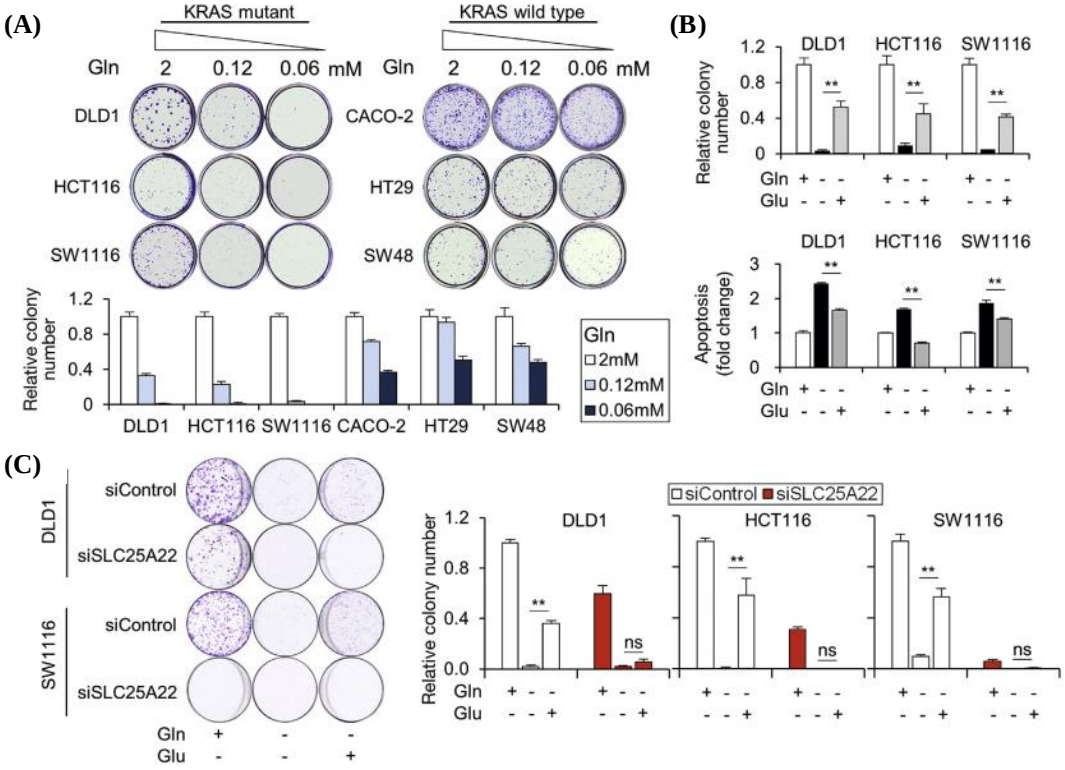

Figure 2.2 KRAS mutant CRC cells were addicted in glutamine. (A) Cell growth in different levels of glutamine (Gln) deprivation obviously inhibited KRAS mutant cell growth, but not KRAS wild-type cells. (B) Relative cell colony and apoptosis with or without supplication of Gln and Glu. (C) Cell growth of control and SLC25A22-silencing cells. (The part of work was conducted by collaborators in CUHK).

2.3.2 Statistical analysis of global metabolomics

Due to the wide dynamic range and good reproducibility, UHPLC-MS is a powerful tool for metabolomics and is capable of systematic profiling of endogenous metabolites to uncover the complex metabolic alterations that arise from gene mutation or aberrant gene expression [136, 137]. In the study, 15 pLKO and 13 shSLC25A22 cell extracts by chilled 80% MeOH were analyzed for global and targeted metabolomics analysis [138].

In the global metabolomics analysis, a total of 6,195 and 5,260 metabolic features were obtained in positive and negative ion mode, respectively (TIC was shown in Figure 2.3 A). In the score plot of PLS-DA model (Figure 2.3 B and C), pLKO samples were separated clearly from the shSLC25A22 samples, suggesting significantly changed features made great contributions to the separation.

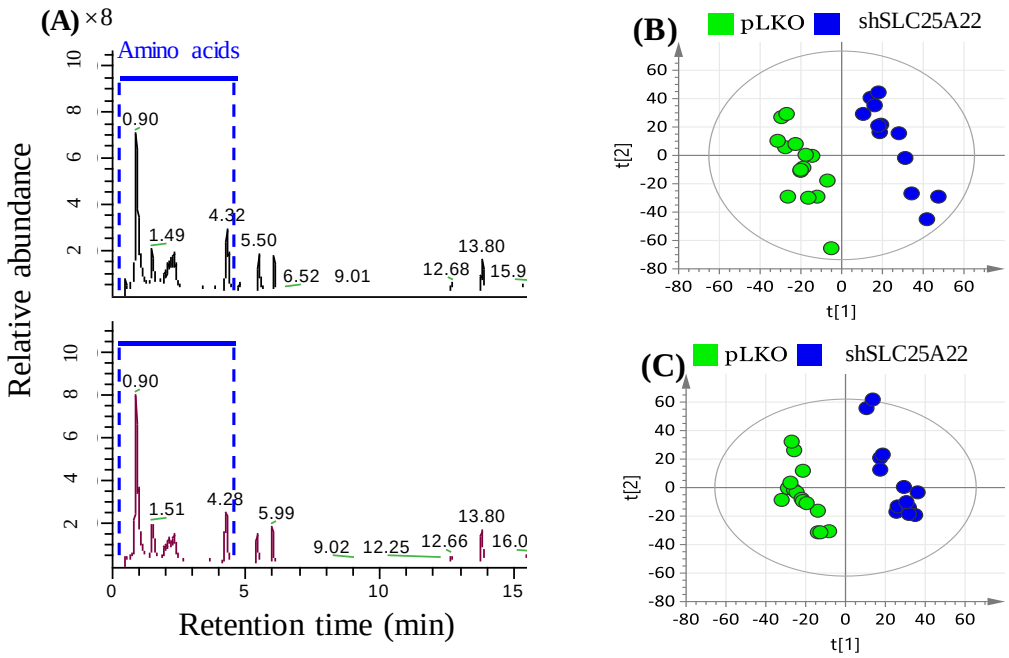

Figure 2.3 Total ion chromatography (TIC) and score plot of PLS-DA model. (A) The TIC of control (pLKO, upper) and knockdown of SLC25A22 (shSLC25A22, lower) cells in positive ion mode of UHPLC-MS. (B) and (C) Score plot in the positive and negative ion mode. [t1]: component 1, [t2]: component 2. Green dot: pLKO sample, blue dot: shSLC25A22 sample.

Among the extracted features, 267 metabolites (175 in positive and 92 in negative mode) were identified. Eventually, 35 metabolites, out of which 16 were confirmed by comparing with authentic standards, were significantly altered with FC of shSLC25A22/pLKO more than 1.1 or less than 0.8 (*t-test*: $p < 0.05$)

through volcano plot screening (Figure 2.4 A) and VIP over 1.0. In the volcano plot, the X-axis was plotted on log2 scale of FC of shSLC25A22/pLKO, while the Y-axis plotted the -log10 scale of p-value. Venn diagram (Figure 2.4 B) showed that 22 and 20 metabolites were found in positive and negative mode of LC-MS, respectively. There were 7 metabolites were simultaneously detected in two modes.

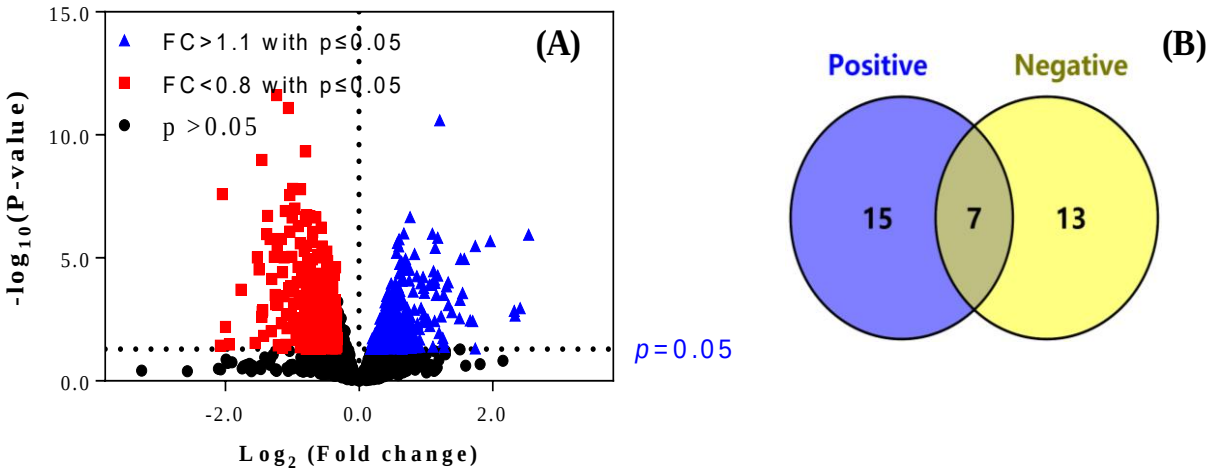

Figure 2.4 Volcano plot in positive mode and Venn diagram.

(A) Volcano plot of global metabolomics in positive mode. (B) Venn diagram of identified metabolites both in positive and negative ion mode of UHPLC-MS.

2.3.3 Differentially expressed metabolites for SLC25A22 knockdown

Overall, specific sets of metabolites were considerably altered in shSLC25A22 cells compared to pLKO cells ($p < 0.05$), such as amino acids, nucleotides, carnitines, lipids, fatty acids, and their derivatives (Table 2.1). The heatmap of top changed 15 metabolites was shown in Figure 2.5. The fold change between shSLC25A22 and pLKO of glutamine and glutamate were 1.33 ($p = 2.6\ e^{-5}$) and 1.29 ($p = 1.1\ e^{-4}$), while the FC of Asp and *N*-acetyl-aspartic acid (Ac-Asp) were of 0.55 ($p = 2.4\ e^{-8}$) and 0.71 ($p = 5.7\ e^{-13}$), suggesting reduced metabolism of Gln and Glu to Asp. As an essential precursor amino acid, Gln can support cancer proliferation [91]. Furthermore, Asp-derived metabolites, particularly asparagine (Asn) and alanine (Ala), were down-regulated in SLC25A22-silenced cells (asparagine, FC = 0.79, $p = 9.8\ e^{-5}$; alanine, FC = 0.75, $p = 4.2\ e^{-9}$) as compared to DLD1-pLKO cells.

In previous reports, some metabolites such as TCA cycle and urea cycle intermediates, nucleotides were found to be up-regulated in CRC patients [77, 85]. Notably, specific amino acids were differentially regulated in colorectal tissues of cancer patients. Alanine, asparagine, glycine, proline and serine were up-regulated, whilst glutamine and glutamate were down-regulated in CRC compared with healthy controls [86, 139]. Alanine was reported to function as alterative carbon

source that fuels tumor metabolism [140]. Moreover, alanine secretion and aspartate could promote pancreatic stellate cell proliferation through autophagy [140] and mitochondrial electron transport chain (ETC) [141]. Asparagine was found to be up-regulated in *KRAS*-mutant CRC via the overexpression of asparagine synthetase (ANSN) and it promotes protein biosynthesis in cancer cells by serving as an amino acid exchange factor regulating the uptake of amino acid and cell proliferation [142, 143]. Consistent with the oncogenic function of SLC25A22 in CRC, knockdown of SLC25A22 down-regulated the biosynthesis of TCA cycle metabolites and up-regulated Asp-derived amino acids (alanine, asparagine and glycine) in CRC, which in turn, impair *KRAS*-mutant CRC cell growth.

Of note, AICAR (5-aminoimidazole-4-carboxyamide ribonucleoside) with the largest FC of 2.8 (p = 1.7 e^{-6}) is an activator of AMP-activated protein kinase (AMPK) pathway, which inhibits cancer cell growth [144, 145]. Importantly, N^1, N^{12}-diacetylsmpermine (DAS) was reduced in SLC25A22 knockdown cells (FC =0.76, p =2.4e^{-2}). Johnson *et al*. found that polyamines, especially DAS as an end-product of polyamine metabolism, was strongly up-regulated in CRC tumor tissues compared to adjacent normal tissues using metabolomics approaches [127].

Here, our global metabolomics analysis showed that DAS was reduced in SLC25A22 knockdown CRC cells.

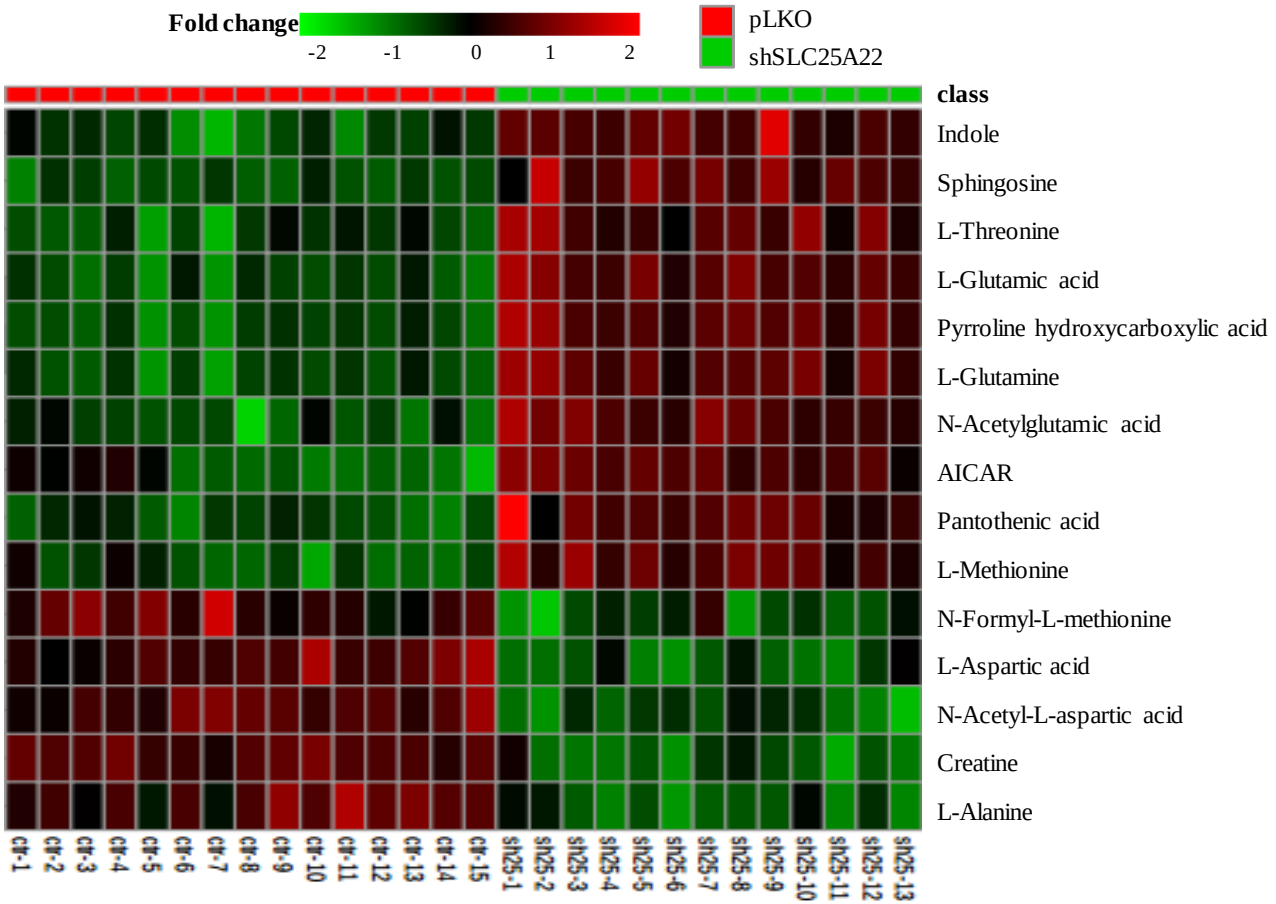

Figure 2.5 Heatmap of the top 15 significantly changed metabolites in the shSLC25A22-silencing cells. The X-axis (column) is sample (ctr: control cell, sh25: shRNA25A22-knockdown cell, the Y-axis is metabolite.

Table 2.1 List of identified metabolites changed significantly between shSLC25A22 and pLKO cell (in the order of descending fold change).

No.	Compound name	m/z	RT/min	FC(s/p)[a]	*P*-value	MS Pattern	*Δppm*	Mode	Classes
1	AICAR	339.0680	1.51	2.82	1.7E-06	110.0352, 97.0283, 127.0614,206.0568	6.0	+/-	Nucleotides and derivatives
2	*N*-Acetylglutamic acid	190.0699	2.09	1.60	9.9E-06	190.0710, 172.0600, 130.0500	5.8	+/-	AAs and derivatives[b]
3	Sphingosine	300.2879	13.38	1.54	2.4E-06	282.2783, 252.2679, 56.0497,69.0698	5.9	+	Glycosphingolipids
4	Glutamine*	147.0756	0.90	1.33	2.6E-05	147.0762, 130.0495, 84.0448, 56.0500	5.5	+	AAs and derivatives
5	Pyrroline hydroxycarboxylic acid	130.0492	0.91	1.31	9.2E-05	84.0447, 130.0493, 56.0505	5.2	+	AAs and derivatives

6	Glutamic acid*	148.0595	0.92	1.29	1.1E-04	84.0446, 102.0547, 130.0497, 148.0600	6.3	+	AAs and derivatives
7	Glutathione*	308.0891	1.58	1.22	1.6E-02	308.0934, 233.0610, 162.0235, 76.0238	6.4	+/-	Peptides
8	Indole	118.0644	6.05	1.21	6.9E-04	118.0648, 91.0540, 65.0386	6.0	+	AAs and derivative
9	Threonine*	120.0649	0.91	1.17	3.6E-02	56.0497, 74.0599, 102.0547, 120.0653	5.5	+	AAs and derivatives
10	Glycerophosphocholine	258.1086	0.91	1.15	1.4E-02	104.1067, 124.9995, 184.0729 86.0962	5.8	+	Glycerophosphocholines
11	Methionine*	150.0575	1.53	1.13	1.1E-02	150.0574, 133.0314, 104.0528, 61.0113	5.5	+	AAs and derivatives
12	Pantothenic acid*	220.1167	4.79	1.10	3.2E-02	90.0548, 220.1175, 202.1069,	5.9	+/-	Vitamins

						184.0964, 72.0443			
13	Creatine*	132.0760	0.95	0.80	0.7E-4	132.0768, 90.0555, 87.0557	5.6	+/-	Carboxylic acids
14	Butyrylcarnitine	232.1530	5.00	0.79	3.5E-03	232.1565, 173.0821, 85.0295	5.7	+	Carnitines
15	Asparagine*	133.0599	0.90	0.79	9.8E-05	133.0602, 87.0551, 74.0242, 70.0293	6.8	+	AAs and derivatives
16	Histidine*	154.0612	0.86	0.78	1.2E-04	154.0613, 93.0446, 137.0346, 110.0711	6.5	-	AAs and derivatives
17	Gamma-glutamyl-L-leucine	261.1430	5.56	0.78	8.2E-07	261.1450,198.1120, 132.1020, 86.0964	5.9	+	AAs and derivatives
18	Xanthine	151.0252	2.04	0.78	1.2E-02	151.0250, 108.0199	6.4	-	Xanthines
19	ADP*	426.0227	1.48	0.78	7.3E-03	426.0227, 158.9245, 78.9575, 134.0462, 328.0456, 272.9573	1.4	-	Nucleotides and derivatives
20	Tyrosine*	180.0659	4.28	0.77	5.0E-08	119.0490, 180.0659, 136.0757,	3.9	-	AAs and derivatives

						163.0391, 93.0332			
21	Phenylalanine*	164.0706	4.28	0.77	7.0E-08	147.0442, 164.0707, 72.0080	6.9	-	AAs and derivatives
22	*N*-Acetyl-L-methionine	190.0538	5.68	0.77	1.7E-06	148.0428, 142.0499, 190.0537, 84.0441, 98.0599	2.7	-	AAs and derivatives
23	N^{1}, N^{12}-Diacetylspermine*	287.2440	0.91	0.76	2.4E-02	100.0763, 171.1498	0.5		Polyamines
24	Gamma Glutamylglutamic acid	277.1014	1.51	0.76	5.5E-03	84.0442, 148.0600, 130.0496, 168.0651, 277.1021	5.9	+	Peptides
25	Uridine diphosphate glucose	565.0485	1.75	0.75	3.6E-02	323.0290, 565.0483, 384.9848, 241.0118, 78.9575, 96.9682	1.4	-	Nucleotides and derivatives
26	*N*-Formyl-L-methionine	176.0380	5.31	0.75	3.5E-11	98.0234, 128.0342, 176.0379, 84.0441, 70.0283	4.1	-	AAs and derivatives
27	Acetylcarnitine	204.1219	1.51	0.75	8.9E-08	85.0282, 204.1227, 60.0809,	5.5	+	Carnitines

						145.0493			
28	Alanine*	90.0545	0.90	0.75	4.2E-09	90.0544	5.3	+	AAs and derivatives
29	Oxidized glutathione*	613.1558	2.43	0.74	5.0E-02	613.1592, 538.1252, 484.1162, 355.0727, 231.0418	5.7	+/-	Oligopeptides
30	*N*-Acetyl-L-aspartic acid	174.0399	1.01	0.71	5.7E-13	88.0390, 130.0499, 58.0282, 174.0399, 156.0291	5.1	-	AAs and derivatives
31	Gamma-Glutamyltyrosine	311.1219	4.76	0.69	8.5E-08	311.1240, 248.0920, 182.0810, 136.0760	6.0	+	AAs and derivatives
32	Uridine diphosphate-*N*-acetylglucosamine	606.0754	2.67	0.69	4.7E-04	606.0750, 384.9849, 282.0388, 402.9953, 323.0287, 158.9244, 78.9574	1.8	-	Nucleotides and derivatives
33	Aspartic acid*	132.0291	0.90	0.55	2.4E-08	132.0291, 115.0025, 88.0399,	8.7	-	AAs and derivatives

						71.0136			
34	Taurine	126.0213	0.91	0.49	1.9E-06	126.0214, 108.0109	5.4	+/-	Primary amines
35	3-Sulfinoalanine	152.0013	0.92	0.48	1.9E-03	88.0390, 152.0017	6.7	-	AAs and derivatives

Notes:

a FC (s/p) represents fold change between shSLC25A22 and pLKO cells.

b AAs and derivatives represent amino acids and their derivatives.

* Represents the metabolite was identified by authentic standard and database, while the unmarked metabolite was identified by database.

2.3.4 Pathway analysis and enrichment analysis of altered metabolites

In the plot of pathway analysis, the larger and darker bubble represents the more significant metabolism. The Pathway analysis of altered metabolites in SLC25A22 knockdown CRC cells compared with control CRC cells uncovered significantly altered metabolites, including Gln, Glu, Ac-Asp, aAsp, Asn and Ala, are involved in the alanine, aspartate and glutamate pathway with pathway impact over than 0.6 (Figure 2.6 A). Additionally, enrichment analysis further demonstrated that altered metabolites were involved in protein synthesis, ammonia recycling, urea cycle, glutamate metabolism, glutathione metabolism and aspartate metabolism (Figure 2.6 B), which further confirmed the significant importance of alanine, aspartate and glutamate metabolism, as well as ammonia metabolism to conduct on the targeted analysis.

The overview of alanine, aspartate and glutamate and ammonia pathway was shown in Figure 2.7. Alanine, aspartate and glutamate metabolism is a part of glutaminolysis, which has been reported as a target for cancer therapy [146]. The alanine, aspartate and glutamate pathway highlighted in green catabolizes glutamine to generate derived amino acids, such as alanine and aspartate (Figure 2.7). Glutamine is taken up by the cells and is converted into glutamate by removing one molecular ammonia. Then glutamate passes through mitochondria via the SLC25A22-encoding glutamate transporter, transforms into α-KG to enter the TCA cycle, generating OAA, aspartate, alanine and asparagine, which could promote cell proliferation. The

pathway highlighted in blue is ammonia metabolism, which includes urea cycle, polyamines biosynthesis and certain amino acids (e.g. aspartate and asparagine). Urea cycle and polyamines are linked by ornithine, which is generated in mitochondria. Polyamines are required for growth of normal and cancer cells, and their levels are frequently up-regulated in carcinogenesis [147, 148].

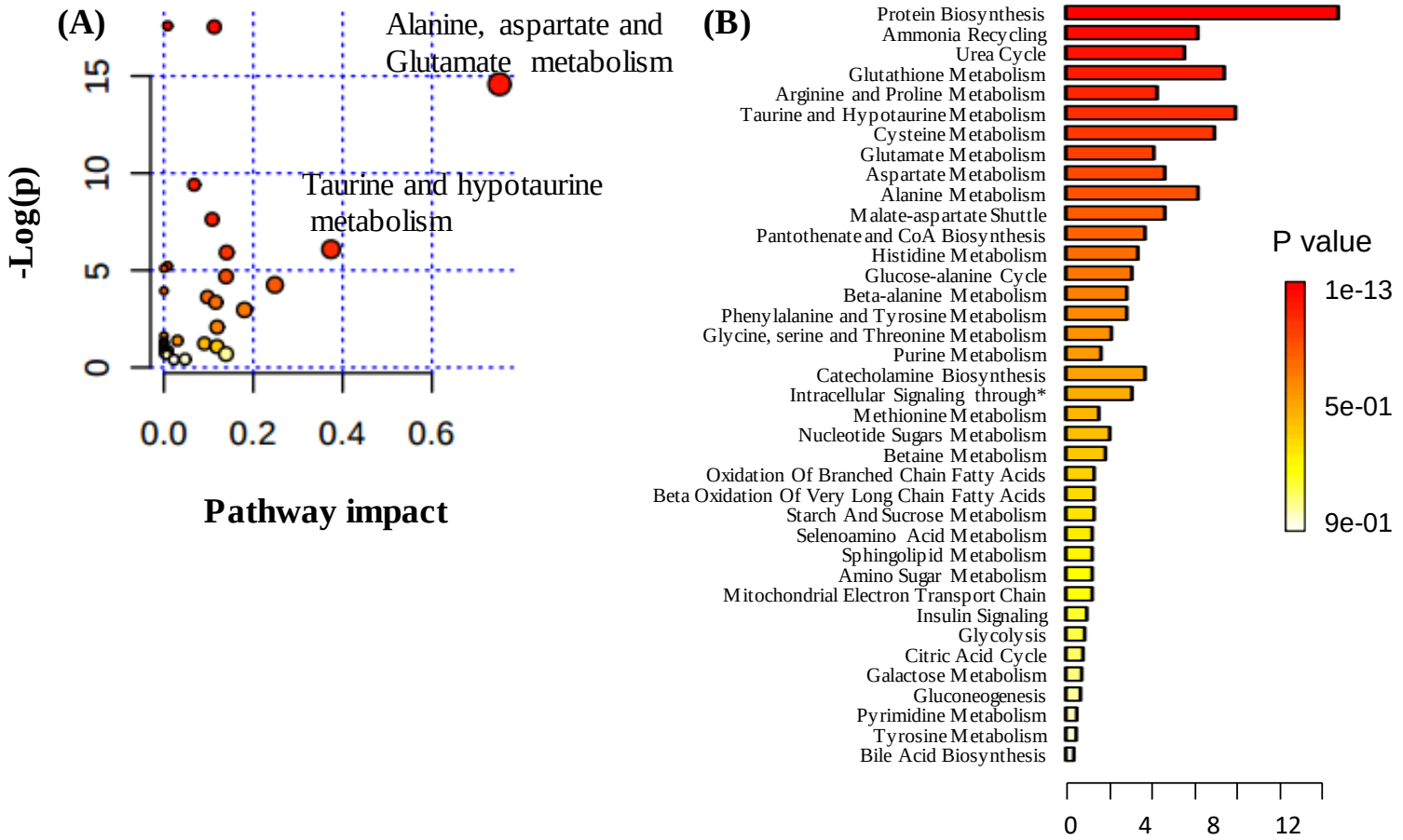

Figure 2.6 (A) Plot of pathway analysis and (B) enrichment analysis.

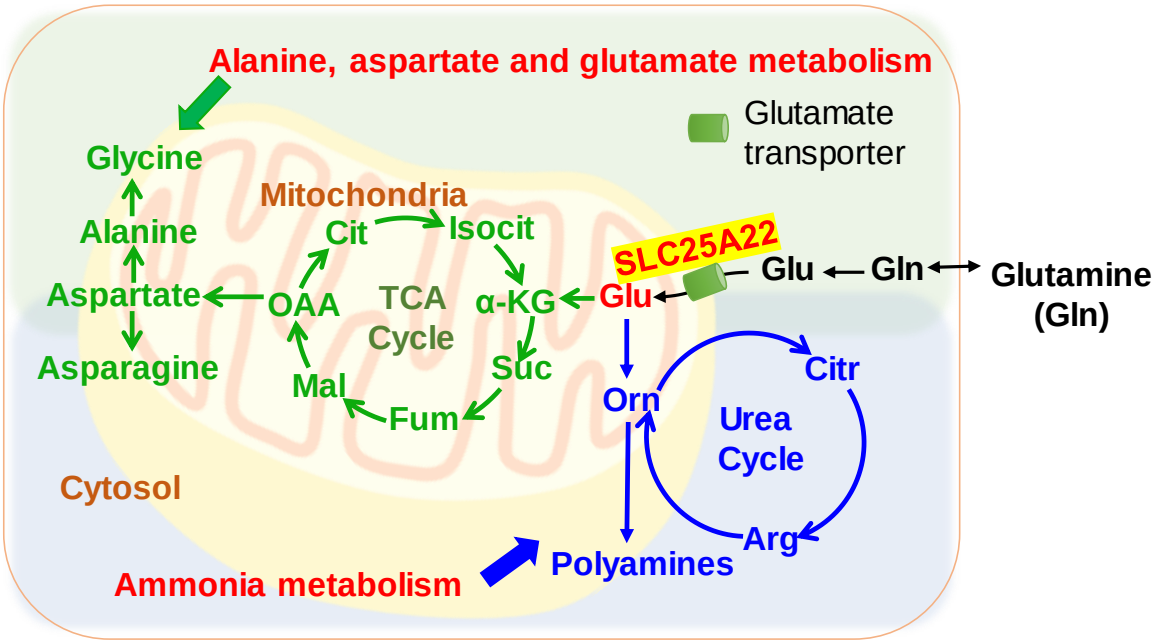

Figure 2.7 Overview of two important pathway due to SLC25A22 knockdown.

Green represented alanine, aspartate and glutamate pathway, blue represented ammonia metabolism, including urea cycle and polyamine metabolism. Glu, glutamate; TCA, tricar-boxylic acid; α-KG, α-keto-glutarate; Suc: succinate; Fum，fumarate; Mal, malate; OAA, oxaloacetate; Cit, citrate; Isocit, isocitrate; Citr, citrulline; Orn, ornithine; Arg, arginine.

2.4 Chapter summary

Cell colony and apoptosis results showed that *KRAS* mutant cells (DLD1, HCT116 and SW1116) were addicted on Gln, even Glu could partially restore cell proliferation and suppress apoptosis. On the basis of LC-MS platform, global metabolomics analysis of shSLC25A22 cells and pLKO cells uncovered significantly

altered metabolites were attributed to the two metabolism (1) alanine, aspartate and glutamate pathway and (2) ammonia metabolism (including urea cycle and polyamines metabolism). In knockdown of SLC25A22 cells, Gln-related amino acids were altered, presenting increased Glu but decreased Asp, Asn and Ala. Methionine, *N*-acetyl-methionine and DAS attributing to ammonia metabolism were perturbed significantly owing to knockdown of SLC25A22. Therefore, to confirm the alteration and source of metabolites, the targeted metabolomics analysis and kinetic isotope analysis, focusing on TCA cycle intermediates, amino acids and polyamines, were conducted by liquid-chromatography coupled with triple-quadrupole mass spectrometer (LC-QqQ MS), which could help better to trace fates of metabolic features caused by overexpression of SLC25A22.

*This Chapter was mainly from my published papers where I am the first and third author as follows:

1. **Li X**, Wong CC*, Cai Z*, *et al.* LC-MS-based metabolomics revealed SLC25A22 as an essential regulator of aspartate-derived amino acids and polyamines in *KRAS*-mutant colorectal cancer. Oncotarget. 2017, 8(60): 101333–101344

2. Wong CC, Qian Y, **Li X**, et al. SLC25A22 Promotes Proliferation and Survival of Colorectal Cancer Cells With KRAS Mutations and Xenograft Tumor Progression in Mice via Intracellular Synthesis of Aspartate. Gastroenterology.2016, 151 (5): 945-960.e6

Chapter 3 Targeted Metabolomics Revealed SLC25A22 as Essential Regulator of TCA Cycle, Aspartate-derived Amino Acids and Polyamines in KRAS-mutant Colorectal Cancer

3.1 Introduction

Based on metabolic profiling of shSLC25A22 cells and pLKO cells, the alanine, aspartate and glutamate metabolism and ammonia metabolism (urea cycle and polyamine) were changed significantly due to knockdown of SLC25A22 of KRAS mutant CRC cells. Therefore, we focus on figuring out alterations of more metabolites in the above-mentioned metabolism by using LC-QqQ MS-based targeted metabolomics, including TCA cycle intermediates, glutamine-derived amino acids, urea cycle intermediates and polyamines. Moreover, the metabolite fates of TCA cycle and derived amino acids, urea cycle intermediates and polyamines were traced via targeted kinetic analysis of DLD1 cells with *KRAS*-mutation using [U-$^{13}C_5$]-glutamine as the isotope tracer. The workflow was shown in Figure 3.1.

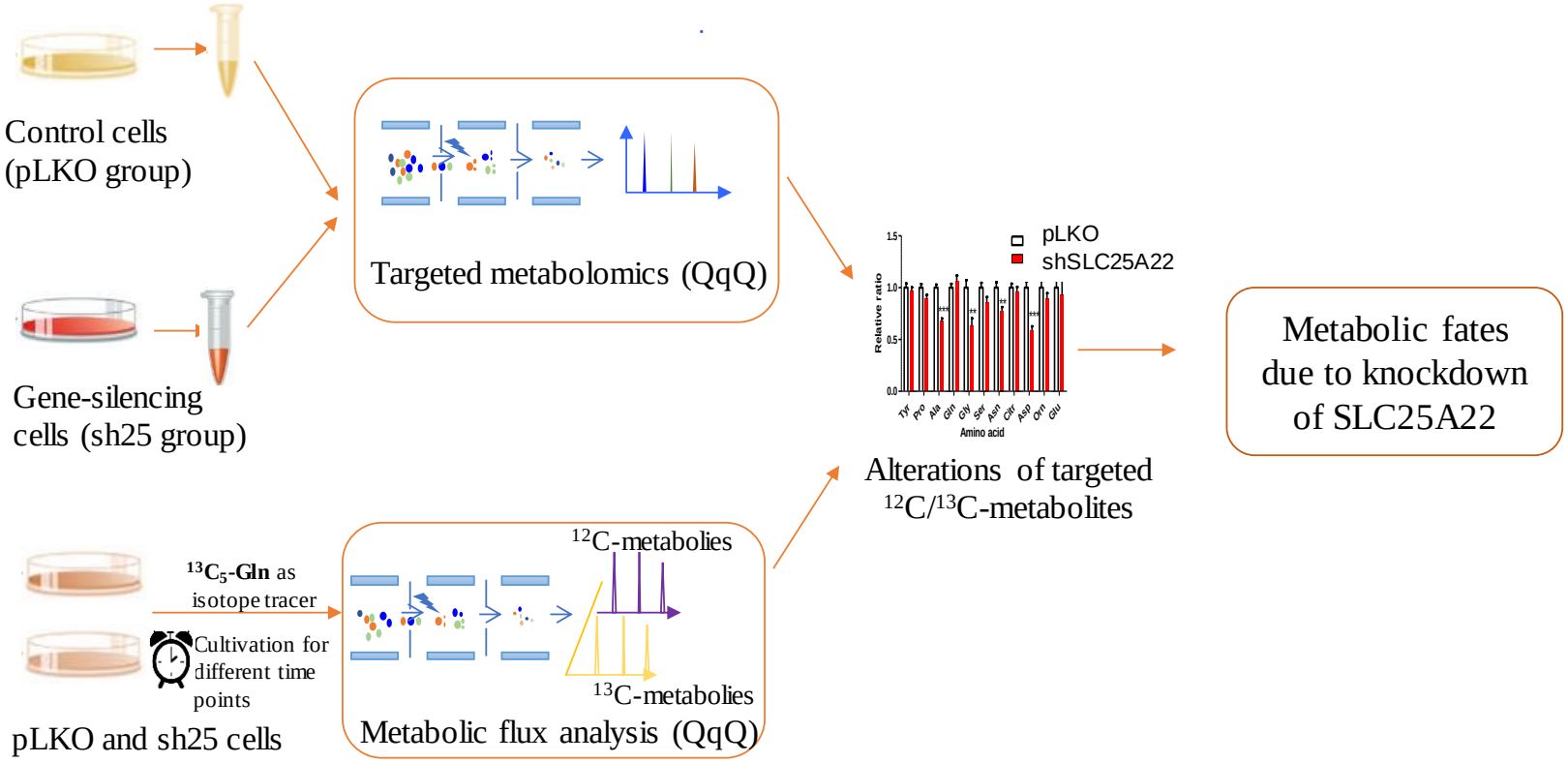

Figure 3.1 Workflow of targeted metabolomics and kinetic metabolomics analysis based on LC-QqQ MS.

3.2 Materials and methods

3.2.1 Chemicals and reagents

Pure water was prepared by Milli-Q system (Millipore, USA). Methanol (MeOH), acetonitrile (ACN), formic acid (FA), ammonium hydroxide and ammonium acetate were of LC grade. All standards of (D/L-) amino acids, TCA cycle intermediates, including citrate (Cit), isocitrate (Isocit), α-ketoglutarate (α-KG), succinate (Suc), fumarate (Fum), oxaloacetate (OAA); polyamines including putrescine (Put), spermidine (Spd), spermine (Spm), N^1-acetylputrescine (Ac-Put) and N^1-acetylspermidine (Ac-Spd) were purchased from Sigma (St. Louis, US). N^1-acetylspermine (Ac-Put), N^1, N^{12}-diacetylspermine (DAS) were ordered from Cayman (MI, US). [U-$^{13}C_5$]-glutamine was obtained from Cambridge isotope laboratory (MA, US).

3.2.2 Cell culture for isotope analysis

The process of cell culture was similar to 2.2.2. For targeted kinetic isotope analysis of TCA cycle intermediates, DLD1-pLKO, DLD1-siSLC25A22 (transiently expressing) and DLD1-shSLC25A22 (stable expressing) cell lines were seeded at a density of 5×10^6 cells/10 cm dish in complete DMEM medium in triplicates. After 24 h, the media were replaced with glutamine-free MEM consisting of 4 mM [$^{13}C_5$]-glutamine. The cells were harvested at the following time points: 0 h, 0.5 h, 1 h and 2 h. Besides, GOT1 (ID: s5954 and s5955) siRNA were purchased from Thermo

Fisher Scientific (Waltham, MA). The culture of knockdown of GOT1 cells and control cells were same to pLKO and shSLC25A22, and the cells were harvested at the time points of 0 h, 0.5 h, 1h and 2 h.For targeted kinetic isotope analysis of polyamine and urea cycle intermediates, DLD1-pLKO and DLD1-shSLC25A22 cell lines were seeded at a density of 2×106 cells/10 cm dish in complete DMEM medium in triplicates. After 24 h, the media were replaced with glutamine-free MEM consisting of 2 mM [$^{13}C_5$]-glutamine. The cells were harvested at the following time points: 0 h, 2 h, 4 h, 8 h, 16 h and 24 h.

3.2.3 Sample preparation

Sample preparation of non-targeted metabolomics was also used for targeted metabolomics analysis (part 2.2.4), while the sample preparation of kinetic isotope analysis was same to part 2.2.4One microliter of cell culture media was collected for lyophilization, the residues were precipitated by 4 mL chilled MeOH and centrifuged. The supernatant was dried again and stored at -80 ℃ until analysis. The residue was re-constituted in 85% ACN for native and ^{13}C-labeled polyamine analysis.

3.2.4 Data acquisition of targeted metabolomics and kinetic isotope analysis using LC-QqQ MS

Targeted metabolomics of label-free metabolites and kinetic isotope analysis were performed by Ultimate 3000 RSLC coupled to Quantiva^{TM} triple-quadrupole MS (QqQ, Thermo Scientific, USA). The Xbridge BEH Amide column (2.1 × 100 mm, 1.8 μm, Waters) was used for metabolites separation at 30 °C. The mobile phases

used for the separation of related amino acids and polyamines were water (A) and ACN (B) both containing 0.1% FA, while for the TCA cycle intermediates were water/ACN (A, v/v, 95:5, pH 9.45) containing 20 mM ammonium acetate and 20 mM ammonium hydroxide and acetonitrile (B). The flow rate was 0.3 mL/min. The LC gradient program was as follows: 0 min, 85 % B; 12 min, 55 % B; 14 min, 20 % B; 16 min, 20 % B; 16.5 min, 85 % B; 22 min, 85 % B. The TSQ MS was also equipped with a heated electrospray ionization (HESI) source. The spray voltages were of 3.5 kV and 3 kV in positive and negative ion mode, respectively. The pressure of sheath and auxiliary gas was set at 30 arb and 10 arb. The temperature of capillary and auxiliary gas was 320 °C and 320 °C. The S-lens RF level was 60 %. The CID gas was set at 1.5 mTorr.

Selected monitoring reaction (SRM) mode was utilized for data acquisition of targeted metabolomics and kinetic metabolic analysis. The SRM transitions were listed in Table 3.1 and Table 3.2, respectively. The targeted metabolomics included TCA cycle intermediates, Glu-derived amino acids, urea cycle intermediates and polyamines. Among them, amino acids, urea cycle intermediates and polyamines were analyzed in positive ion mode, while the TCA cycle intermediates were in negative ion mode. The analytes separation was performed in segments to increase the sensitivity.

Table 3.1 SRM transitions of TCA cycle intermediates, polyamines and related amino acids in targeted metabolomics analysis by using LC-QqQ MS.

	Metabolite	Abbreviation	Polarity	Precursor Ion	Product Ion	CE[a] (V)
	Citrate	Cit	Negative	191	87	25
	Isocitrate	Isocit	Negative	191	73	25
	α-ketoglutarate	α-KG	Negative	145	101	8
TCA cycle	Succinate	Suc	Negative	117	73	15
Intermediates	Fumarate	Fum	Negative	115	71	10
	Malate	Mal	Negative	133	115	12
	Oxaloacetate	OAA	Negative	131	87	15
	4-Cl-Phenylalanine	IS[b]	Negative	198	181	15
	Glutamate	Glu	Positive	148	84	15
	Glutamine	Gln	Positive	147	84	10
	Aspartate	Asp	Negative	132	88	15
Related	Asparagine	Asn	Positive	133	74	15
amino acids	Alanine	Ala	Positive	90	44.3	10
	Proline	Pro	Positive	116	70	18
	Ornithine	Orn	Positive	133	70	20
	Citrulline	Citr	Positive	176	70	10

	Arginine	Arg	Positive	175	70	15
	Putrescine	Put	Positive	89.1	72.1	12
	N^1-Acetylputrescine	AcPut	Positive	131.1	114.2	12
	N^1-Acetylputrescine	AcPut	Positive	131.1	72.1	18
	Spermidine	Spd	Positive	146.1	72.1	15
	Spermidine-2	Spd	Positive	146.1	112.1	15
	N^1-Acetylspermidine	AcSpd	Positive	188.2	72.1	20
Polyamines	N^1-Acetylspermidine-2	AcSpd	Positive	188.2	100.1	18
	Spermine	Spm	Positive	203.2	112.1	20
	Spermine-2	Spm	Positive	203.2	129.1	12
	N^1-Acetylspermine	AcSpm	Positive	245.2	129.2	15
	N^1-Acetylspermine-2	AcSpm	Positive	245.2	112.2	20
	N^1,N^{12}-diacetylspermine	DAS	Positive	287.2	100.1	25
	N^1,N^{12}-diacetylspermine-2	DAS	Positive	287.2	171.2	18
	4-Cl-Phenylalanine[b]	IS	Positive	200	154	15

Note: [a] represents collision energy, [b] represents internal standard.

Table 3.2 SRM transitions of TCA cycle intermediates, polyamines and amino acids in metabolic kinetic analysis by using LC-QqQ MS.

Class	Metabolite	Polarity	Precursor Ion	Product Ion	CE (V)
TCA cycle inter-mediates	α-KG	Negative	145	101	8
	$^{13}C_5$-α-KG	Negative	150	105	8
	Suc	Negative	117	73	15
	$^{13}C_4$-Suc	Negative	121	76	15
	Fum	Negative	115	71	10
	$^{13}C_4$-Fum	Negative	119	74	10
	Mal	Negative	133	115	12
	$^{13}C_4$- Mal	Negative	137	119	12
	OAA	Negative	131	87	15
	$^{13}C_4$- OAA	Negative	135	90	10
	Cit	Negative	191	87	25
	$^{13}C_4$- Cit	Negative	195	91	25
	Isocit	Negative	191	73	25
	$^{13}C_4$-Isocit	Negative	195	76	25
	4-Cl-Phenylalanine	Negative	198	181	15
Related amino acids	Gln	Positive	147	84	20
	$^{13}C_5$-Gln	Positive	152	88	20
	Glu	Positive	148	84	15

	$^{13}C_5$-Glu	Positive	153	88	15
	Asp	Positive	134	74	15
	$^{13}C_4$-Asp	Positive	138	76	15
	Asn	Positive	133	74.2	15
	$^{13}C_4$-Asn	Positive	137	76	15
	Ala	Positive	90	44.3	10
	$^{13}C_3$-Ala	Positive	93	46.3	10
	Pro	Positive	116	70	18
	$^{13}C_5$-Pro	Positive	121	74	18
Urea cycle amino acids	Orn	Positive	133.1	70	20
	$^{13}C_5$-Orn	Positive	138	74	20
	Arg	Positive	175	70.2	15
	$^{13}C_5$-Arg	Positive	180	74	15
	Citr	Positive	176	159.1	10
	$^{13}C_5$-Citr	Positive	181	163.1	10
	IS	Positive	200	154	15
Polyamines	Put	Positive	89.1	72.1	12
	Put-$^{13}C_4$	Positive	93.1	76.1	12
	AcPut	Positive	131.1	114.2	12
	AcPut-2	Positive	131.1	72.1	18
	AcPut-$^{13}C_4$*	Positive	135.1	118.1	12
	AcPut-$^{13}C_4$-2	Positive	135	76.1	18

Spd*	Positive	146.1	72.1	15
Spd-2	Positive	146.1	112.1	15
Spd-$^{13}C_4$*	Positive	150.1	76.1	15
Spd-$^{13}C_4$-2	Positive	150.1	116.1	15
AcSpd*	Positive	188.2	72.1	20
AcSpd-2	Positive	188.2	100.1	18
AcSpd-$^{13}C_4$*	Positive	192.2	76.1	20
AcSpd-$^{13}C_4$-2	Positive	192.2	104.1	18
Spm*	Positive	203.2	112.1	20
Spm-2	Positive	203.2	129.1	12
Spm-$^{13}C_4$*	Positive	207.2	116.1	20
Spm-$^{13}C_4$-2	Positive	207.2	133.1	12
AcSpm*	Positive	245.2	112.2	20
AcSpm-2	Positive	245.2	129.2	15
AcSpm-$^{13}C_4$*	Positive	249.2	116.2	20
AcSpm-$^{13}C_4$	Positive	249.2	133.2	15
DAS*	Positive	287.2	100.1	25
DAS-2	Positive	287.2	171.2	18
DAS-$^{13}C_4$*	Positive	291.2	104.1	25
DAS-$^{13}C_4$-2	Positive	291.2	175.2	18

Notes: [a] represents collision energy, * represented quantitative transition.

3.2.5 Statistical analysis

For analysis of cell samples, the peak area of each SRM transition was integrated and normalized by IS and total protein content. The peak areas of ^{13}C-metabolites generated from ^{13}C-Gln (authentic ^{13}C-metabolites) were obtained by deducting the peak areas of native ^{13}C-labeled analytes from detected ^{13}C-metabolites; while the native ^{13}C-labeled analytes were calculated form the peak areas of ^{12}C-metabolites according to the ratio of ^{13}C in native ^{12}C (1.1 %) and number of ^{13}C-labeled carbon (N). The following formula was used to calculate the peak area of ^{13}C-metabolits: $A_{\text{authentic } ^{13}\text{C-metabolites}} = A_{\text{detected } ^{13}\text{C-metabolites}} - 1.1\ \%\ N * A_{^{12}\text{C-metabolites}}$. Relative or absolute intensities of metabolites between DLD1 control and SLC25A22 knockdown cells were obtained to reveal the alterations of targeted metabolites. The relative ratios of shSLC25A22 cells were conducted by setting the level of control cells as 1.

3.2.6 Western blot

Total proteins were extracted using Cytobuster™ Protein Extraction Reagent (EMD Millipore), denatured in loading buffer, and then separated by sodium dodecyl sulfate polyacrylamide gel electrophoresis (SDS-PAGE). Antibodies for ornithine decarboxylase (ODC, ab66067) and spermidine/spermine N^1-acetyl

transferase (SAT, ab105220) were obtained from Abcam (Cambridge, MA). The part of work was conducted by collaborators in CUHK.

3.2.7 3-(4,5-dimethylthiazol-2-yl)-2,5-diphenyltetrazolium bromide (MTT) assay

Cell growth curve was performed using MTT assay (Sigma-Aldrich, St. Louis, MO). Briefly, DLD1 cells were seeded into 96 well plates (1 x 10^3 cells per well) overnight, followed by the addition of polyamines for 48 h. At the end of the incubation, MTT (0.5 mg/mL) was added to the medium for 4 h, and the reaction was stopped by the addition of 0.1 N HCl in 10 % SDS. After overnight incubation, the plates are analyzed on a microplate reader (570 nm). The part of work was conducted by collaborators in CUHK.

3.3 Results and discussion

3.3.1 Optimization of LC-MS conditions

Targeted metabolites including TCA cycle intermediates, amino acids, urea cycle and polyamines with strong hydrophilic ability, performed poor retention in RP column. Thus, HILIC complementing RP, normal phase (NP) and ion chromatography (IC) was chosen for polar compounds separation. Two HILIC columns were compared in the optimization of LC separation system [64, 138, 149]. The targeted analytes showed relative broad peaks and poor separation in Luna NH_2 column (100×2 mm, 3 μm). The column was also reported shorter lifespan over than pH 9.0 [138]. Alternatively, BEH amide column was adopted to

obtain better retention and peak symmetry at pH range of 2-12 [149]. The amide-modified stationary phase of the UPLC HILIC column allowed the use of high proportion of organic mobile phase, which resulted in ideal solvent evaporation and good sensitivity in ESI-MS analysis [150]. The optimization of buffer salt concentration and LC gradient program indicated that polar analytes could be retained more strongly in higher salt concentration and lower percentage of organic mobile phase. The method could provide relative sufficient peak intensity of most amino acids, TCA cycle and polyamines intermediates with good peak shape and separation without derivatization [151, 152]. However, the HILIC method was limited in short column life [138], absolute quantification and insufficient sensitivities of several amino acids such as histidine, arginine and ornithine due to peak tailing.

The heated electrospray ionization (HESI) probe was utilized to deliver better desolvation, thus enhancing ion-transfer efficiency and detection sensitivity. To obtain high absolute abundance of precursor and product ions in triple quadrupole mass spectrometer, collision energy was optimized manually for all SRM transitions by injecting single compound via the infusion pump. The highest intensity of major product ion was chosen from intensities of different CE (Figure 3.2). Other mass spectrometric parameters, including the probe voltage, temperatures of ion transfer tube and vaporizer, flow rates of sheath gas and auxiliary gas were optimized separately by using both a mixed standard solution and the cell extract.

In the metabolite isotope analysis, the precursor and product ions of the native and ^{13}C-labeled metabolites were selected from the full scan MS analysis and parallel reaction monitoring (PRM) mode with stepped CE by using HR MS.

The example of Gln was shown in Fig. 3.3 A-D, the molecular ion (*m/z* 147.08) of Gln lost a hydroxyl and amide group and generated the main product ion *m/z* 84.04. The fragments *m/z* 130.05 and *m/z* 102.05 were formed by losing –OH and then –CO from the molecular ion of Gln. For the ^{13}C-labeled Gln, the precursor and product ions were detected as *m/z* 152.09 with 5 ^{13}C-labeled carbons and *m/z* 88.06 with 4 ^{13}C-labeled carbons, respectively.

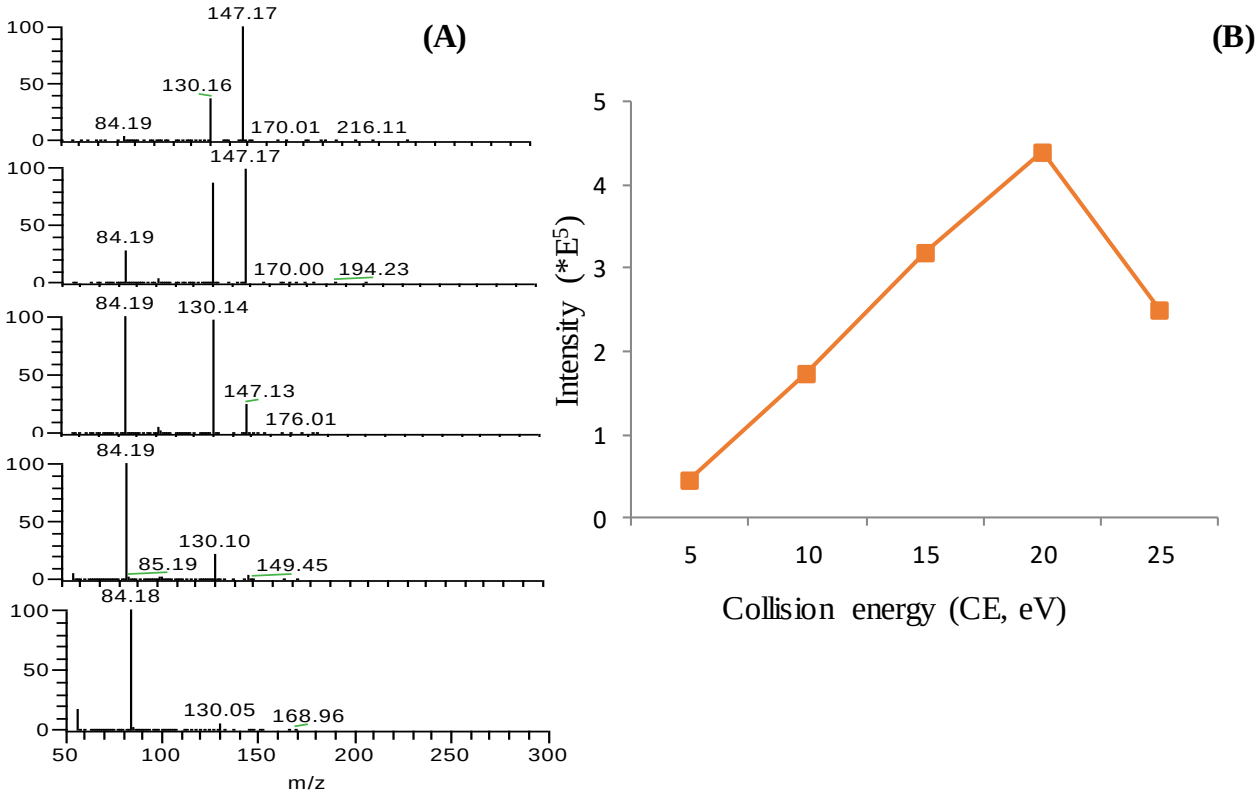

Figure 3.2. Optimization of collision energy (CE) with an example of Gln m/z 147.1. (A) Product ions of mass spectra of Gln *m/z* 147.1 generated by different CE, (B) The intensity of major fragment ion (*m/z* 84) generated with CE of 5, 10, 15, 20, 25 eV.

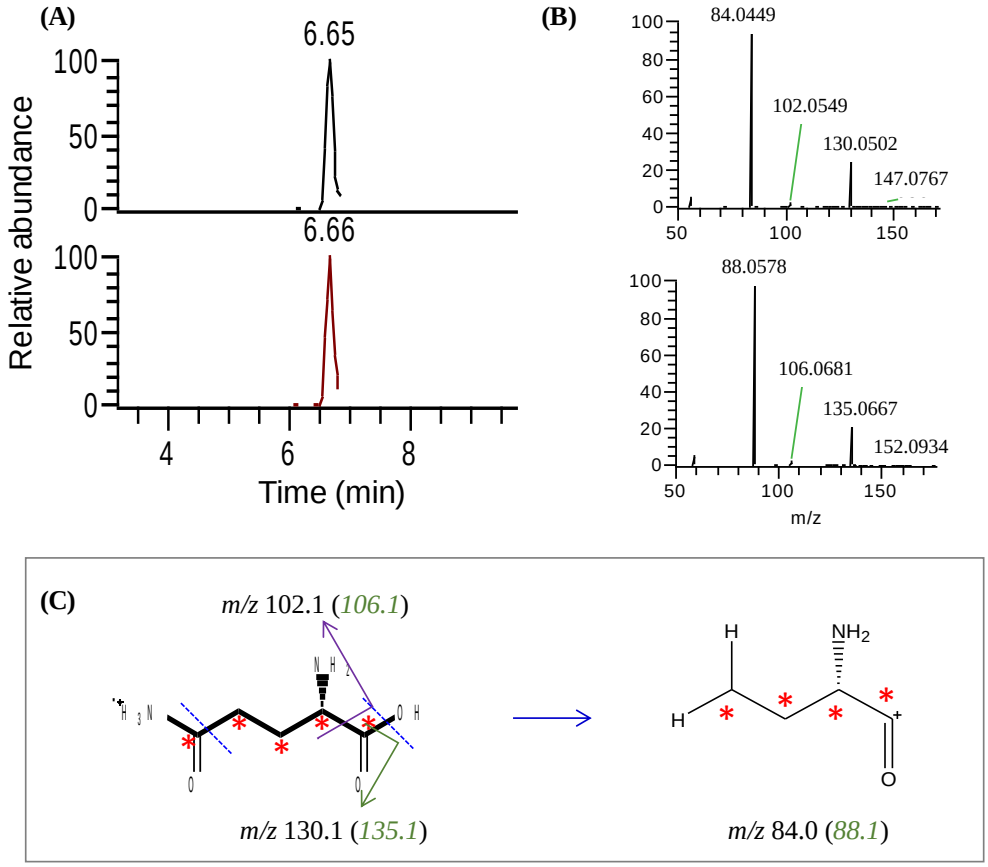

Figure 3.3 MS pattern and fragmentation of native and ^{13}C-labeled of Gln. (A) Chromatograms of native Gln (upper) and ^{13}C-Gln (lower), (B) and (C) product ions of ^{12}C-/^{13}C- Gln, (D) fragmentation pattern of $^{13}C_5$-labled-Gln, the asterisk represented ^{13}C-labeled carbon.

3.3.2 Targeted analysis of TCA cycle and derived amino acids using LC-QqQ MS

Glutamine serving as carbon and nitrogen source, can provide energy for cancer cell growth and survival through TCA cycle and nitrogen metabolism.

Glutamine metabolism starting from glutamine intake, generates aspartate and its derived amino acids (including alanine, glycine and serine) through TCA cycle, which could be metabolized to pyruvate (Figure 3.4, highlighted in green). On the other hand, glutamine could also participate in nitrogen metabolism via urea cycle and polyamine metabolism [90, 153] (Figure 3.4, highlighted in blue). In the urea cycle, ornithine is converted to citrulline in mitochondrial and both were transferred into cytoplasm. However, urea cycle is generally expressed in periportal hepatocytes, and also has been reported at a low level in enterocytes [154]. Moreover, Orn can be converted into putrescine in required of ODC. Spermidine and spermine are resulted from Put obtaining one or two propyl amine group from S-adenosylmethionine (SAM). Furthermore, the acetylated polyamines, including N^1-acetylpurtrescine (Ac-Put), N^1-acetylspermidine (Ac-Spd), N^1-acetylspermine (Ac-Spm) and N^1, N^{12}-diacetylspermine (DAS) are yielded through spermidine/spermine N^1-acetyltransferase (SAT) and pass through cell membrane to extracellular matrix. Amino acid-derived polyamines play important roles in normal and cancer cell growth. Previous studies have been proven that inhibition of polyamine synthesis is ineffective on clinical anticancer trials, but it is effective on preclinical cancer chemoprevention trials [155]. Targeted analysis was thus performed on these metabolic pathways.

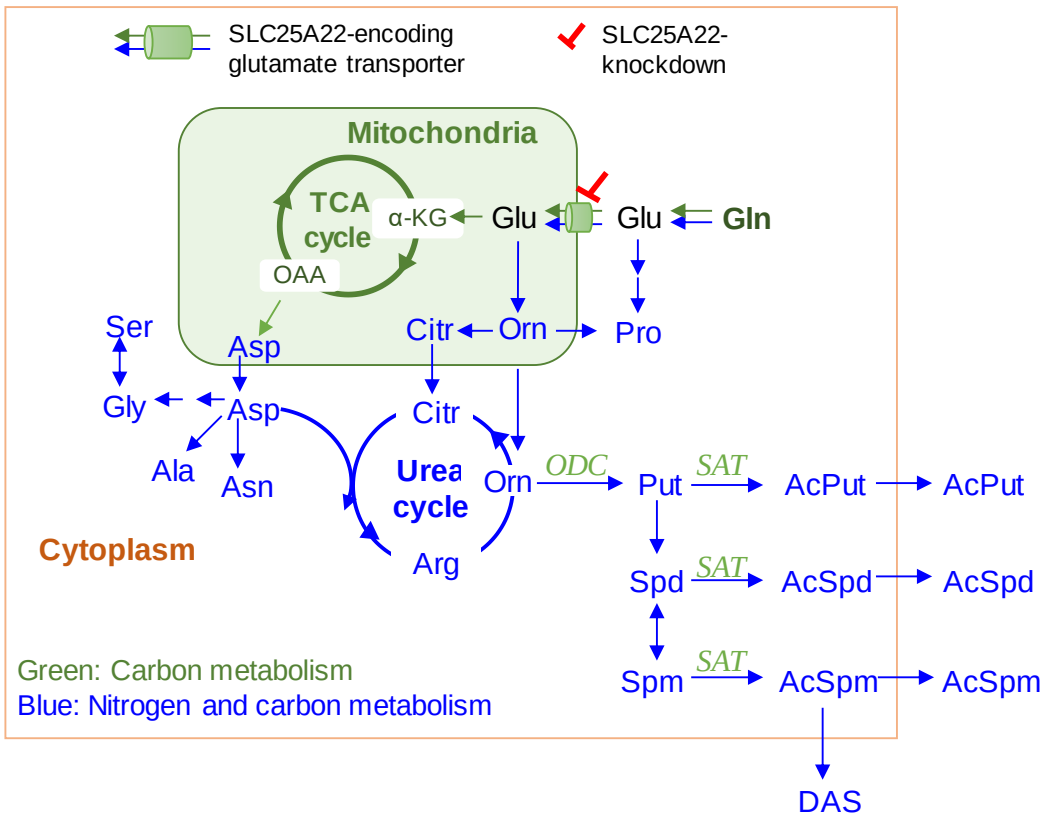

Figure 3.4 Scheme overview of glutamine metabolism, involving alanine, aspartate and glutamate metabolism (green), as well as urea cycle and polyamine metabolism (blue).

As shown in Figure 3.5 A, when the expression of SLC25A22 was knocked down in DLD1-shSLC25A22 cells, TCA cycle intermediates tended to be down-regulated, especially malate ($p < 0.05$) and fumarate ($p < 0.05$), which was in agreement with our previous study [121]. The relative ratio of aspartate was strongly reduced in shSLC25A22 cells ($p < 0.001$). Moreover, levels of alanine, asparagine and glycine as down-stream of Asp were significantly reduced in

shSLC25A22 cells, which were likely a consequence of reduced Asp levels (Figure 3.5 B). Levels of SLC25A22 expression in cells did not affect glutamine, glutamate, serine and proline differentially.

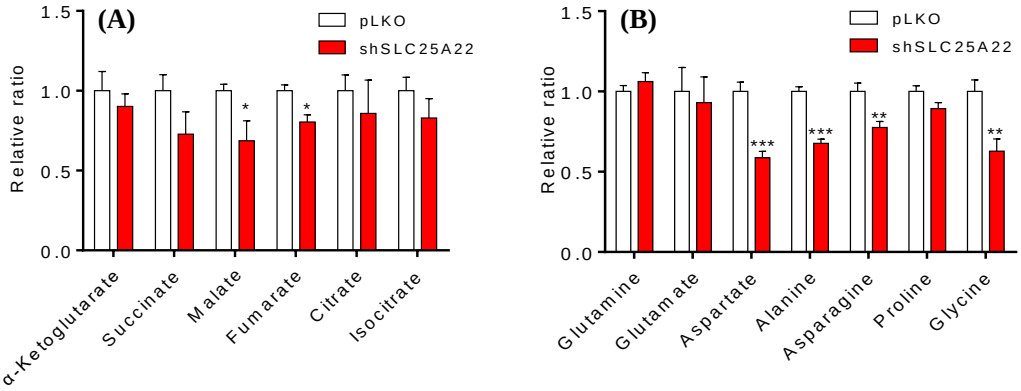

Figure 3.5 Relative ratio of (A) TCA cycle intermediates and (B) related amino acids between pLKO and shSLC25A22 cells.

3.3.3 Kinetic isotope analysis of TCA cycle intermediates and derived amino acids using [U-$^{13}C_5$]-Gln as isotope tracer

To investigate more effects of SLC25A22 on alanine, aspartate and glutamate pathway, DLD1 cells transfected with siSLC25A22 or shSLC25A22 were incubated with 2mM [U-$^{13}C_5$]-Gln for 2 hours and the intracellular metabolites were analyzed by usingLC- QqQ MS. After incubation of 2 h in siSLC25A22 and shSLC25A22 cells, the relative ratios of ^{13}C-labeled and total TCA cycle intermediates were significantly decreased in comparison with pLKO

cells, especially succinate, fumarate and malate (p <0.05) (shown in Figure 3.6). Whilst, $^{13}C_5$-glutamine, $^{13}C_5$-glutamate and $^{13}C_5$-α-KG were altered without significant differences, indicating the metabolites were not affected by knockdown of SLC25A22. α-Ketoglutarate can be generated from glutamate via transaminases that are present in the cytosol (GOT1/PSAT1); whereas α-ketoglutarate–succinate conversion proceeds in the mitochondria via 2 steps. As SLC25A22 knockdown only inhibited glutamate transport into mitochondria, it will not affect α-ketoglutarate synthesis in cytosol. Mitochondria-dependent formation of succinate and downstream metabolites from α-ketoglutarate were reduced by SLC25A22 knockdown, consistent with its role in inhibiting alanine, aspartate and glutamate pathway. Moreover, the down-regulation of OAA (p < 0.01) and OAA-derived $^{13}C_4$-aspartate (p < 0.01) were observed in SLC25A22 silencing cells (Figure 3.6). Moreover, the incorporation of U-$^{13}C_5$-Gln into nonessential amino acid was traced, then found that $^{13}C_4$-asparagine (p < 0.01) was down-regulated in shSLC25A22 cells. Because $^{13}C_4$-aspartate is mainly derived from $^{13}C_5$-Gln through TCA cycle, indicating that SLC25A22 knockdown impairs alanine, aspartate and glutamate pathway.

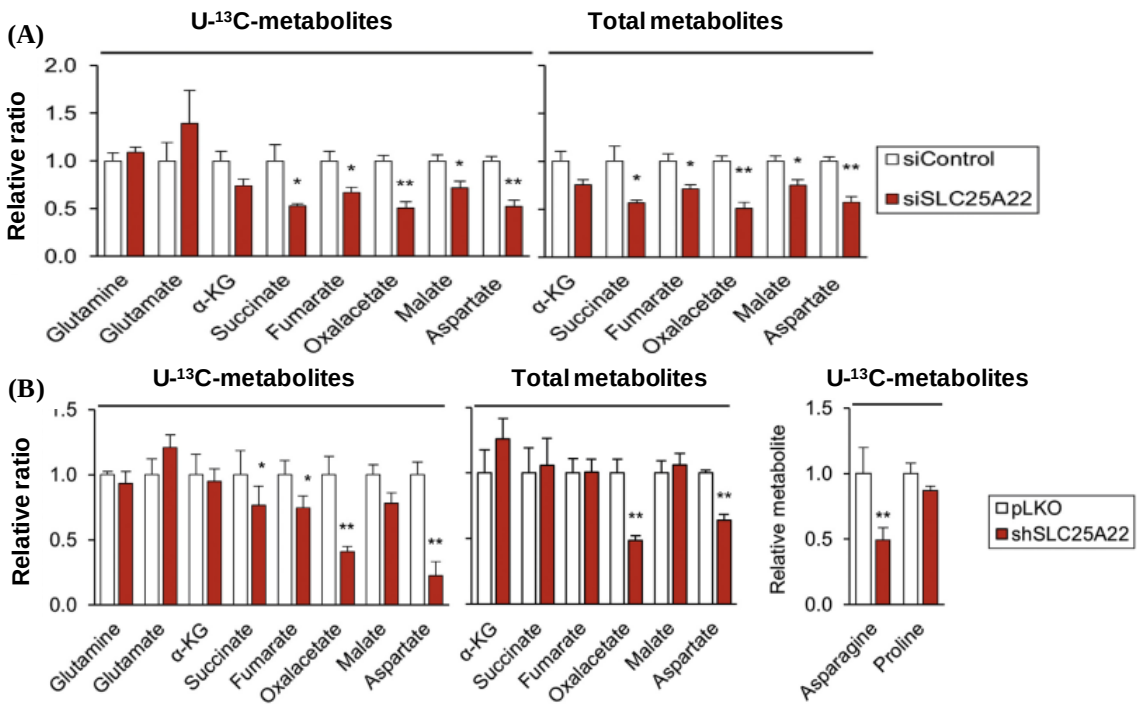

Figure 3.6 Relative ratio of ^{13}C-labeled and total metabolites between pLKO and SLC25A22-knockdown cells.

(A) Relative ratio of ^{13}C-labeled and total metabolites between pLKO and siSLC25A22 cells. (B) Relative ratio of ^{13}C-labeled and total metabolites between pLKO and shSLC25A22 cells.

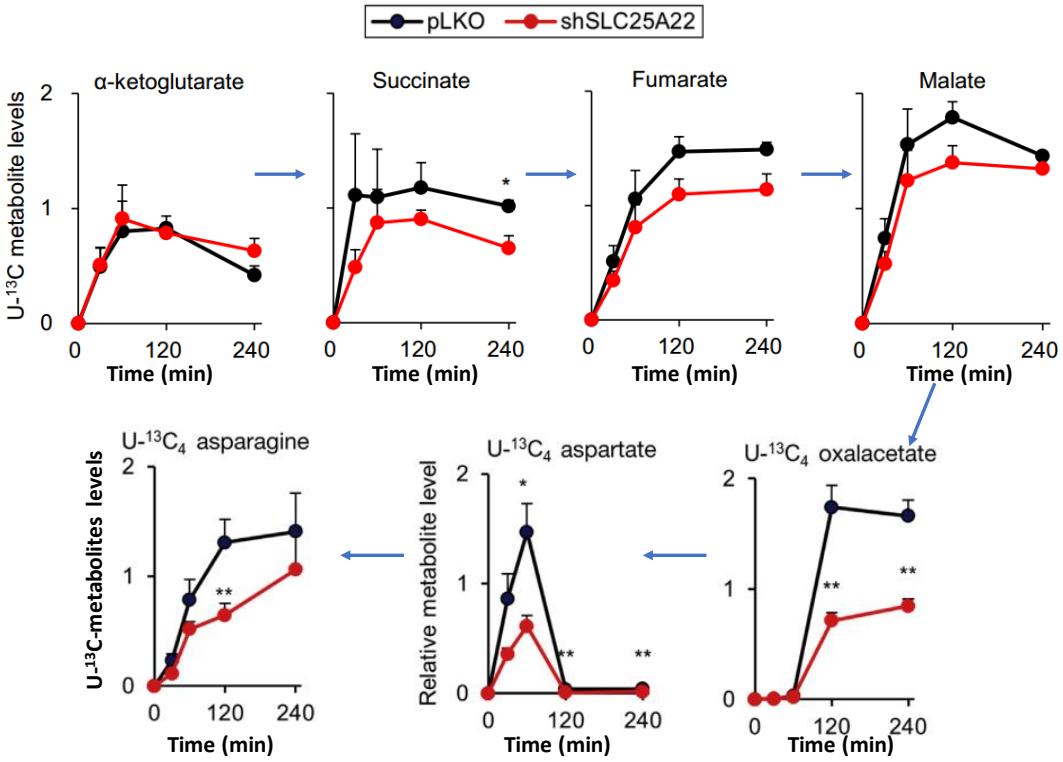

Figure 3.7 Metabolic flux analysis of ^{13}C-labeled TCA cycle intermediates and derived amino acids following labeling of pLKO cells and stably expressing SLC25A22 cells with 4 mM [U-$^{13}C_5$]-Gln.

We monitored the ^{13}C-glutamine kinetic flux mates in DLD1 pLKO cells and stably expressing SLC25A22 (shSLC25A22) cells. ^{13}C-labeled TCA cycle intermediates including $^{13}C_4$-succinate, $^{13}C_4$-fumarate and $^{13}C_4$-malate reached their peaks at 60 or 120 min (shown in Figure 3.7). Intriguingly, $^{13}C_4$-oxalacetate and $^{13}C_4$-aspragine reached their peaks at 240 min, while the $^{13}C_4$-aspratate reached its peak at 60 min, of which is the down- and up-stream metabolites of

$^{13}C_4$-oxalacetate and $^{13}C_4$-aspragine, respectively. These data were consistent with a model whereby $^{13}C_4$-labeled carbons were incorporated into aspartate (via GOT2 in the TCA cycle), exported out of mitochondria via SLC25A12/13, and channeled to oxaloacetate and asparagine in the cytosol, and that SLC25A22 knockdown suppressed these metabolic pathways (Figure 3.8 A). Due to technical limitations, we were unable to differentiate the cytosolic and mitochondrial oxaloacetate pools. Nevertheless, knockdown of GOT1 in DLD1 cells increased U-$^{13}C_4$-labeled aspartate but suppressed U-$^{13}C_4$-oxaloacetate at 120–240 minutes, which implied that oxaloacetate was being formed from aspartate via GOT1 (Figure 3.8 B). Based on our data, we hypothesize that SLC25A22 silencing impairs alanine, aspartate and glutamate metabolism, and the reduced aspartate levels may in turn suppress biosynthesis of oxaloacetate and asparagine in the cytosol.

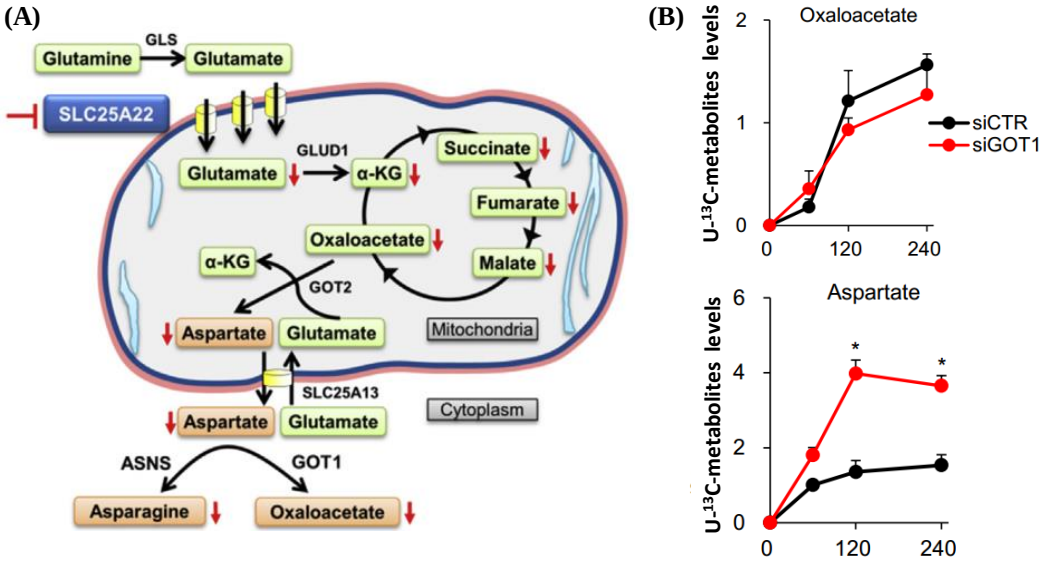

Figure 3.8 Schematic illustrating the effects of SLC25A22 on alanine, aspartate and glutamate pathway (A) and relative ratio of $^{13}C_4$-Oxalacetate and $^{13}C_4$-aspartate between control (siCTR) and transiently expressing knockdown of GOT1 (siGOT1) cells.

On the one hand, aspartate plays a vital role in anabolism and redox homeostasis [156], our collaborator observed that aspartate supplementation into culture medium can rescue the antiproliferation in DLD1, SW116 and HCT116 cells caused by SLC25A22-knockdown. Moreover, aspartate also reserved the induction of apoptosis due to SLC25A22 silencing. The control cells showed no sensitive to aspartate contrastively.

On the other hand, oxaloacetate is converted from aspartate and α-KG via the transaminase GOT1 in cytosol, whether OAA is required for the *KRAS* mutant CRC cell growth needed to investigate. OAA could rescue colony formation in knockdown of SLC25A22 cells (Figure 3.9 A). If Asp-derived OAA is essential for cell viability, the rescue effect of aspartate in knockdown of SLC25A22 cells was possible to depend on GOT1. Thus, in the stably expressing shSLC25A22 DLD1 and HCT116 cell lines, the knockdown of GOT1 abolished the rescue effect of aspartate on colony formation (Figure 3.9 B). Furthermore, knockdown of GOT1 did not affect the siSLC25A22 cells, but inhibited cell viability in siControl cells (Figure 3.9 C). The above findings indicated that GOT1 might function downstream of SLC25A22, so that the effect of GOT1 on cell viability is diminished on silencing of SLC25A22. We could conclude that upon knockdown of SLC25A22, Asp-derived OAA through GOT1 could inhibit the cell growth in *KRAS* mutant CRC cells.

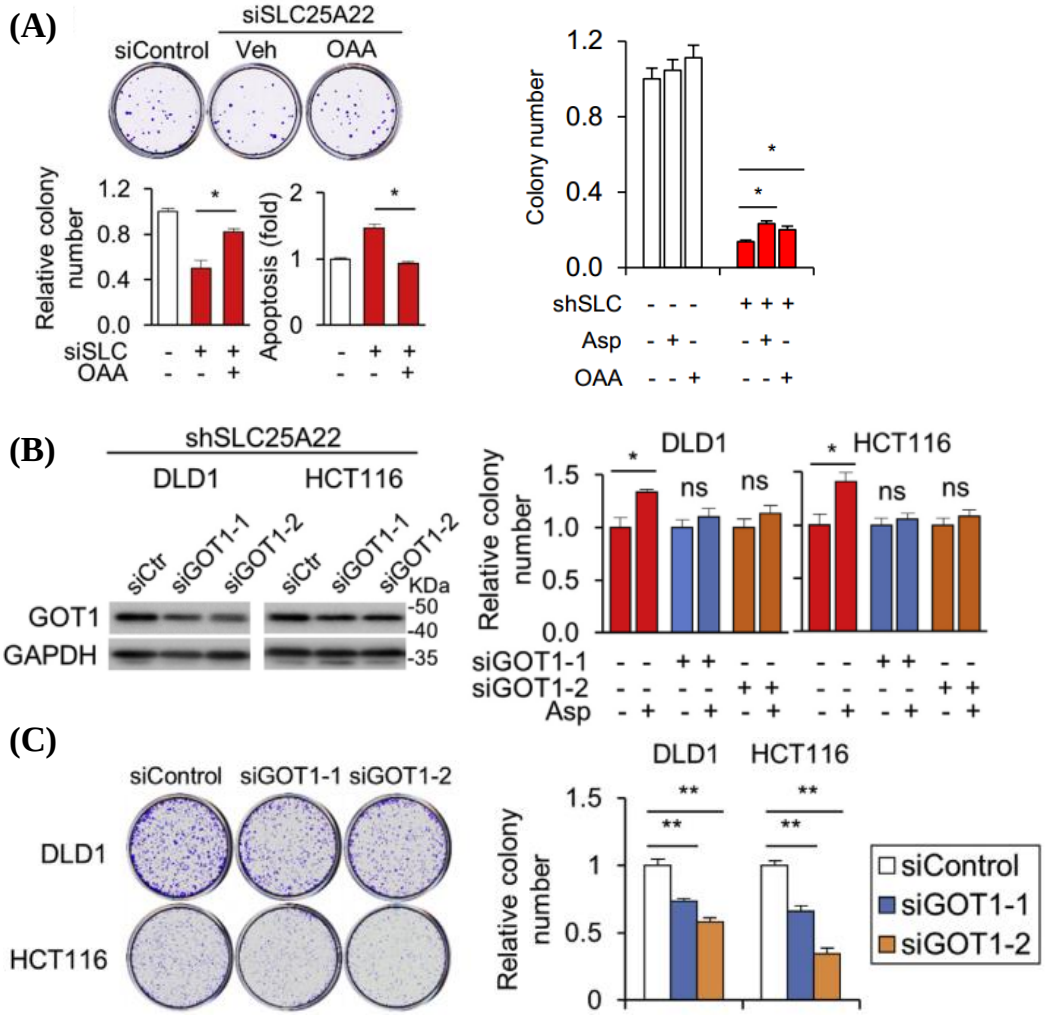

Figure 3.9 (A) OAA rescued cell viability and suppressed apoptosis (left), and rescued cell proliferation ability (right) in SLC25A22 silenced SW1116 cells. (B) Knockdown of GOT1 knockdown inhibited rescue effect of aspartate on colony formation in shSLC25A22 cells. (C) GOT1 knockdown had no effect on siSLC25A22 cells but suppressed cell viability in parental DLD1 and HCT116 cells.

3.3.4 Targeted metabolomics analysis of urea cycle and polyamine by using UHPLC-QqQ MS analysis

In the targeted analysis, urea cycle metabolites such as ornithine, citrulline and arginine were not significantly altered except for Asp, which functions as an intermediate to generate arginosuccinate (Figure 3.10 A). On the other hand, ornithine-derived polyamines putrescine, spermine and acetylated polyamines were suppressed in DLD1-shSLC25A22 cells (Figure 3.10 B). These data indicated that knockdown of SLC25A22 expression profoundly affected synthesis of polyamines, but not altered synthesis of urea cycle (except for Asp).

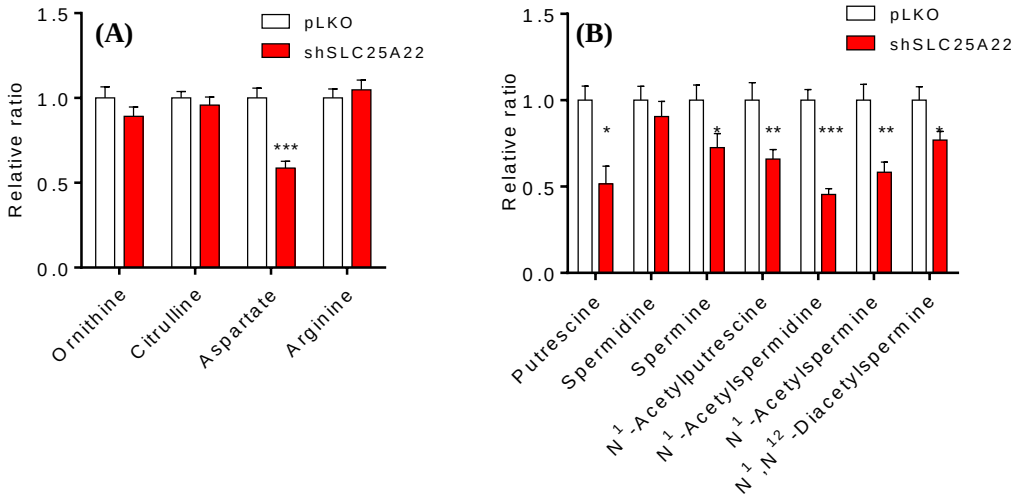

Figure 3.10 Relative ratio of urea cycle amino acids and polyamines between pLKO and shSLC25A22 cells.

(A) Relative ratio of urea cycle amino acids between pLKO and shSLC25 A22 cells, (B) Relative ratio of polyamines between pLKO and shSLC25 cells. * p < 0.05, ** p < 0.01, and *** p < 0.001. Error bar represented the SEM.

3.3.5 Metabolic kinetic isotope analysis of polyamines using [U-$^{13}C_5$]-Gln as isotope tracer

We also traced the metabolic fates of aspartate-derived amino acids and polyamines from 0 to 24 h by using [U-$^{13}C_5$]-Gln as isotope tracer. $^{13}C_4$-Asp, $^{13}C_4$-Asn and $^{13}C_3$-Ala were labelled when using $^{13}C_5$-Gln as carbon source [157]. Results demonstrated that ^{13}C-labled Asp, Asn and Ala were significantly reduced in shSLC25A22 cells in comparison with those in the control pLKO cells at time points starting from 4 h (p < 0.05) (Figure 3.11), while $^{13}C_5$-Gln and $^{13}C_5$-Glu accumulated in the shSLC25A22 cells from 4 h. Of note, the intensity of [U-$^{13}C_3$]-alanine in shSLC25A22 cells at each time point was close to 0.5-fold compared to that in control pLKO cells, indicating a strong reduction in the levels of this metabolite. Moreover, tendencies of ^{12}C-metabolites were similar to ^{13}C-metabolites (shown in Figure 3.12), suggesting that SLC25A22-mediated glutamine metabolism is important for the biosynthesis of derived amino acids. The native and ^{13}C-labeled proline, resulting from ornithine and glutamate simultaneously, were up-regulated in shSLC25A22 cells from 6 h without significantly difference.

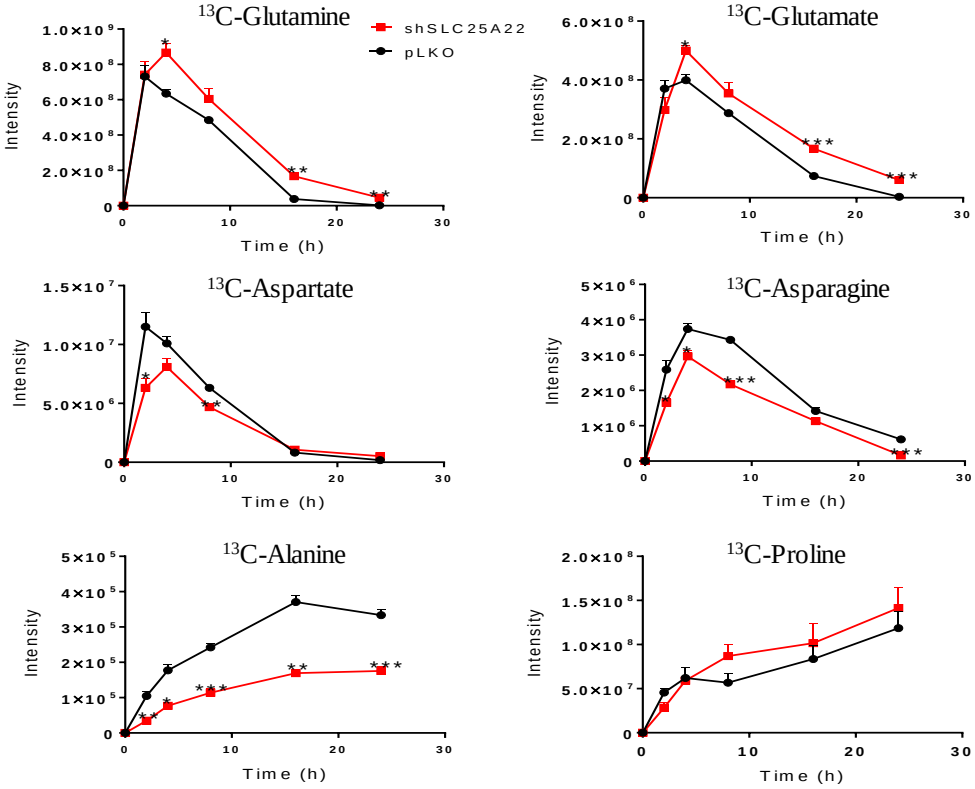

Figure 3.11 Relative ratio of ^{13}C-labeled Gln-derived amino acids between shSLC25A22 and pLKO cells.

* $p < 0.05$, ** $p < 0.01$, and *** $p < 0.001$. Error bar represented the SEM.

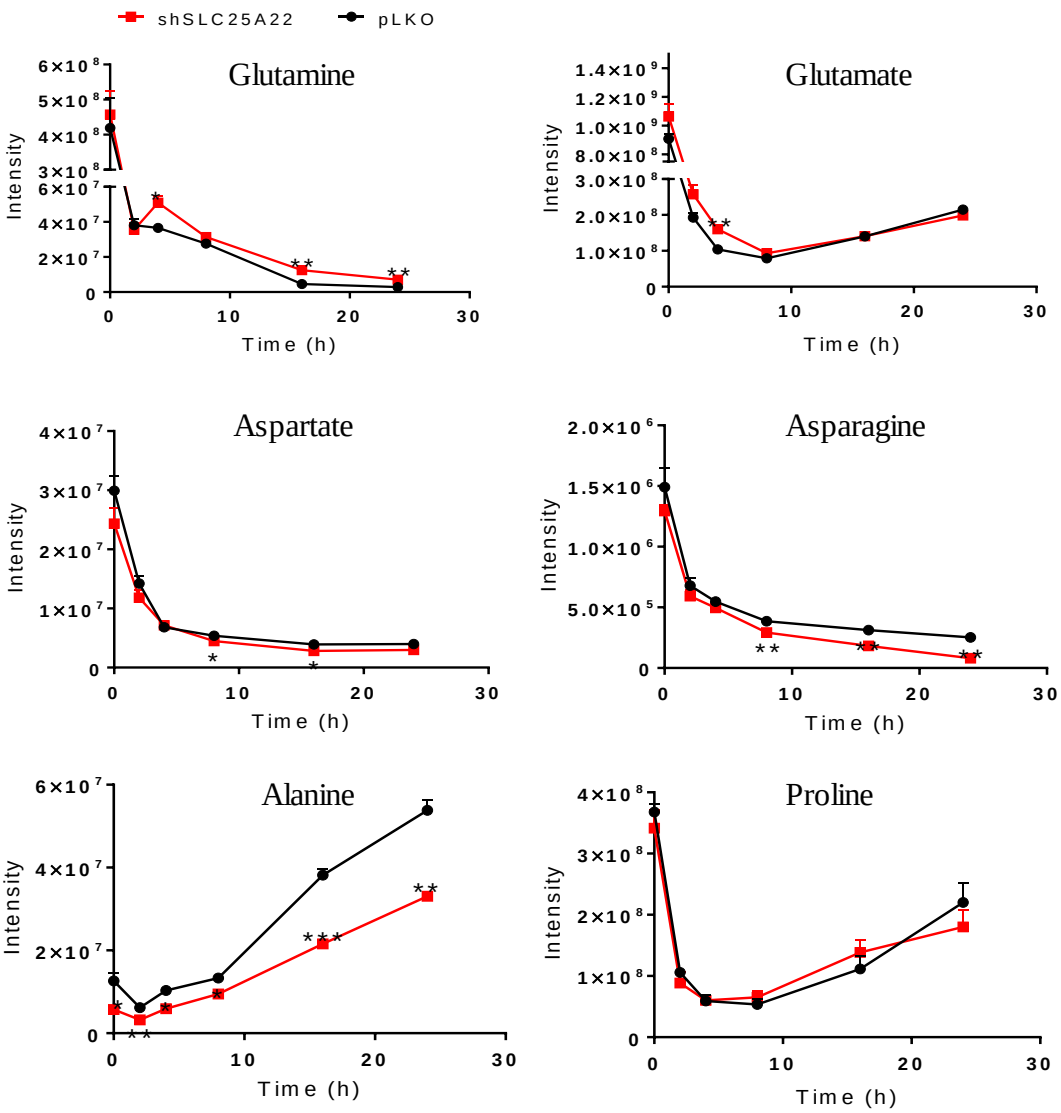

Figure 3.12 Relative ratio of native Gln-derived amino acids between shSLC25A22 and pLKO cells.

* $p < 0.05$, ** $p < 0.01$, and *** $p < 0.001$. Error bar represented the SEM.

The [U-$^{13}C_5$]-ornithine in urea cycle derived from [U-$^{13}C_5$]-Gln can be converted into [U-$^{13}C_4$]-putrescine via *ODC* and then further metabolized into spermidine and spermine, which are acetylated and exported via passive diffusion across the cell membrane [148]. The overview of ^{13}C-labeled carbon was shown in Figure 3.13. And Figure 3.14 showed that [U-$^{13}C_5$]-ornithine were reduced in shSLC25A22 cells compared with control pLKO cells before 2 h, while it was up-regulated from 4 h to 24 h, which may promote proline accumulation in shSLC25A22 cells. However, other $^{13}C_5$-urea cycle intermediates were not detected both in pLKO and shSLC25A22 cells. On the other hand, most of $^{13}C_4$-labeled polyamine intermediates except $^{13}C_4$-N^1-acetylputrescine at 4 h, were down-regulated in the SLC25A22 knockdown cells ($^{13}C_4$-N^1-acetylspermine and $^{13}C_4$-N^1, N^{12}-diacetylspermine were not detected). Of note, both $^{12}C/^{13}C$-polyamines in the DLD1-shSLC25A22 cells and DLD1-shSLC25A22 conditioned cell culture media were significantly reduced compared to DLD1-pLKO cells and media (Figure 3.15, the data of media were not shown here). These data indicated that silencing of SLC25A22 significantly impaired the flux of glutamine-derived carbons into polyamine biosynthesis, while it did not affect the urea cycle synthesis except for ornithine.

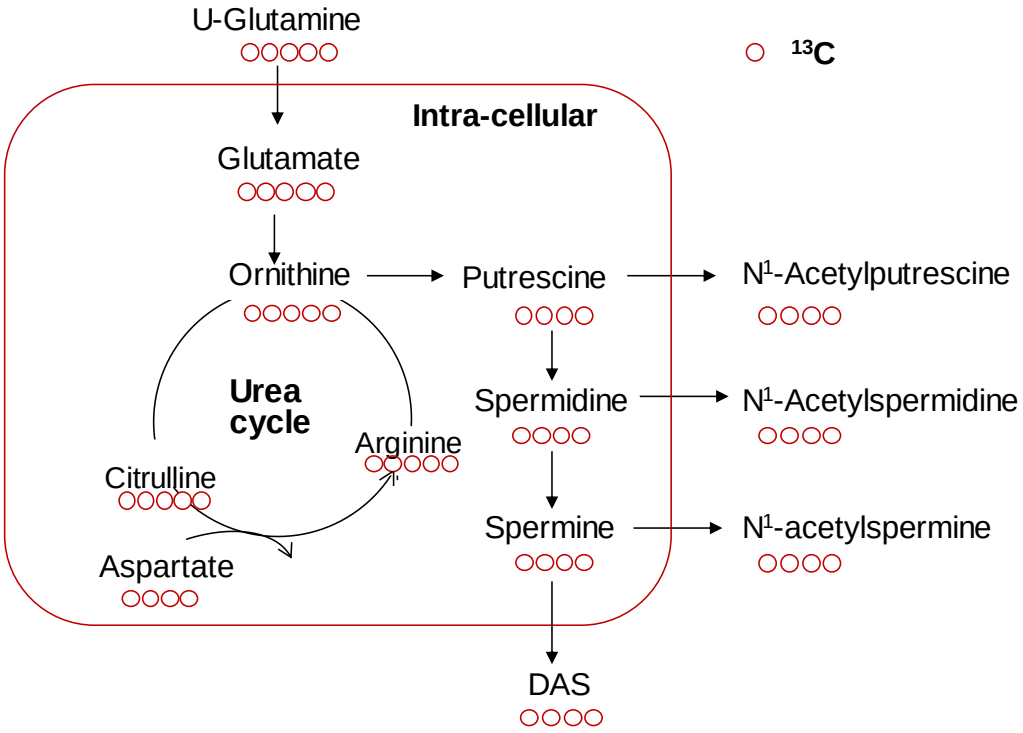

Figure 3.13 Overview of ^{13}C-labeled carbon skeleton of urea cycle and polyamines using [U-$^{13}C_5$]-Gln as isotope tracer. Red circle represented ^{13}C.

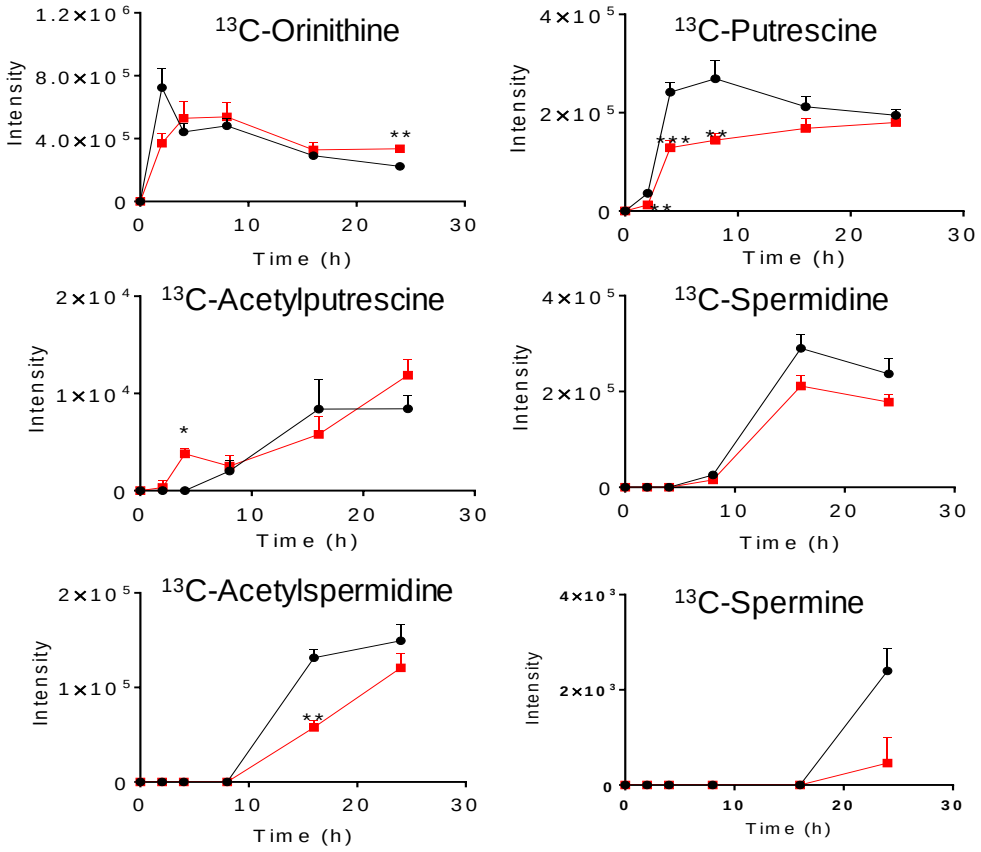

Figure 3.14 Flux of ^{13}C-labeled urea cycle intermediates and $^{13}C_4$-polyamines in shSLC25A22 and pLKO cells.

* $p < 0.05$, ** $p < 0.01$, and *** $p < 0.001$. Error bar represented the SEM.

Apart from the aforementioned metabolites, we unveiled that SLC25A22 knockdown had a profound impact on polyamine metabolism. Polyamines derived from ornithine are required for normal and cancer cells growth [147, 148], and their levels are frequently up-regulated in carcinogenesis. Johnson *et al.* found that polyamines, especially DAS as an end-product of polyamine metabolism, were strongly up-regulated in CRC tumor tissues compared to adjacent normal

tissues by using metabolomics approach [127]. Here, global metabolomics analysis has shown that DAS was reduced in silencing of SLC25A22 cells. Targeted analysis of polyamines and urea cycle metabolites demonstrated that polyamines were remarkably decreased in knockdown of SLC25A22 cells. However, urea cycle intermediates were not sufficiently labelled by [U-$^{13}C_5$]-Gln, suggesting the urea cycle was not triggered by the knockdown of SLC25A22. Previous reports indicated that increased polyamine metabolism could enhance cancer growth, migration and metastasis [158, 159], while polyamines depletion could inhibit cancer cell proliferation, migration and invasion via SAT1 mediation [160]. Exogenous addition of some polyamine metabolites promoted growth of DLD1 cells, which confirmed their potential role as oncometabolites in *KRAS*-mutant CRC. Taken together, SLC25A22-induced production of polyamines represents a novel mechanism whereby SLC25A22 mediates its oncogenic effect in *KRAS*-mutant CRC.

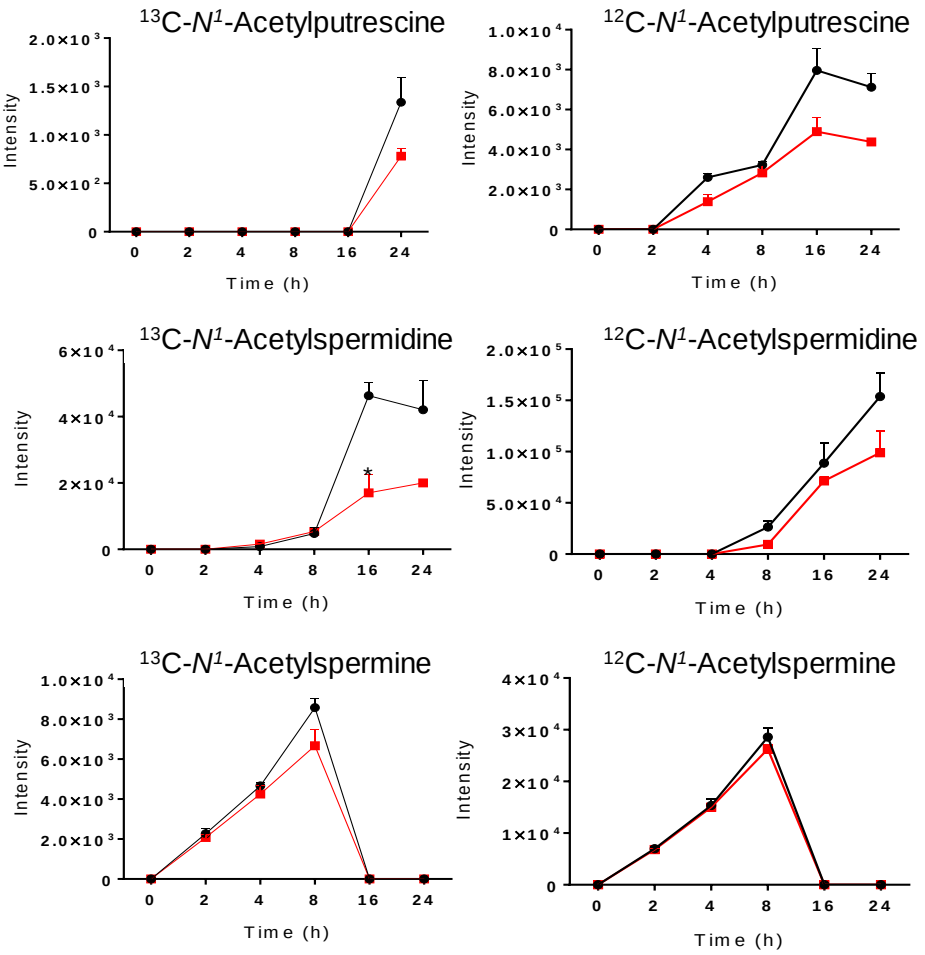

Figure 3.15 Intensities of native and ^{13}C-labeled polyamines in shSLC25A22 and pLKO cells.

* $p < 0.05$. Error bar represented the SEM.

3.3.6 Western blot analysis of polyamine biosynthetic enzymes

We validated whether the altered polyamine metabolism dysregulated expression of enzymes involved in polyamine biosynthesis. However, western blot analysis revealed that *ODC* expression was not significant different in SLC25A22-silenced DLD1 cells, HCT116 cells and SW1116 cells; whilst

expression of spermidine/spermine N^1-acetyltransferase 1 (*SAT1*) was induced by knockdown of SLC25A22 (Figure 3.16 A). The results suggested that the suppression of polyamines biosynthesis is likely to a direct consequence of reduced glutamine flux. We thus speculated that induced *SAT1* expression might reflect an attempt to up-regulate polyamine metabolism which in turn could compensate for the reduced carbon flux from glutamine.

3.3.7 Role of polyamines in the proliferation of *KRAS*-mutant CRC cells

We examined whether polyamines play a role in cell proliferation in *KRAS*-mutant CRC cells. We incubated DLD1 cells with six polyamines at 1.25/2.5 µM or 2.5/5 µM, and then examination cell viability by MTT assay. Our results showed that N^1-acetylputrescine and N^1-acetylspermidine promoted CRC cell growth at both doses (Figure 3.16 B).

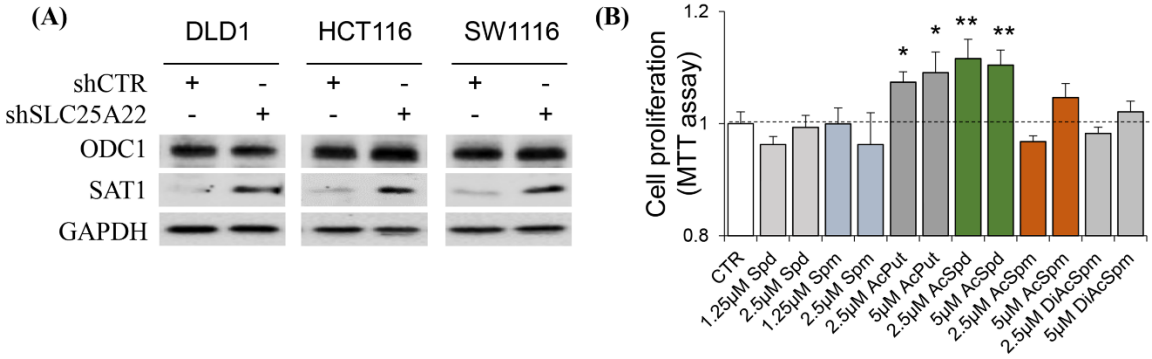

Figure 3.16 Western blot and MTT analysis.

(A) Western blot of *ODC* and *SAT1* in shSLC25A22 and pLKO cells, (B) Cell proliferation in MTT assay. * $p < 0.05$, ** $p < 0.01$. Error bar represented the SEM.

3.4 Chapter summary

In summary, the data obtained through LC-MS-based targeted metabolomics and kinetic isotope analysis indicated that SLC25A22 knockdown inhibited the biosynthesis of TCA cycle, aspartate and derived amino acids, such as alanine, asparagine and glycine, which could reduce cell proliferation in *KRAS* mutant CRC cells. As the downstream product of aspartate, oxaloacetate was obviously decreased, and it is essential for cell survival required GOT1 in knockdown of SLC25A22 cells. Moreover, decreased levels of polyamines were generated from less glutamine intake due to knockdown of SLC25A22 in *KRAS*-mutant CRC cells. The addition of polyamine into culture medium can modulate CRC cell growth. Thus, our studies demonstrated that SLC25A22 is an essential regulator of the metabolic system of *KRAS*-mutant colorectal tumor via TCA cycle, aspartate/derived amino acids and polyamines, and its overexpression promotes tumor cell growth, which could provide more insights into *KRAS*-mutant CRC therapy with treatment of polyamine-inhibitor.

*This Chapter was mainly from my published papers where I am the first and third author as follows:

1. **Li X**, Wong CC*, Cai Z*, *et al.* LC-MS-based metabolomics revealed SLC25A22 as an essential regulator of aspartate-derived amino acids and polyamines in *KRAS*-mutant colorectal cancer. Oncotarget. 2017, 8(60): 101333–101344

2. **Li X**, Wong CC, Cai Z*, *et al*. Determination of amino acids in colon cancer cells by using UHPLC-MS/MS and [U-$^{13}C_5$]-glutamine as the isotope tracer. Talanta. 2017, 1 (162): 285-292

3. Wong CC, Qian Y, **Li X**, et al. SLC25A22 Promotes Proliferation and Survival of Colorectal Cancer Cells With KRAS Mutations and Xenograft Tumor Progression in Mice via Intracellular Synthesis of Aspartate. Gastroenterology. 2016, 151 (5): 945-960.e6

Chapter 4 LC-MS-based Urinary and Serum Metabolomics Study of Rheumatoid Arthritis

4.1 Introduction

Rheumatoid arthritis (RA) is a chronic, systemic inflammatory autoimmune disorders [94, 98]. It can cause severe consequences on individuals such as intensive pain and joint destruction, even disability and increased mortality worldwide [95]. According to the Global Burden of Disease Study 2010, the global prevalence of RA was approximately 0.2%, which had been ranked as the 42nd cause of global disability [161]. Additionally, there are some complications associated with RA, such as neurologic complications, lung disease, cardiovascular disease and osteoporosis [162-164]. Generally, RA is considered to be affected by multigenetic and environmental factors (micro-organisms, smoking, stress, *etc.*) [95, 98]. Cytokines play crucial roles during the course of RA through imbalanced activities between pro-inflammatory and anti-inflammatory cytokines, such as interleukin (IL)-1, IL-6, tumor-necrosis factor (TNF)-α, *etc.*, which are helpful for RA diagnosis [94, 97, 98]. However, the etiology of rheumatoid arthritis is still unclear [97]. Moreover, it is also challenging for early diagnosis and treatment of RA [98, 165].

Metabolomics is widely applied as a powerful approach to characterize the metabolic phenotype in response to multifactorial stimulus among disease or drug therapy, diet, gut microbiomes and genetics [166, 167]. Metabolomics study has

been applied in discovering altered metabolites in biological samples, and provided evidences of the diagnosis and prognosis of RA [168, 169]. NMR and MS coupled with UHPLC or GC are two major technologies for metabolomics study. UHPLC-MS is popularly utilized for metabolomics study due to its advantages of high sensitivity, wide dynamic range and good reproducibility [22, 170]. In recent years, previous metabolomics studies on RA mainly focused on discrimination from other types of arthritis and therapeutic evaluation of targeted drug or traditional Chinese medicines based on murine models [19, 99, 100, 103, 171, 172]. The findings from serum or synovial fluid (SF) revealed some metabolites, including urea cycle and TCA cycle intermediates, amino acids and purine metabolites were perturbed - due to inflammation or immune activities [171, 172]. However, rare studies are simultaneously integrated with the metabolomics findings from urine and serum samples of RA patients comparing with healthy counterparts.

Interaction of microbiomes with human hosts is promising to provide new insights into pathogenesis of RA [108, 173]. Of note, composition and proportion of bacterial species are perturbed in responding to RA, which also can be partially restored after therapy [110, 111]. Additionally, epidemiologic research unveiled that gastrointestinal infection could diminish the risk of RA [174]. However, investigations on association of GM-derived metabolites with RA are insufficient.

In the study, based on MS nontargeted and targeted metabolomics, we aimed to find out differentially expressed urinary and serum metabolites in RA patients in comparison with healthy controls, and furtherly to investigate association of GM-derived intermediates with RA. The nontargeted metabolomics was performed by HR orbitrap MS or GC-MS, and the targeted analysis of metabolites in tryptophan and polyamine metabolism was conducted by using LC-QqQ MS.

4.2 Materials and methods

4.2.1 Chemicals and reagents

Methanol (MeOH), acetonitrile (ACN), formic acid (FA) were of LC grade. Pure water was prepared by Milli-Q purification system (Millipore, USA). Metabolites in tryptophan and phenylalanine metabolism, including tryptophan (Trp), kynurenine (KYN), 3-hydroxylkynurenine (HKYN), kynurenic acid (KYNA), anthranilic acid (AA), 3-hydroxyanthranilic acid (HAA), quinolinic acid (QA), indole, indole-3-proponic acid (IPA), 3-indoleacetic acid (IAA), 3-indolecetonitrile, serotonin, melatonin, 5-hydoxyindoleacetate (5HIAA), phenylalanine (Phe), phenyllactic acid (PLA), tyrosine (Tyr), L-Dopa, dopamine, noradrenaline, epinephrine were obtained from Sigma-Aldrich (MO,US). The internal standards (IS) including D_5-L-tryptophan, D_4-serotonine creatinine sulfate complex, D_4-dopamine hydrochloric acid were purchased from C/D/N Isotopes (Quebec, Canada), 4-chloro-kynurenine (4-Cl-KYN) from Toronto Research Chemicals Inc. (Toronto, Canada) and 4-chloro-phenylalanine from

Sigma-Aldrich (MO, USA). Standard stock solutions were prepared in proper solvent for mass spectrum verification and targeted analysis. All above standard solutions were stored at -20 ℃.

4.2.2 Sample collection

In the study, RA patients and healthy controls were recruited in Guanghua Integrative Medicine Hospital, Shanghai, China. Urine and serum samples were collected from 50 RA patients and 50 healthy controls following the same protocol. RA patients who met the American College of Rheumatology (ACR) criteria were enrolled [175]. There were 74 % female patients aged 27-73, and 26 % male patients aged 51-68. For the RA patients, erythrocyte sedimentation rate (ESR) and C reactive protein (CRP) were collected. Another group of 50 healthy volunteers including 64 % female (aged 21-62) and 36 % male (aged 21-62), was enrolled by routine physical examination. The age of enrolled RA individuals and healthy controls is without significant difference. The clinical characteristics of 100 human subjects were shown in Table 4.1. And the part of work was conducted by collaborators in School of Chinese Medicine (SCM).

Urine and serum samples were prepared within 30 min after collection. All samples were stored at -80 ℃ until analysis. The study protocol was approved by the Ethical Committee of Guanghua Integrative Medicine Hospital and Hong Kong Baptist University. Informed consents were obtained from all participants or their legal representatives before sample collection. Questionnaires including diet

information, dietary habits, smoker/un-smoker and basic treatment were conducted before collecting sample, and the different habits (*e.g.* complete vegetable diet, alcohol consumption) were excluded. In addition, patients who suffered from severe cardiovascular, lung, liver, kidney, hematologic or mental disease and women who were pregnant, breast-feeding or planning to become pregnant were excluded from the RA group. Furthermore, the patients continuously receiving non-steroidal anti-inflammatory drugs (NSAID) or corticosteroids for over six months, or patients and volunteers receiving above mentioned medicine within one month were excluded.

4.2.3 Sample preparation

4.2.3.1 Urine preparation

Urine samples were thawed on ice. 100 μL of urine was precipitated by 100 μL chilled MeOH with 4-Cl-Phe (0.5 μg/mL), and vortexed for 30 s, and centrifuged at 15,000 g for 10 min. The supernatants were divided into three parts: 20 μL-aliquot pooled together from each sample as quality control samples, 80 μL-aliquot for global metabolomics analysis, and 80 μL-aliquot for targeted metabolites analysis after lyophilization. The residues for targeted analysis were reconstituted in 5 % ACN with 4-Cl-KYN (0.5 μg/mL), D_5-Trp (0.25 μg/mL) and D_4-dopamine (0.25 μg/mL).

Table 4.1 Demographical and clinical information of urine samples in the study.

	RA (n=50)	Control (n=50)
Demography		
Age (years), mean (median)	55.0 (56)	53.5 (50)
Female/male	37/13	32/18
Female age mean±SD (min, max)	53.1±11.3 (27, 73)	45.1±11.0 (21, 62)
Male age mean±SD (min, max)	59.8±6.1 (51, 68)	38.9±14.9 (21,62)
Disease activity parameters		
Disease Duration (months)	34.3 (17.6)	[6] NA
[1]DAS28, mean (median)	3.6 (3.1)	NA
[2]ESR (mm/h), mean±SD	39.8±33.4	NA
[3]CRP (mg/L), mean±SD	14.14±22.18	NA
Autoantibody status		
[4] RF-positive	76%	NA
[5]ACPA-positive	72%	NA

Notes:

[1] DAS: disease activity score, [2] ESR: erythrocyte sedimentation rate, [3] CRP: C-reactive protein, [4] RF: rheumatoid factor, [5] ACPA: anti-citrullinated protein antibody. [6] NA: not applicable.

4.2.3.2 Serum preparation

Serum samples were thawed in 0 ℃. 100 μL of serum was extracted by 400 μL chilled MeOH and vortexed for 30 s, then centrifuged at 15,000 g for 10 min. The supernatants were divided into three aliquots for lyophilization. One-aliquot of residue was redissolved in 150 μL 50 % MeOH with 0.5 μg/mL 4-Cl-Phe for LC-MS-based global metabolomics analysis. One-aliquot (with 0.5 μg/mL 4-Cl-Phe and 0.5 μg/mL heptadecanoic) of residue for GC-MS-based global metabolomics analysis after derivatization as follows. The residue was derivatized by 30 μL of methoxamine (20 mg/mL in pyridine) at 30 °C for 30 min and 60 μL of BSTFA with 1% TMCS at 60 °C for 60 min. One-aliquot of residue for targeted metabolomics analysis, was reconstituted in 150 μL 50% ACN with final concentration of 4-Cl-Phe (0.5 μg/mL), 4-Cl-KYN (0.5 μg/mL), D_5-Trp (0.25 μg/mL) and D_4-dopamine (0.25 μg/mL). All samples were stored at -80 °C until analysis.

Quality control (QC) samples for global metabolomics are required to monitor repeatability and stability of LC-MS and GC-MS analysis. In the study, QC sample was prepared by pooling together of equal volume of each sample. Blank sample was prepared by using reconstituted solvent.

4.2.4 Global metabolomics

The LC-MS-based global metabolomics data were acquired by using ultra-high performance liquid chromatography coupled with Q Exactive Focus

Orbitrap mass spectrometer (QE MS, Thermo Scientific, USA). Ten μL of prepared urine or serum sample was injected into a 100 mm × 2.1 mm, 1.8 μm particle size HSS T3 (Waters, Milford, USA) equipped in Ultimate 3000 rapid separation liquid chromatography (RSLC) for separation at 30 ℃. The mobile phases were water (A) and ACN (B) both with 0.1% FA. The LC gradient program was as follows: 0 min, 2 % B; 1 min, 2 % B; 19 min, 100 % B; 21 min, 100 % B; 21.1 min, 2 % B; 25 min, 2 % B. The flow rate was 0.3 mL/ min. The sample room was set at 4 ℃. The MS parameters were as follows. The spray voltage was 3.5 kV and 3 kV in positive and negative ion mode, respectively. The pressure of sheath and auxiliary gas was set at 40 arb and 10 arb, respectively. The temperature of capillary and auxiliary gas was both 320 °C. The S-lens RF level was 60 %. The scan range was 70-1000 (*m/z*). The resolution was 35,000. The maximum inject time (max IT) was 100 ms. Automated gain control (AGC) was set at 1×10^{6} ions. The urine samples were analyzed at randomly. The samples were run in order of "1 QC sample-10 real samples-1 QC sample-1 blank sample" [19].

The GC-MS-based global metabolomics data were acquired by using an Agilent 7890B gas chromatography coupled with a 5977A mass spectrometer (Agilent, Folsom, CA). Metabolites were separated in DB-5 ms capillary column (30 m × 250 μm i.d., 0.25 μm film thickness, coated with 5%-diphenyl crossed-linked 95% dimethylpolysiloxazne, Agilent J&W Scientific, Folsom, CA)

in splitless mode. The flow rate was set at 1.0 mL/min with helium as carrier gas. Metabolites detection was performed in electron impact ionization source. The temperature of injection, transfer interface and ion source were 260, 250, 200 °C, separately. The full scan range was m/z 50-650. Electron impact energy was 70 eV. The solvent delay was 5 min. The GC gradient oven program was set as follows: initially set at 70 °C for 2 min, followed by raising to 200 °C with a rate of 5 °C/min, then increased to 300 °C with a rate of 20 °C/min, and kept at 300 °C for 2 min.

4.2.5 Targeted metabolomics

For targeted metabolomics, the metabolites in tryptophan and phenylalanine metabolism, and amino acids were compared between RA and control samples by using UHPLC-QqQ MS (Thermo Scientific, USA). The HSS T3 column (100 mm × 2.1 mm, 1.8 μm, Waters, USA) was utilized. The mobile phase was water with 0.1% FA (A) and ACN with 0.1% FA (B). The flow rate: 0.25 mL/min. LC gradient program was as follows: 0 min, 2 % B; 2 min, 2 % B; 3.5 min, 30 % B; 6 min, 95 % B; 8 min, 95 % B; 8.5 min, 2 % B, 12 min, 2 % B. The sample room was set at 6 ℃. The MS parameters in positive mode were set as bellows. Spray voltage: 3.5 kV, sheath gas pressure: 35 arb, auxiliary gas pressure: 10 arb, capillary temperature: 350 °C, and auxiliary gas temperature: 320 °C, CID gas: 1.5 mTorr. The SRM transitions of metabolites in tryptophan and phenylalanine metabolism were

shown in Table 4.2. The solutions were prepared with referring to our published paper [176].

Table 4.2 SRM transitions of metabolites in tryptophan and phenylalanine metabolism in targeted metabolomics analysis using LC-QqQ MS.

Classes	Compound	Precursor ion	Product Ion	CE (eV)
Tryptophan and kynurenine metabolism	Tryptophan	205	188	12
	Serotonin	177	160	12
	Melatonin	233	174	15
	Kynurenine	209	94	10
	Quinolinic acid	168	150	10
	Anthranilic acid	138	120	12
	3-Hydroxyanthranilic acid	154	136	15
	Kynurenic acid	190	144	18
	3-Hydroxykynurenine	225	208	12
	Indole	118	91	20
	3-Indoleacetonitrile	157	130	15
	3-Indolpropionic acid	190	130	15
	5-Hydroxyindoleacetic acid	192	146	20
Phenylalanine metabolism	Phenylalanine	166	120	15
	Tyrosine	182	136	15
	L-Dopa	198	152	22
	Dopamine	154	137	12
	Noradrenaline	170	135	10
	Epinephrine	184	166	10
IS	D_4-5HT	181	164	12
	4-Cl-Phenylalanine	200	154	15
	4-Cl-KYN	243	226	12
	D_5-Tryptophan	210	192	12
	D_4-Dopamine	158	141	12

4.2.6 Data processing and metabolites identification

MS data was processed as previously reported method [177, 178]. For LC-MS data, raw data files (*.raw*) in global metabolomics study were converted into CDF files using RawFileReducer (Thermo Scientific, USA) [179]. The GC-MS data were exported to NetCDF by DataAnalysis (Agilent, CA, US). Ion features were extracted and picked up by using XCMS software and CAMERA, implemented with the open-source R statistical language (v 3.3.3) [131]. A three-dimensional CSV file consisting of *m/z*, retention time (RT) and signal intensity was obtained after peak extraction, RT correction, integration, alignment and annotation through setting the following parameters [179]. The noise of LC-MS and GC-MS was set at proper threshold after tests. As for LC-MS data, the mass error and RT error were set as ± 5 ppm and 12 s. The variables were filtered by 80 % rule, meaning that the missing value of ion intensity were removed [132].

The data sets from LC-MS and GC-MS were performed by multivariate and univariate statistical analysis by using SIMCA-P 13.0 software (Umetrics, Umea, Sweden) and SPSS (v18, IBM, NY, US). To evaluate the reliablity of data, the PCA class plot of QC samples in LC-MS (positive and negative) and GC-MS were obtained by using SIMCA-P. The orthogonal partial least squares-discriminant analysis (OPLS-DA) was performed after Pareto scaling of result matrix. The variables importance in projection (VIP) over 1.0 or/and fold

change (FC) between RA and controls over 1.1 and less than 0.9 were used to find out differentially expressed urinary and serum biomarkers [180]. The choice of FC depended on the number of metabolic features, aiming for screening approximately 3-4 hundred metabolic features. The MS/MS spectra of significant features discovered from LC-MS were obtained by stepped collision energy (10, 25, 40 eV) at the resolution of 70,000 and isolation window of 0.6 amu. Therefore, the significantly changed metabolites were identified by comparing accurate mass, retention time, MS/MS pattern and isotope pattern of metabolites in QC samples with those of authentic standards or database, *e.g.* METLIN (www.metlin.scripps.edu), HMDB (www.hmdb.ca/), mzCloud (www.mzcloud.org), *etc*. The pathway analysis, correlation analysis and receiver operating characteristic curve (ROC) analysis of altered metabolites was performed on MetaboAnalyst 3.0 (www.metaboanalyst.ca/) [181]. For metabolites identification performed on GC-MS, their RT and MS spectrum in samples were compared with those in NIST library or authentic standards, here the similarity of Match index and R Match index was over 700 [182].

The semi-quantification of targeted metabolites, including some amino acids, indole-derivatives, and other compounds in tryptophan and phenylalanine metabolism, were processed by using Xcalibur (Thermo Scientific, USA).

4.3 Results

4.3.1 Metabolic phenotype of urine and serum of RA patients

On basis of LC-MS and GC-MS platform, we conducted on metabolic profiling of RA patients and healthy controls whose GM were neither interfered by diet nor medicine. The workflow of metabolomic study was shown in Figure 4.1. Global metabolic signatures of prepared urine and serum are primarily captured by high-resolution MS to discover changed metabolites and pathways in response to RA inflammation. The significantly altered compounds correlated to gut microbiome are targeted analyzed by using LC-QqQ MS.

In the global metabolomics analysis, the samples were injected randomly to exclude instrumental bias. Principle component analysis (PCA) class plot of all QC samples showed that QC samples were mostly within 2 times of standard deviation (SD) (Figure 4.2), demonstrating that the reproducibility and reliability of MS were acceptable in the metabolomics study [183, 184]. In the score plots of OPLS-DA model, urine and serum samples of RA patients (red dots) were clearly separated from those of healthy controls (green dots), as shown in Figure 4.3 A-C and Figure 4.4 A-B (both with 1 predictive component and 2 orthogonal components), suggesting that there were altered metabolites making contributions to the distinction between two groups. R^2X, R^2Y and Q^2 closer to 1 are good indicators of a good PCA/PLS-DA/OPLS-DA model, which possesses good capability of discrimination of different groups or factors. In addition, permutation

test (n=200) was used to evaluate whether the models were overfitted. In the permutation test, the R2 value represents the explanation capability of model to fit to the data, while Q2 value represents the capability of model to predict data. The Y-axis intercepts of R2 less than 0.4 and Q2 less than 0 indicate that model is not overfitted in permutation validation, as shown in Figure 4.3 D from GC-MS data [185].

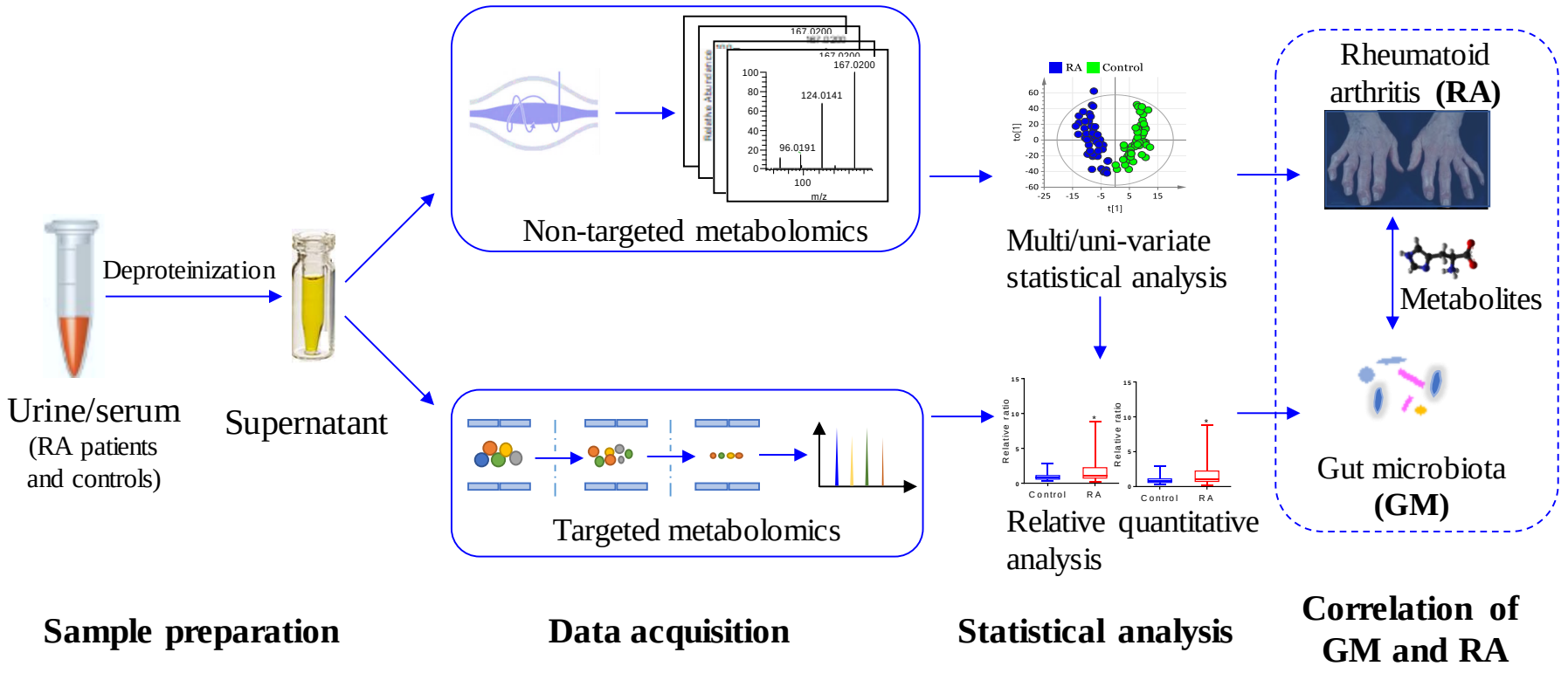

Figure 4.1 Workflow of global and targeted metabolomics analysis of RA patients by using LC-HRMS and LC-QqQ MS.

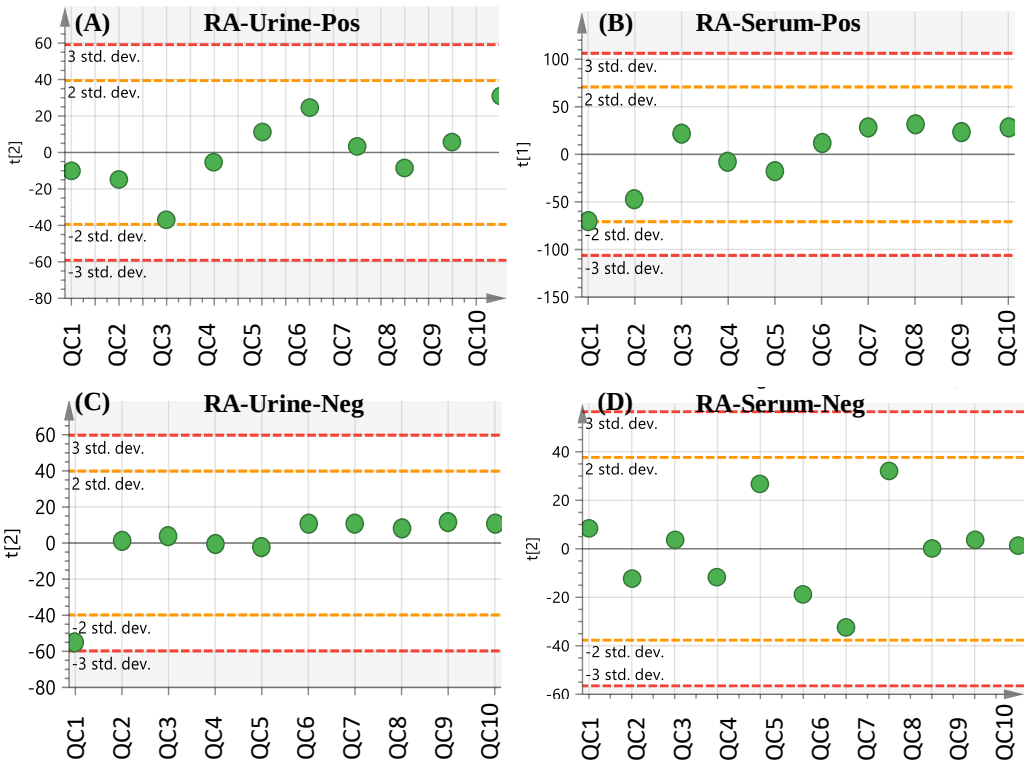

Figure 4.2 Principle component analysis (PCA) class plots of QC samples.

(A) Positive mode of RA urine sample, (B) Positive mode of RA serum sample, (C) Negative mode of RA urine sample, (D) Negative mode of RA serum sample.

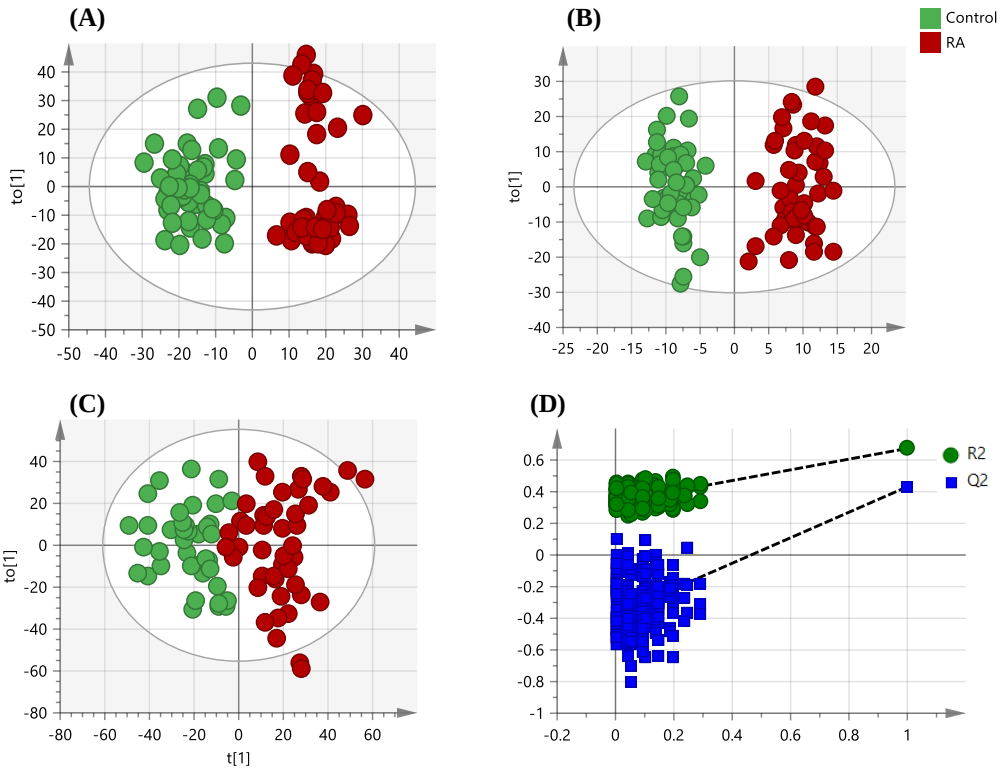

Figure 4.3 Score plots of OPLS-DA model of serum samples.

(A) Score plot from data of LC-MS positive ion mode (R^2X=0.217, R^2Y=0.913, Q^2 =0.675), (B) Score plot from data of LC-MS negative ion mode (R^2X=0.118, R^2Y=0.932, Q^2=0.524), (C) Score plot from data of GC-MS positive (R^2X=0.637, R^2Y=0.727, Q^2=0.496), (D) validation plot of permutations (n=200) based on data of GC-MS (Intercepts: R2=0.332, Q2= -0397).

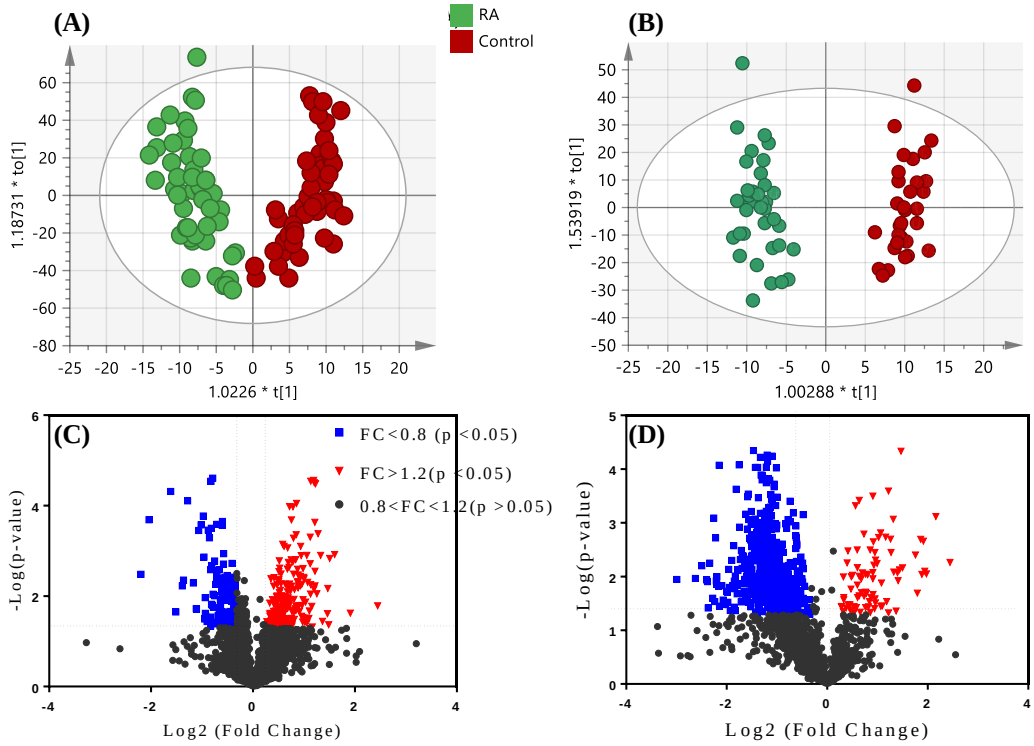

Figure 4.4 Score plots and volcano plots of OPLS-DA model of urine samples. (A) Score plot from data of LC-MS positive ion mode (R^2X=0.315, R^2Y=0.884, Q2(cum)=0.449), (B) Score plot from data LC-MS negative ion mode (R^2X=0.388, R^2Y=0.903, Q2(cum)=0.391), (C) Volcano plot of all features in positive ion mode, (D) Volcano plot of all features in negative ion mode.

4.3.2 Abnormal metabolites in response to RA

4.3.2.1 Abnormal metabolites in urine samples

A total of 32 abnormal metabolites between RA and healthy controls (p <0.05) were obtained in urine samples, including 22 and 10 metabolites in positive and negative ion mode, respectively. The differentially expressed

compounds between RA group and control group with VIP >1 and p <0.05 were shown in Table 4.3, including amino acids and derivatives, acylcarnitines and organic acids, *etc*. These metabolites were mostly classified into tryptophan and kynurenine metabolism, phenylalanine and tyrosine metabolism, purine metabolism, and so on (Figure 4.5A). Additionally, other 39 abnormal metabolites with VIP >1 but without significant differences (including 34 and 5 in positive and negative ion mode) between two groups were listed in Table 4.4. The changed metabolites were attributed into caffeine metabolism, tryptophan metabolism, acylcarnitine metabolism, *etc* (Figure 4.5B). Taking a view of above perturbed metabolites, the metabolites and derivatives from tryptophan and phenylalanine pathway play critical roles in RA, thus it is meaningful to investigate alterations of more metabolites in the tryptophan, phenylalanine and tyrosine pathway by using targeted metabolomics.

Aromatic amino acids, especially those in tryptophan and phenylalanine metabolism are closely associated with inflammatory response to disease or disorders [186]. Among the significantly changed metabolites, tryptophan metabolism intermediates showed up-regulation in the inflammatory individuals, including 5-hydroxy-tryptophan (FC=1.5, p <0.05), L-kynurenine (FC=1.8, p <0.01), 3-hydroxykynurenine (FC=2.8, p < 0.01), 3-hydroxyanthranilic acid (FC=1.7, p < 0.001), 5-hydroxyindoleacetic acid (FC=1.8, p < 0.01) and indolelactic acid (FC=1.8, p < 0.05); while indoxyl sulfate as derivative from indoxyl showed down-regulation in RA patients (FC=0.4, p < 0.05).

Phenylacetate and phenyllactic acid transformed from phenylalanine via microbiomes, were up-regulated but phenylalanine down-regulated (FC=0.9, p >0.05) in RA patients. The markedly elevated levels of the two above phenolic acids were consistent with higher ROS release in RA patients [187]. Specifically, phenolic acids are able to increase ROS production in mitochondrial and neutrophils, resulting in inflammation associated with tissue damage [188-190]. Additionally, phenylacetate is an active metabolite of phenylbutyrate, which can reduce neuroinflammation [191]. Whilst other phenylalanine metabolites were not changed resulting from arthritis inflammation.

TCA cycle as an aerobic process plays a critical role of energy metabolism, providing NADH or precursors for many biochemical reactions. We found that citric acid and *cis*-aconitic acid in TCA cycle were obviously decreased in patients' urine with RA, suggesting the anaerobic catabolism might be the major energy source for inflammatory individuals [192]. Moreover, it is worth pointing out the *N*-acetylcadaverine an acetylated polyamine generated by gut microbiome, was obviously increased in RA patients with the FC of 2.8 (p <0.001) [148].

Generally, phase II conjugated-metabolites after glucuronidation, acetylation, sulphation or glycine, *etc*, can increase their water solubility and then are excreted to urine, leading to reduced toxicity because of elimination of harmful moieties of endo/xenobiotics [193, 194]. In the study, we found that most conjugates, involving glycine-conjugates (vanilloylglycine), *N*-acetylvaline, sulfates (phenol sulphate and pyrocatechol sulfate), showed lower levels (FC <0.5) in patients with

RA. It implicated decreased capability of detoxification by phase II reactions. In particular, galactosylhydroxylysine as a biomarker of bone resorption in serum and urine was elevated in RA patients, indicating that more galactosylhydroxylysine from bone damage were excreted into urine [195, 196].

Table 4.3 Altered metabolites with significant differences in urine samples based on platform of UHPLC-MS.

Classes	Metabolites	HMDB ID	MW	RT/min	FC (RA/Ctr)	*p*-value	VIP	MS pattern	Mode	Δ (ppm)
Tryptophan and kynurenine metabolism	3-Hydroxyanthranilic acid[1]	HMDB01476	153.0426	4.62	1.72	1.1E-04	2.92	80.0505, 108.0453, 136.0401	+	2
	5-Hydroxy-L-tryptophan[2]	HMDB00472	220.0848	4.26	1.54	1.5E-02	1.89	158.0584,175.0848, 132.0431, 221.0897	+	2
	3-Hydroxykynurenine[1]	HMDB0011631	224.0797	2.15	2.84	1.5E-03	2.43	208.0606,190.0500,180.0657, 110.0604,162.0551, 136.0395,152.0708, 99.0082,74.0237	+	2
	Kynurenine[1]	HMDB00684	208.0848	3.88	1.83	4.9E-03	2.17	94.0654,192.0651, 146.0597, 118.0651, 174.0546	+	2
	Indolelactic acid[1]	HMDB00671	205.0739	7.77	1.81	1.7E-02	1.87	118.0646, 130.0654, 146.0602, 160.0759, 170.0602, 188.0708,206.0814	+	2
	Dihydrobiopterin[2]	HMDB00038	239.1018	2.13	0.70	4.8E-02	1.38	196.0831,204.0883,222.0987,240.1094	+	2
	Indoxyl sulfate[2]	HMDB00682	213.0096	6.67	0.41	1.2E-02	14.92	79.9559, 80.9637, 132.0444, 212.0018	-	4
Phenylalanine	Phenylacetate[2]	HMDB0040733	136.0524	6.42	1.32	4.5E-02	1.54	65.0392,91.0547,94.0415, 109.0650,	+	2

and tyrosine								122.0360, 119.0490, 137.0592		
metabolism	Phenyllactic acid[1]	HMDB00779	166.0630	8.65	2.28	2.8E-05	3.19	121.0646,167.0698, 95.0494, 91.0545, 149.0230	+	2
	Dopamine[1]	HMDB00073	153.0790	1.71	1.39	5.6E-03	2.20	91.0546, 119.0492, 137.0596,154.0861	+	2
	Phenol sulphate[2]	HMDB60015	173.9987	5.81	0.45	9.8E-03	10.98	93.0332, 172.9905, 79.9559	-	4
TCA cycle intermediates and derivatives	Mesaconic acid/Citraconic acid (isomer)[1]	HMDB0000749 /HMDB00634	130.0266	0.98	0.35	2.1E-03	1.77	85.0291, 129.0181	-	4
	Cis-Aconitic acid [1]	HMDB00072	174.0164	1.01	0.32	4.7E-03	2.47	111.0075, 94.0285, 85.0280, 129.0182, 173.0082	-	3
	Citric acid[1]	HMDB00094	192.0270	0.98	0.44	3.8E-02	5.25	111.0074, 87.0073, 67.0191, 57.0330, 191.0191	-	3
Purine metabolism	Cytosine[1]	HMDB00630	111.0433	0.94	1.98	2.4E-03	2.29	112.0501,95.0238, 69.0450, 67.0294, 68.0134, 52.0187	+	1
	Hypoxanthine[1]	HMDB00157	136.0385	1.83	0.76	4.0E-02	1.62	137.0454, 110.0349, 119.0351, 94.0402, 55.0298,67.0296	+	2
	Guanine[1]	HMDB0000132	151.0494	1.45	0.60	5.5E-03	2.11	152.0554, 110.0342,128.0445,	+	2

								82.0399,55.0294		
Acylcarnitine metabolism	6-Keto-decanoylcarnitine[2]	HMDB13202	329.2202	8.01	0.52	2.4E-02	1.71	85.0289,253.1434,330.2274	+	3
	Malonylcarnitine[1]	HMDB02095	247.1056	1.45	1.31	2.8E-02	1.67	85.0293,144.1026,204.1242, 248.1139	+	2
	3-hydroxydecanoy carnitine[2]	HMDB61636	331.2359	7.48	1.74	2.3E-02	1.77	85.0290, 60.0817,332.2479	+	3
Ornithine and polyamine metabolism	N-Acetylcadaverine[2]	HMDB02284	144.1263	0.95	2.77	6.8E-03	2.09	145.1326, 128.1063, 69.0702,86.0600	+	2
	N-(3-acetamidopropyl) pyrrolidin-2-one[2]	HMDB61384	184.1212	4.56	1.27	2.5E-02	1.85	70.0656,126.0911, 98.06101, 143.1174, 167.1174, 185.1278	+	3
	Vanilloylglycine[2]	HMDB60026	225.0637	5.25	0.31	3.3E-03	1.05	224.0563, 180.0658, 164.0343, 123.0440, 100.0227, 74.0232	-	3
Phase II metabolism	N-acetylvaline[2]	HMDB0011757	159.0895	4.31	0.48	1.8E-02	1.04	116.0703, 112.0755, 114.0911, 158.0813, 58.0282,140.0707	-	4
	Pyrocatechol sulfate[2]	HMDB59724	189.9936	5.42	0.44	3.1E-03	5.76	109.0282,188.9857	-	4
	Testosterone glucuronide[2]	HMDB03193	464.2410	10.09	0.60	9.9E-03	1.85	271.2050, 289.2156, 189.1271,465.2475	+	3
	Galactosylhydroxylysine[2]	HMDB00600	324.1533	0.73	1.40	2.0E-02	1.77	307.1500, 163.1073,	+	2

	Hexanoylglycine[2]	HMDB00701	173.1052	7.32	1.91	8.0E-04	2.70	128.0704,145.0968,325.1598, 174.1113, 99.0804, 76.0393, 71.0856	+	2
Others	N-Acetylneuraminic acid[2]	HMDB00230	309.1060	1.09	1.83	2.5E-03	2.27	274.0921, 310.1141, 292.1026, 250.0922, 232.0817, 167.0340, 121.0286,112.0396,60.0452	+	2
	Threonic acid[2]	HMDB00943	136.0372	0.90	1.40	4.7E-02	1.91	75.0071, 59.0122, 117.0180, 135.0288	-	4
	Gluconic acid[1]	HMDB0000625	196.0583	0.89	2.09	1.5E-03	2.47	75.0071, 59.0122, 99.0074, 195.0504, 177.0397	-	2
	Glutamylphenylalanine[2]	HMDB00594	294.1216	5.57	1.61	1.1E-02	1.99	120.0813, 166.0868, 84.0452,278.1030,295.1297	+	3

Notes:

[1]represents the compound identified by commercial available chemicals, [2] represents the compound identified by comparing exact mass of parent ion and MS fragmentation of samples with those of database (Metlin or/and HMDB), MW represents molecular weight, FC represents fold change.

Table 4.4 Altered metabolites without significant differences in urine samples.

Classes	Metabolites	HMDB ID	MW	RT/min	FC (RA/Con)	*p*-value	VIP	Mode	MS pattern	Δ (ppm)
caffeine metabolism intermediates and derives	Caffeine[2]	HMDB01847	194.0804	5.76	0.41	1.3E-01	1.18	+	138.0669, 110.0721, 69.0458,83.06124,195.0887	3
	1-Methyluric acid[2*]	HMDB03099	182.0440	3.63	0.26	8.5E-02	2.13	-	181.0360, 138.0299, 108.0442, 83.0237, 96.0190	3
	3-methylxanthine[2]	HMDB0001886	166.0491	4.12	0.17	1.0E-01	1.67	-	165.0406,122.0298,65.9970	4
	Xanthine[1*]	HMDB0000292	152.0334	2.08	0.78	6.5E-02	1.39	+	55.0299,82.0405,110.0351,128.0455,153.0406	2
purine metabolism	Adenosine[1]	HMDB00050	267.0968	3.09	1.15	2.0E-01	1.09	+	136.0618, 268.1039	2
	Uric acid[2]	HMDB00289	168.0283	1.90	1.70	5.1E-02	3.10	-	167.0200 124.0142, 96.0190,69.0079	3

intermediates and derives	5-Methylcytidine[2]	HMDB00982	257.1012	1.62	1.21	1.2E-01	1.23	+	258.1072, 126.0654, 109.0392	2
	5'-Methylthioadenosine[2]	HMDB01173	297.0896	4.87	1.33	1.3E-01	1.18	+	136.0608,163.0410,298.0945	3
	7-Methylguanine[2]	HMDB00897	165.0651	1.73	0.89	1.3E-01	1.11	+	166.0730,124.0507,149.0464, 107.0248	2
	3-Hydroxyhippuric acid[2]	HMDB0006116	195.0532	7.24	0.15	3.1E-01	2.76	-	93.0333, 150.0550,194.0453	3
tyrosine metabolism intermediates and derives	Tyrosine[1]	HMDB00158	181.0739	2.48	1.61	1.2E-01	1.28	+	165.0532, 136.0745, 119.0483, 123.0432,91.0540, 95.0488,182.0796	2
	Homovanillic acid sulfate[2]	HMDB0011719	262.0147	5.05	0.37	5.4E-02	1.09	+	181.0498,261.0076, 166.0261, 135.0442, 119.0489,	2
	Hydroxyphenylacetylgly-cine[2]	HMDB00735	209.0688	3.30	1.44	5.9E-02	1.46	+	210.0765, 192.0660, 150.0554,	2
histidine metabolism	Histidine[1]	HMDB00177	155.0695	1.01	0.78	1.6E-01	1.09	+	110.0714,156.0766, 93.0451, 83.0608,56.0502	2

intermediates	*N*-Acetylhistidine[2]	HMDB32055	197.0800	0.95	0.88	2.3E-01	1.12	+	110.0717, 83.0610, 156.0769,180.0769,198.0875	2
acylcarnitines	3-Methylglutarylcarnitine[2]	HMDB00552	289.1525	4.42	1.36	1.6E-01	1.20	+	85.0288, 231.0859,290.1593,129.0544,60.0814,	3
	Hexanoylcarnitine[2]	HMDB00756	259.1784	7.14	1.29	2.0E-01	1.04	+	260.1854,201.1120,85.0289	3
	Glutarylcarnitine[2]	HMDB13130	275.1369	3.29	1.19	1.4E-01	1.16	+	85.0292,144.1023,276.1448	2
	Methylmalonylcarnitine[1]	HMDB0013133	261.1212	2.32	0.82	7.7E-02	1.36	+	85.0290, 103.0393	2
ornithine and polyamine metabolites and derivatives	Homocitrulline[2]	HMDB00679	189.1113	0.95	1.18	1.4E-01	1.15	+	84.0805,127.0870,144.1134, 190.1192, 173.0925	2
	N^1-Acetylspermidine[2]	HMDB01276	187.1685	0.87	1.21	9.8E-02	1.18	+	72.0817, 100.0764, 114.0919,171.1496, 188.1762	2
	N-Acetylhistamine[2]	HMDB13253	153.0902	0.95	1.59	8.8E-02	1.37	+	95.0609, 112.0873, 83.0610,68.0503,136.0481,154.0975	2

	Valerylglycine[2]	HMDB0000927	159.0895	0.97	3.07	1.4E-01	1.14	+	160.0955,114.0907, 142.0805,96.0804	1
	2-Methylbutyrylglycine[2]	HMDB0000339	159.0895	5.30	1.25	1.7E-01	1.23	+	55.0559, 72.0819, 114.0910	3
Phase II conjugates	Dihydroferuloylglycine[2]	HMDB41725	253.0950	5.90	1.81	1.0E-01	1.29	+	137.0591, 179.0694, 76.0396, 254.1010	3
	7-Ketodeoxycholic acid[2]	HMDB00391	406.2719	11.45	0.64	1.1E-01	1.21	+	335.2363,353.2468,371.2574,389.2679, 407.2785,	3
	Hydroxyprolyl-Histidine[2]	HMDB28865	268.1172	1.45	0.81	1.4E-01	1.06	+	269.1227, 156.0759, 110.0709,223.1175,251.1123	2
dipeptides	Beta-aspartyl-*L*-glutamic acid[2]	HMDB11164	262.0801	1.31	1.29	1.7E-01	1.05	+	70.0292,84.0447,102.0550,148.0599,164.9200,182.0442,199.0706,245.0758, 263.0864	2
	Prolyl-Aspartate[2]	HMDB02335	230.0903	1.53	1.15	1.2E-01	1.27	+	231.0962, 70.0654,	2
	Prolylhydroxyproline[2]	HMDB0006695	228.1110	1.44	1.33	1.4E-01	1.18	+	70.0660,132.0660,211.0719,229.1189	2

	Glycylproline[2]	HMDB00721	172.0848	0.96	1.16	1.9E-01	1.01	+	70.0651,173.0904, 127.0854, 116.0697	2
	2-Hydroxycinnamic acid[2]	HMDB0002641	164.0473	5.52	1.54	8.0E-02	1.61	+	165.0543,147.0437,137.0595, 123.0440, 119.0492, 91.0545,79.0547	3
	N_2-Succinyl-L-ornithine[2]	HMDB01199	232.1059	1.88	1.23	1.7E-01	1.11	+	233.1130 216.0870 170.0810	3
	Threoneopterin[2]	HMDB00727	253.0811	1.45	1.27	1.4E-01	1.12	+	254.0889,236.0783,206.0678,218.0677,190.0728,154.0727,182.0677,154.0727	2
others	Spermine dialdehyde[2]	HMDB13076	200.1525	5.23	0.54	1.2E-01	1.03	+	86.0967,128.1067,145.1331,183.1486, 201.1590	2
	4-O-Methylgallic acid[2]	HMDB13198	184.0372	6.99	0.45	1.2E-01	1.21	+	139.0290,167.0340,185.0447,97.0288, 111.0446,69.0342	2
	Cis-5-Decenedioic acid[2]	HMDB13227	200.1049	6.97	1.28	1.1E-01	1.25	+	155.1070, 137.0964, 165.0901,	2

									183.1021,201.1126	
	Ethylbenzene[2]	HMDB59905	106.0783	6.69	1.36	1.0E-01	1.27	+	91.0549,79.0550,65.0394,53.0395,95.0498,107.0497	2
	Lactic acid[2]	HMDB00190	90.0317	0.99	0.47	8.9E-02	1.33	-	71.0143	5

Notes:

[1]represents the compound identified by commercial available chemicals, [2] represents the compound identified by comparing exact mass of parent ion and MS pattern of sample with those of database (Metlin or/and HMDB),

MW represents molecular weight, FC represented fold change, * represents metabolites belonged into purine metabolites.

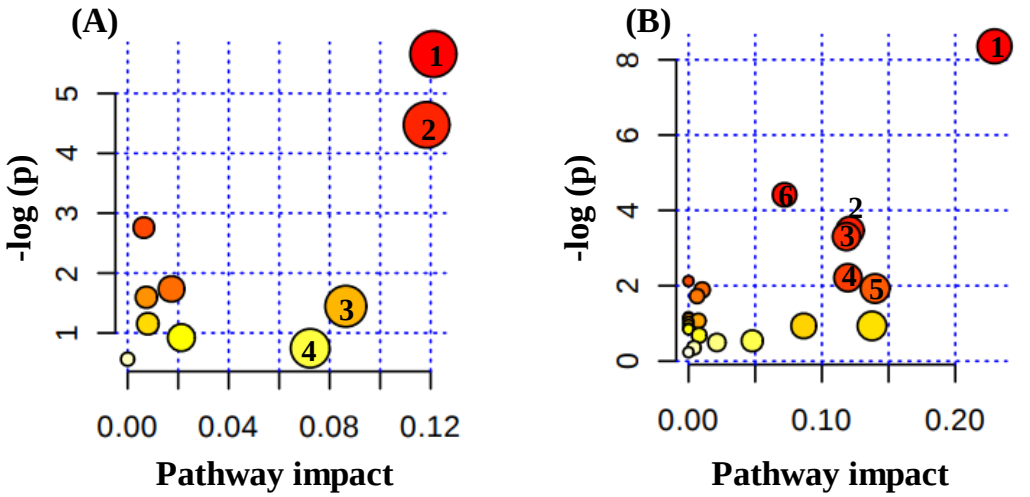

1: Tryptophan metabolism
2: Citrate cycle (TCA cycle)
3: Pentose phosphate pathway
4: Tyrosine metabolism

1: Caffeine metabolism
2: Tryptophan metabolism
3: Citrate cycle (TCA cycle)
4: Tyrosine metabolism
5: Histidine metabolism
6: purine metabolism

Figure 4.5 Pathway analysis of altered metabolites in urine samples.

(A) Pathway analysis plot of significantly changed metabolites (p <0.05), (B) Pathway analysis plot of changed metabolites without significant differences between RA and control groups.

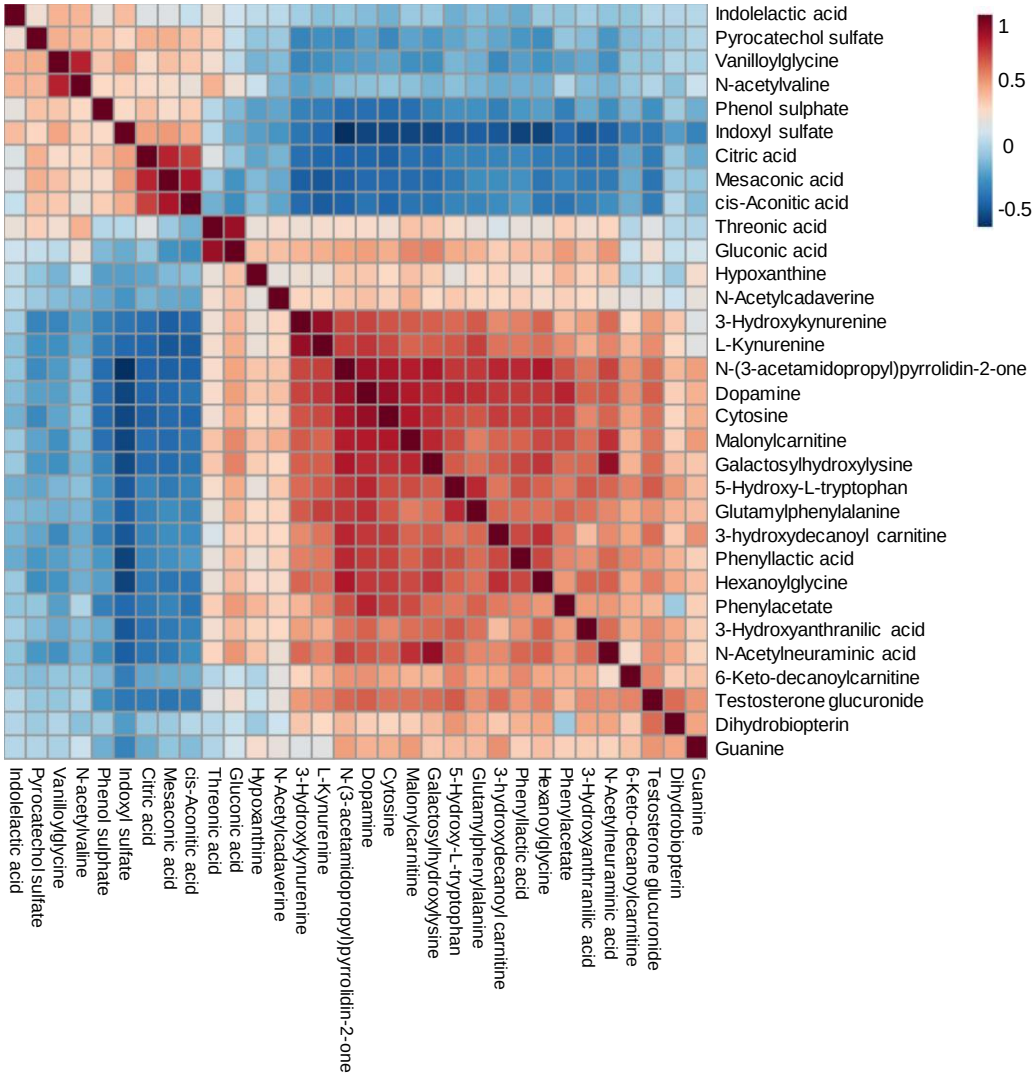

Figure 4.6 Correlation analysis of altered metabolites in urine samples.

4.3.2.2 Abnormal metabolites in serum samples

Based on OPLS-DA model from LC-MS and GC-MS data, a total of 34 abnormal metabolites were significantly changed in response to RA, including 18 metabolites found in positive ion mode of LC-MS, 10 metabolites in negative ion mode of LC-MS and 8 metabolites from GC-MS (2 metabolites found both in negative and positive ion mode of LC-MS, 2 metabolites found both in positive

ion mode of LC-MS and GC-MS, as shown in Figure 4.7A, Table 4.5 and Table 4.6). The metabolites were classified into amino acids and derivatives, acylcarnitines, organic acids and derivatives, fatty acids, *etc*. According to Figure 4.7B, pathways including glycine, serine and threonine metabolism, aminoacyl-tRNA biosynthesis, tryptophan metabolism were important for arthritis inflammation.

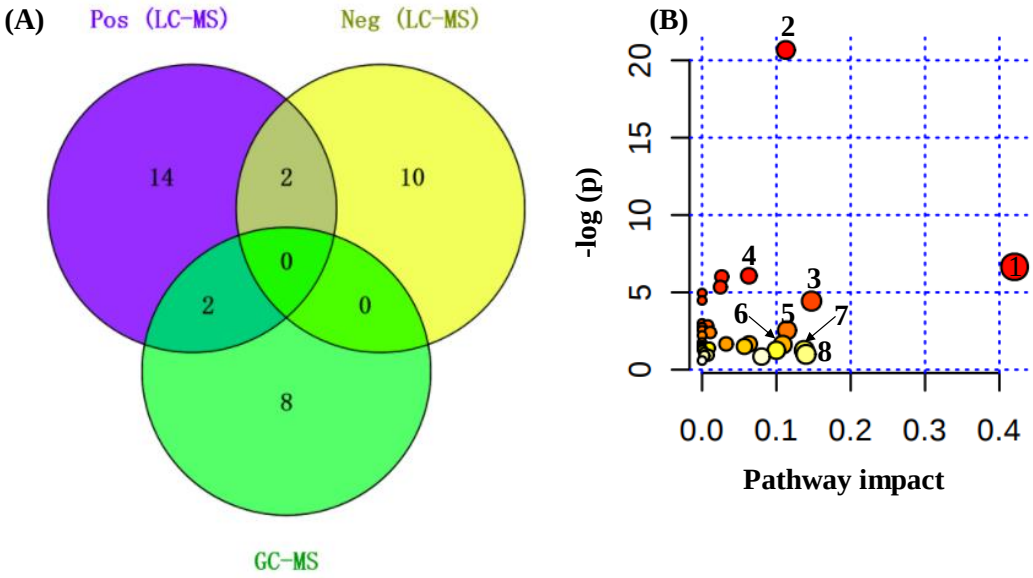

Figure 4.7 Venn diagram (A) and pathway analysis (B) of altered metabolites in serum samples.

(A) Venn diagram of altered metabolites, (B) pathway analysis plot, 1: Glycine, serine and threonine metabolism, 2: Aminoacyl-tRNA biosynthesis, 3: Lysine degradation, 4: Cysteine and methionine metabolism, 5: Ascorbate and aldarate

metabolism, 6: Tryptophan metabolism, 7: Pyruvate metabolism, 8: Histidine metabolism.

Tryptophan metabolism is closely associated with inflammation and immune system in RA patients [19, 99, 197]. In serum samples, tryptophan metabolism intermediates were perturbed in RA patients. Indolelactic acid as a product of tryptophan was up-regulated (FC=1.44, p <0.01) in RA individuals comparing with healthy controls, while tryptophan, indoxyl sulfate were significantly down-regulated. Moreover, indole-derived indoleacrylic acid (FC=0.87, p <0.001), 1H-Indole-3-carboxaldehyde (FC=0.87, p <0.001), 3-indoleproponic acid (FC=0.87, p >0.05) were decreased in arthritis patients.

Phenylalanine metabolites, level of phenyllactic acid and *p*-cresol sulfate in inflammatory patients was 1.5-fold of healthy controls. Due to the capability of *Lactic acid bacteria* (LAB), phenyllactic acid was produced from phenylalanine and could inhibit bacteria growth [198]. Here, up-regulation of phenyllactic acid in inflammatory arthritis (FC=1.57, p <0.0001) complement with the finding of overexpression of *Lactobacillus salivarius* in RA individuals, *esp.* under active RA inflammatory condition [111].

Lactic acid is likely to be accumulated in inflammatory conditions, and it is converted from food carbohydrates by lactic acid bacteria (LAB) [199]. As reported, lactic acid, indolelactic acid and phenyllactic acid are inflammatory mediators, which can inhibit proinflammatory cytokine IL-6 [199]. Furthermore,

comparing with healthy controls, amino acids were altered in RA patient blood samples (Figure 4.8). Tryptophan, methionine, valine, isoleucine, threonine, lysine and histidine belonging to essential amino acids, were down-regulated in RA suffers with or without significant differences, suggesting insufficient amino acids for energy metabolism and protein biosynthesis. Meanwhile, level of conditional essential amino acid in RA including tyrosine and glycine were also less than that of healthy controls, while cystine as product of cysteine was increased. Tryptophan, threonine, lysine, alanine were down-regulated in patients with RA, which is similar to previous studies [18, 19]. Additionally, as a substrate donor of the TCA cycle, valine was lower level in inflamed individuals [200], which is of the same tendency to TCA cycle intermediates detected in urine samples. Serine and alanine as alternative nutrient like glucose in cancer cells were also decreased in RA individuals [201].

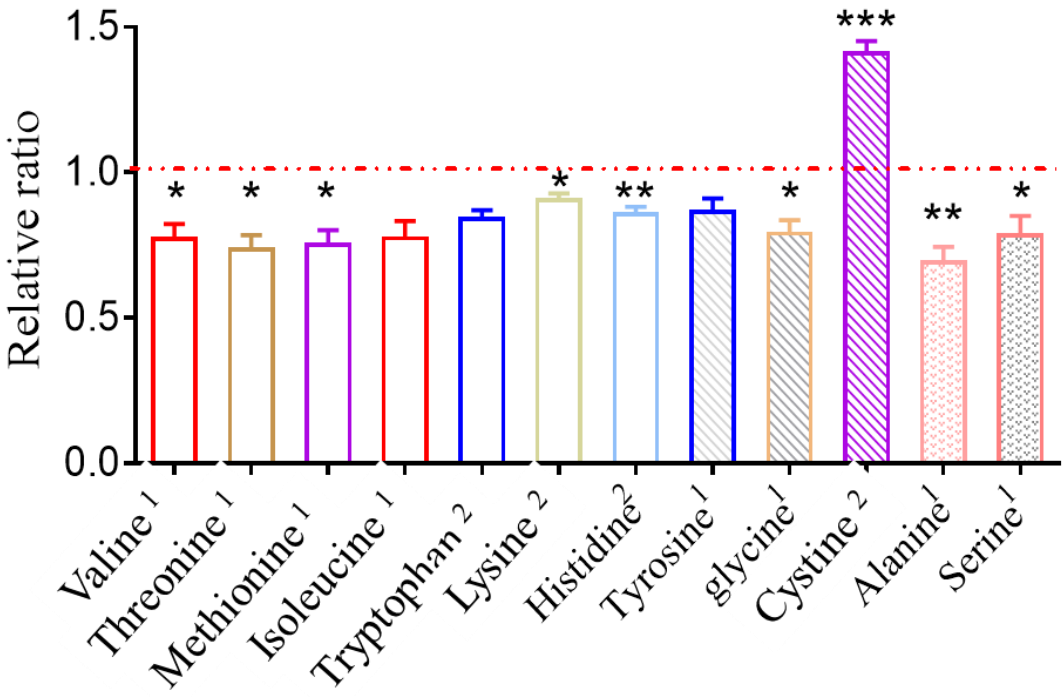

Figure 4.8 Relative ratio of altered amino acids of RA patients compared with healthy controls.

[1] represents the amino acids analyzed by using GC-MS, [2] represents the amino acids analyzed by using LC-MS. Error bar represented SEM. * $p < 0.05$, ** $p < 0.01$, *** $p < 0.001$.

Table 4.5 Altered metabolites in serum samples based on platform of LC-MS.

Metabolism	Metabolites	HMDB ID	Exact mass	RT/min	FC (RA /Ctr)	*p*	VIP	MS Pattern	Mode	Δ(ppm)
Tryptophan and indole metabolism	Tryptophan*	HMDB0000929	204.0899	5.52	0.86	2.1E-01	2.4	203.0821, 159.0923, 142.0657, 116.0501, 74.0244,	-	4
	Indolelactic acid	HMDB0000671	205.0739	8.08	1.44	2.4E-03	1.9	204.0661, 158.0606,142.0657, 116.0501, 72.9927,128.0501,	+/-	4
	Indoleacrylic acid	HMDB0000734	187.0633	5.45	0.87	1.8E-04	1.6	188.0702, 170.0602,115.0540, 89.0400	+	0
	1H-Indole-3-carboxaldehyde	HMDB0029737	145.0528	5.45	0.87	2.1E-04	1.5	91.0541, 118.0649, 146.0598	+	0
	3-Indolepropionic acid*	HMDB0002302	189.0790	9.89	0.28	4.3E-03	0.7	130.0651, 172.0756, 190.0862, 55.0182	+	1
	Indoxyl sulfate*	HMDB0000682	213.0096	6.89	0.84	2.8E-01	2.4	132.0450,79.9570, 80.9648	-	4
phenylalanine	3-Phenyllactic acid*	HMDB00748	166.0630	7.67	1.57	3.3E-05	1.5	165.0552, 147.0446,	-	7

and tyrosine metabolism	*p*-cresol sulfate	HMDB0011635	188.0143	7.80	1.52	1.9E-01	7.8	119.0498,72.9927 107.0498, 79.9570, 80.9648, 187.0066	-	6
	Salicylic acid*	HMDB0001895	138.0317	9.10	2.52	1.4E-01	1.6	93.0342, 137.0239, 65.0393	-	10
cysteine and methionine metabolism	Methionine*	HMDB0000696	149.0510	1.47	0.86	2.7E-03	1.1	133.0318, 150.0584, 104.0529, 87.0264, 61.0501	+	0
	Cystine	HMDB0000192	240.0238	0.88	1.36	4.9E-07	1.5	74.0235, 120.0112, 122.0268,151.9832, 241.0306	+	1
	Serine*	HMDB0000187	105.0426	0.87	0.91	4.0E-02	0.6	60.0445, 70.0652, 88.0394, 106.0499		4
	Methionine sulfoxide	HMDB0002005	165.0460	1.48	0.78	2.1E-06	1.6	74.0237, 102.0550, 149.0267, 166.0533	+	1
lysine biosynthesis and degradation	Pipecolic acid	HMDB0000716	129.0790	0.94	1.62	1.1E-03	1.6	84.0808, 130.0863	+	1
	Lysine*	HMDB0000182	146.1055	0.76	0.90	1.0E-02	1.3	84.0809, 130.0863, 67.0543	+	0
fatty acid	Hexanoylcarnitine*	HMDB0000756	259.1784	7.41	1.37	8.2E-03	1.1	85.0285,260.1854, 201.1121,	+	1

metabolism								60.0809		
	2-Octenoylcarnitine	HMDB0013324	285.1940	8.62	0.74	2.7E-03	1.7	85.0285, 227.1276, 286.2010	+	0
	LysoPC(22:6)	HMDB0010404	567.3325	14.69	1.21	3.4E-02	1.3	184.0733, 104.1070, 568.3395	+	0
	LysoPC(18:2)	HMDB0010386	519.3325	14.66	0.78	4.2E-04	1.5	104.1068, 184.0730, 520.3392, 502.3285	+	0
	LysoPC(18:3)	HMDB0010387	517.3168	13.83	0.81	4.6E-01	1.1	104.1070, 184.0732, 518.3238	+	1
ascorbate and aldarate metabolism	Ascorbic acid*	HMDB0000044	176.0321	1.51	0.72	6.8E-02	1.1	87.0084, 115.0032, 175.0243, 59.0134	-	7
others	C16 sphingosine-1-phosphate	HMDB0060061	351.2175	12.06	0.79	2.6E-03	0.5	78.9587,350.2096, 173.4071	-	2
	Gulonic acid	HMDB0003290	196.0583	0.92	1.25	2.0E-02	0.7	75.0084,129.0188,195.0505	-	6
	Histidine*	HMDB0000177	155.0695	0.87	0.88	8.2E-03	0.9	137.0352,110.0719,93.0454	+/-	8
	Bilirubin	HMDB0000054	584.2635	14.83	0.75	1.7E-02	0.6	285.1240,253.1343,583.2557	-	2
	Uric acid	HMDB0000289	168.0283	0.96	0.90	4.5E-02	4.2	167.0206,124.0148,96.0200,69	-	7

								.0091		
	Citric acid*	HMDB0000094	192.0270	0.97	7.32	3.1E-01	3.4	111.0083,191.0193,129.0189,87.0084	-	6
	Glycyl-valine	HMDB0028854	174.1004	2.18	2.59	1.2E-02	2.2	72.0809, 118.0863,129.1022	+	1

Note:

*represents compound identified by authentic standard.

Table 4.6 Altered metabolites in serum samples based on platform of GC-MS.

Metabolism	Match	RT/min	VIP	HMDB ID	FC (RA /Ctr)	*p*	Fragmentation ions	Match	R match
Pyruvate metabolism	Lactic acid (2TMS)	7.62	7.2	HMDB00190	1.35	1.4 E-02	147,73,117,191,148,190,45,75,133,118	958	965
Cysteine and	Methionine (2TMS)	17.40	0.9	HMDB00696	0.76	9.8 E-03	176, 128, 73,147,61,45	766	793
methionine	Alanine (2TMS) [1]	8.45	1.8	HMDB00161	0.69	6.3E-03	116,73,147,117,190,45	938	942
metabolism	Serine (3TMS)	14.20	2.0	HMDB00187	0.76	3.5E-02	204,73,218,147,100,205,45,	930	934
BCAA metabolism	Valine (2TMS)	10.90	4.3	HMDB00883	0.78	2.4E-02	144,73,218,145,147,100	943	945
	Isoleucine (2TMS)	12.68	3.0	HMDB00172	0.79	1.1E-01	158,73,218,159,45,147,74,100	832	873
Glycine, serine and threonine metabolism	Threonine (3TMS)	14.80	2.0	HMDB00167	0.77	3.3E-02	73,117,218,219,147,101,291,56,45	921	924
lysine biosynthesis and degradatioin	N-α-Acetyl-L-Lysine (3TMS)	23.60	0.6	HMDB01550	0.80	2.4E-02	174,73,175,86,156,75,59	748	780

Note:

[1] represents alanine belonged to glycine, serine and threonine pathway.

4.3.3 Targeted metabolomics study of tryptophan and phenylalanine metabolites

For screening more metabolites in tryptophan and phenylalanine metabolism, we performed on target analysis of 19 compounds by using LC-QqQ MS, due to advantages of high-throughput, good sensitivity and reproducibility. Method validation of determination of the above compounds was conducted, including linearity, precision, recovery, LOD and LOQ. The results of method validation showed good linearity (r^2 > 0.9906), intra-day precision (< 5.0 %) and inter-day precision (< 13.1 %) and sensitivity (shown in Table 4.7), indicating the method is reliable and reproducible and could be successfully applied in biological samples.

Table 4.7 Method validation of metabolites in tryptophan and phenylalanine metabolism by using LC-QqQ MS.

No.	Metabolites	Linearity range (ng mL^{-1})	r^2	Intra-day Precision (RSD %)	Inter-day precision (RSD %)	LOD (RSD %)	LOQ (RSD %)	Recovery (RSD %)
1	3-Indolepropionic acid	2.5-5000	0.9906	3.3	0.6	0.3	0.9	100.6
2	Indole	50-5000	0.9992	0.9	2.7	15	50	ND
3	3-Indoleacetonitrile	50-5000	0.9988	4.6	2.4	3	9	95.8
4	5-Hydroxyindoleacetic acid	2.5-5000	0.9946	5	11.6	0.3	0.9	98.5
5	Noradrenaline	50-5000	0.9978	1.4	2	10	40	98.9
6	Epinephrine	50-5000	0.9989	0.9	2.1	4	12	98.4
7	Dopa	5.0-5000	0.9958	0.9	1.7	1	3	96.5

8	Quinolinic acid	10-5000	0.9974	1	1.2	2.5	10	97.9
9	Dopamine	5.0-5000	0.9972	0.7	1.7	2	5	96.1
10	3-Hydroxykynurenine	2.5-5000	0.9994	0.5	3.2	1	2.5	101.1
11	Tyrosine	2.5-5000	0.9988	1	1.3	1	2.5	99.4
12	Serotonin	5.0-5000	0.9993	0.5	1.7	1	4	99.8
13	Kynurenine	2.5-5000	0.9975	0.6	2.3	NP	< 2.5	99.3
14	Phenylalanine	2.5-5000	0.9922	0.6	3.4	NP	< 2.5	96.1
15	3-Hydroxyanthranilic acid	50-5000	0.9991	0.5	3.4	10	45	102.7
16	Tryptophan	2.5-5000	0.9949	2.9	3.1	NP	< 2.5	103.7
17	Kynurenic acid	2.5-5000	0.9969	0.8	1.7	0.3	1	95.7
18	Anthranilic acid	5.0-5000	0.9939	0.8	7.9	2	5	93.6
19	Melatonin	2.5-5000	0.9922	3	4.7	NP	<2.5	98.3

Notes:

ND represents not detected, NP represents not performed.

On basis of abnormal urinary metabolites in global metabolomics, in targeted metabolomics analysis 5 metabolites were up-regulated with significant differences in RA patients (Figure 4.9), namely kynurenine, 3-hydroxykynurenine, anthranilic acid, 3-hydroxyanthranilic acid and 5-hydroxy-indoleacetic acid. In view of tryptophan-kynurenine metabolism (Figure 4.10), most urinary tryptophan derived metabolites were up-regulated apart from kynurenic acid (KYNA), which serves as anti-inflammatory mediator through reducing production of pro-inflammatory cytokines in nervous diseases [202]. In the targeted analysis of phenylalanine metabolites, no significant alteration of most metabolites was observed except up-regulated dopamine (Figure 4.11).

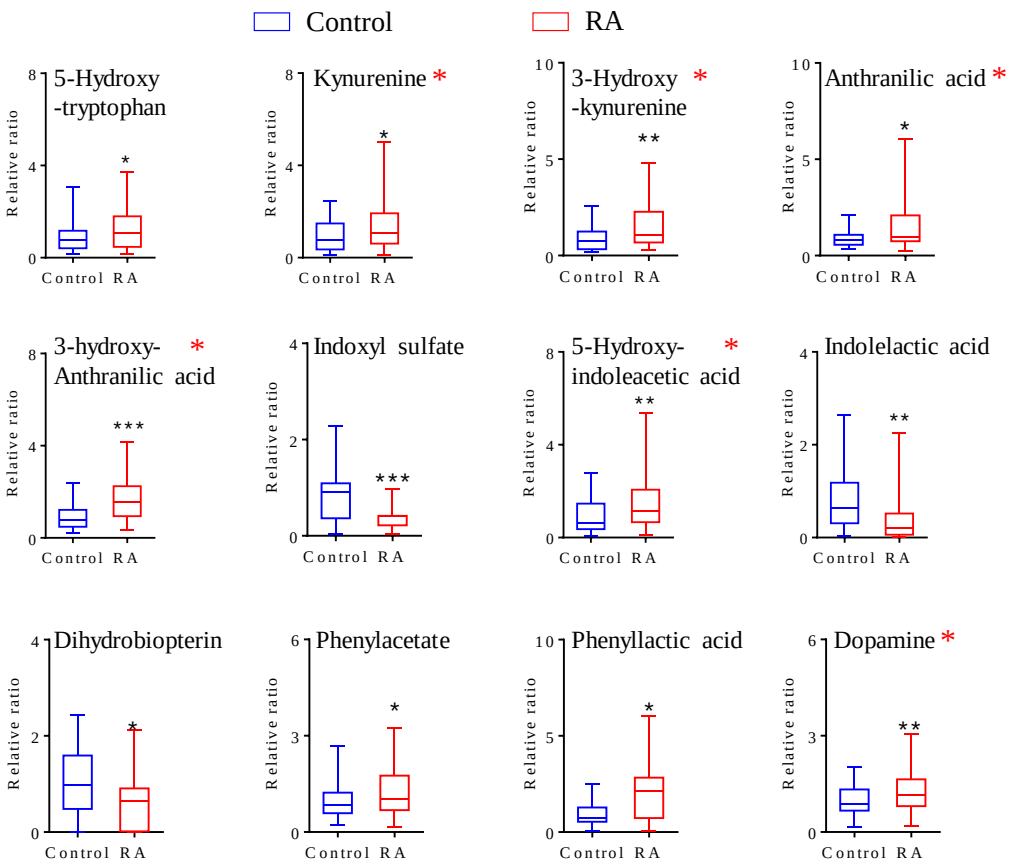

Figure 4.9 Significantly altered urinary metabolites in tryptophan and phenylalanine metabolism in responding to RA.

Red * represents metabolites detected by using LC-QqQ MS. * p <0.05, ** p <0.01, *** p <0.001.

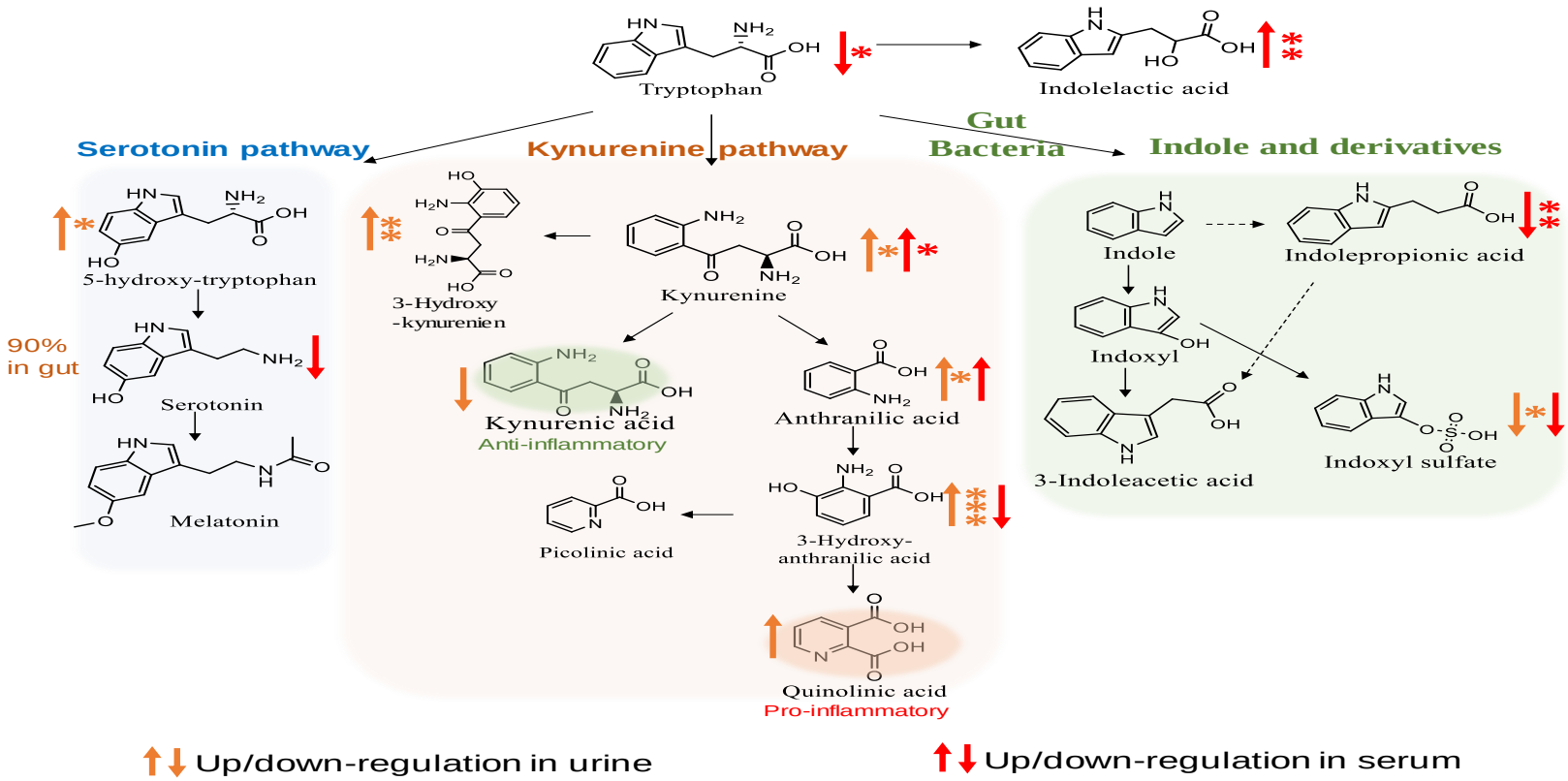

Figure 4.10 Alteration of urinary and serum metabolites in tryptophan phenylalanine metabolism. Yellow arrows represent up/down-regulation in urine of RA patients, while red arrows represent up/down-regulation in serum of RA patients compared with levels of those metabolites in healthy controls. * p <0.05, ** p <0.01, *** p <0.001.

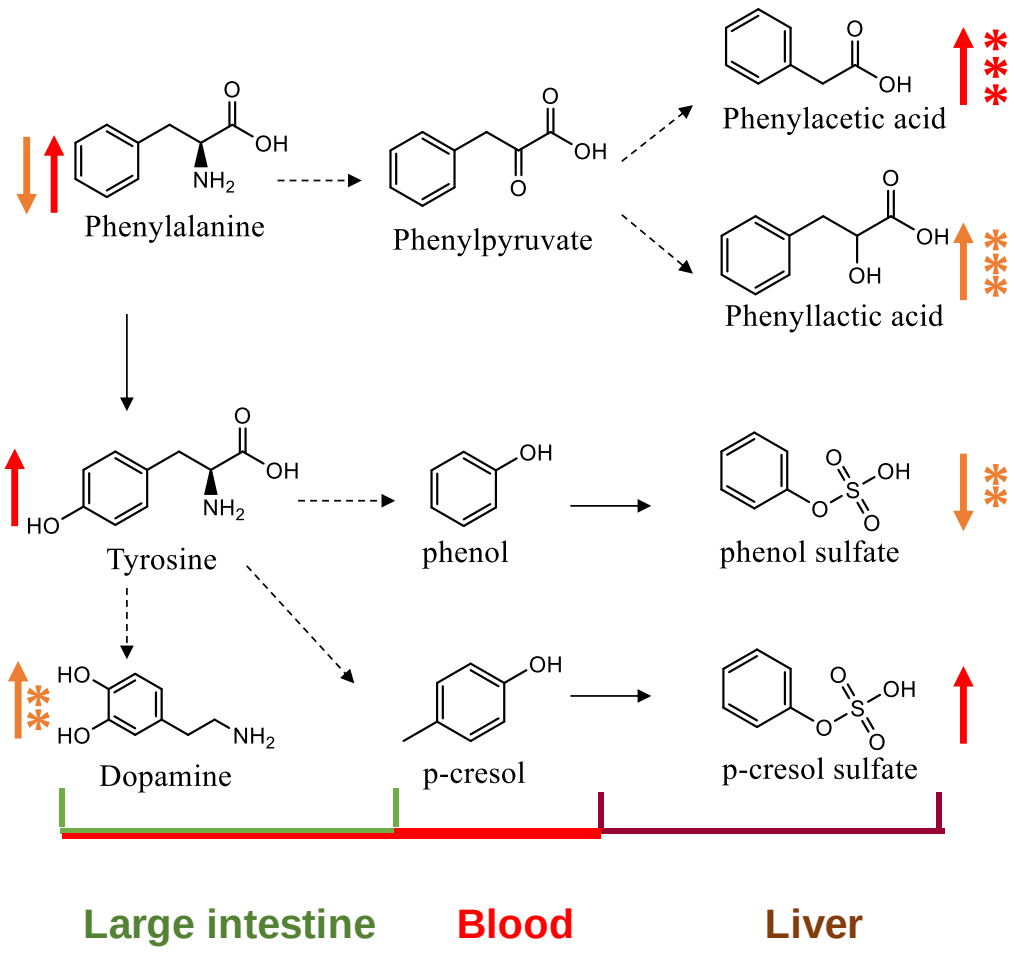

Figure 4.11 Alteration of urinary and serum metabolites in phenylalanine metabolism.

Yellow arrows represent up/down-regulation in RA patients' urine, while red arrows represent up/down-regulation in RA patients' serum compared with levels of those metabolites in healthy controls. * p <0.05, ** p <0.01, *** p <0.001.

For serum metabolites in tryptophan metabolism, on the one hand, KYN and 5HIAA were markedly up-regulated while tryptophan and HKYN decreased in RA individuals (Figure 4.12 and Figure 4.10). The results showed that tryptophan metabolism may be activated in response to RA inflammation. Moreover, by combining global metabolomics analysis, we found that tryptophan and tryptophan-derived metabolites were reduced probably resulting from catabolism by microbials, such as indoleacrylic acid (p <0.001), 3-indolpropionic acid (IPA, p <0.01) and indoxyl sulfate (FC=0.84, p >0.05), while indolelactic acid (p <0.01) was increased in serum of patients with RA. However, kynurenic acid and quinolinic acid serving as anti-inflammatory and pro-inflammatory mediator, were not detected in serum in part due to less volume of sample by using this quantitative method. On the other hand, targeted phenylalanine metabolites were not changed significantly.

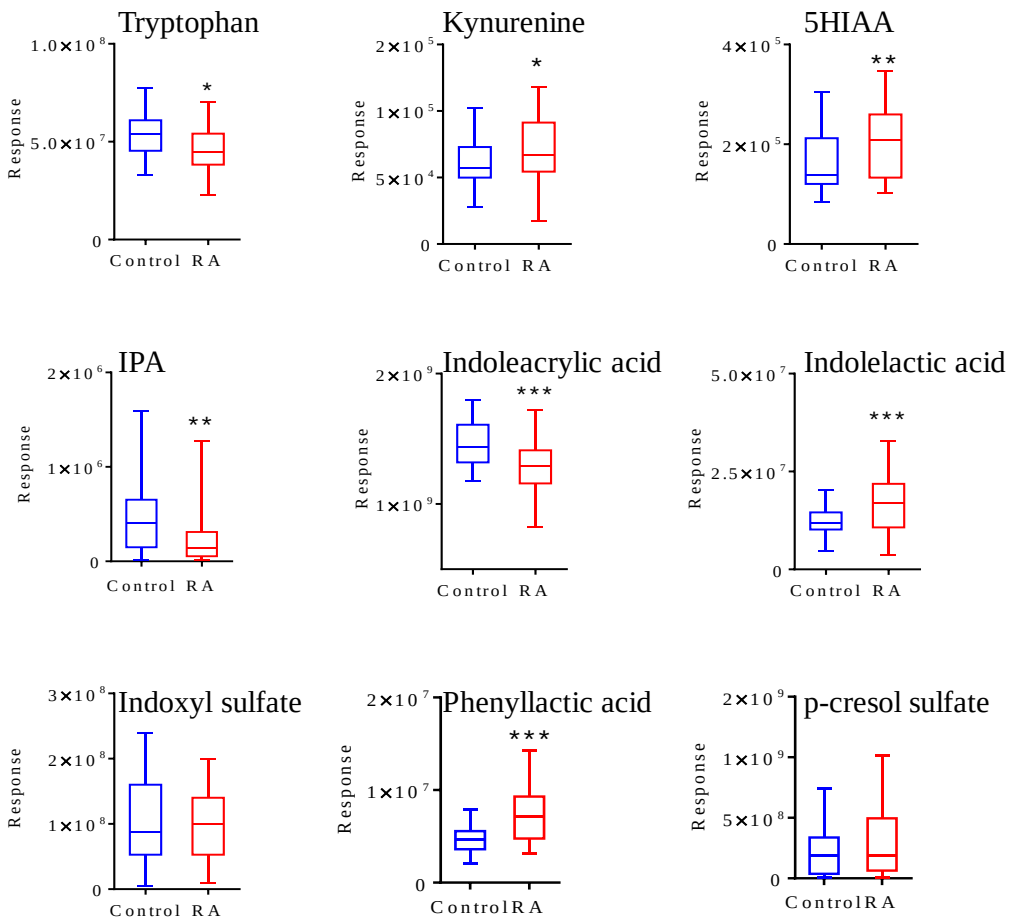

Figure 4.12 Altered metabolites of tryptophan and phenylalanine metabolism in serum.

5HIAA: 5-hydoxyindoleacetic acid, IPA: 3-indoleproponic acid. Red * represented metabolites detected by using LC-QqQ MS. * p <0.05, ** p <0.01, *** p <0.001.

Enzyme indoleamide-(2,3)-dioxygenase (IDO) and *tryptophan-2,3-dioxygenase* (TDO) is the first step to rate-limited catalyze the conversion of kynurenine from tryptophan. IDO contributes to oxidative stress by producing

harmful oxygen and hydroxyl radicals which may promote production of inflammatory cytokines, such as IL-6, TNF-α [203]. Therefore, IDO activity regulates cellular immune or inflammatory response. The ratio of kynurenine over tryptophan (KYN/Trp) is to evaluate IDO activity. In our study, IDO activity (KYN/Trp ratio, Figure 4.13) was obviously increased in the arthritis individuals due to significantly up-regulated KYN but almost the same level of Trp, which is consistent with serum samples from RA patients [204].

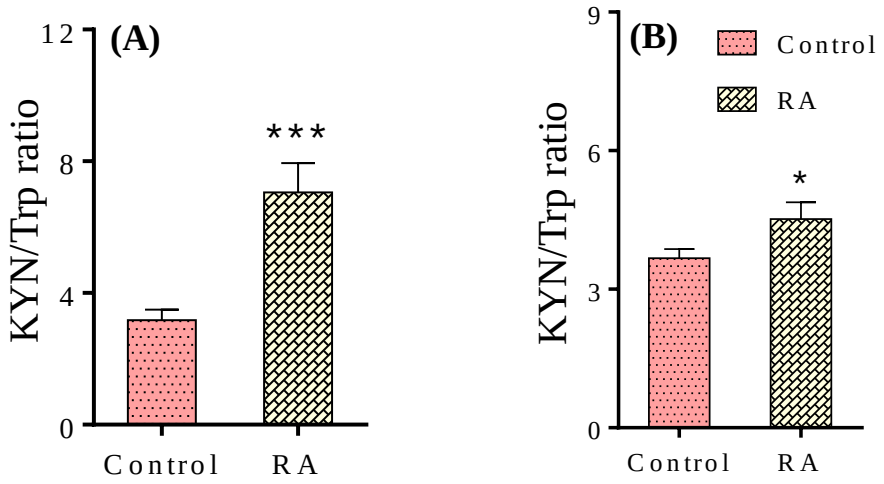

Figure 4.13 IDO activity (KYN/Trp) in urine (A) and serum samples (B).

Error bar represents SEM, * p <0.05, *** p <0.001.

4.3.4 Association of microbiome-derived metabolites with RA

As well known, tryptophan, phenylalanine and tyrosine as aromatic amino acid can be converted into indoles and phenols through gut microbiomes in

mammalians [205]. Intriguingly, apart from changes of most kynurenine pathway intermediates in RA patients, there were alteration of intestinal bacterial-related metabolites, such as indolelactic acid, HIAA, indoxyl sulfate and *p*-cresol sulfate. Moreover, malfunctions of gut microbiome may affect biosynthesis and utilization of host amino acids [206, 207]. In turn, the perturbation of amino acids as precursors for SCFAs may lead to imbalance of SCFAs which participate into the pathogenesis of many diseases [206, 208, 209].

Based on the altered metabolic features and microbiome-associated intermediates, we compared plots of receiver operating characteristic curve (ROC) analysis by using MetaboAnalyst as shown in Figure 4.14. For urinary metabolites, the area under the curve (AUC) of microbiome-related metabolites up to 0.881 (95% CI: 0.8-0.952), was close to AUC of all abnormal metabolites as 0.91 (95% CI: 0.837-0.975) caused by RA. According to the ROC curve from serum metabolites shown in Figure 4.15, AUC of metabolites in tryptophan and phenylalanine metabolism up to 0.84 (95% CI: 0.75-0.941), was close to AUC of all abnormal metabolites as 0.876 (95% CI: 0.771-0.978). The findings showed that microbiome-derived metabolites, in particular aromatic amino acid-derived metabolites such as indoles and phenols were closely associated with inflammation of RA, which was also consistent and in complement with previous studies [105, 111, 173].

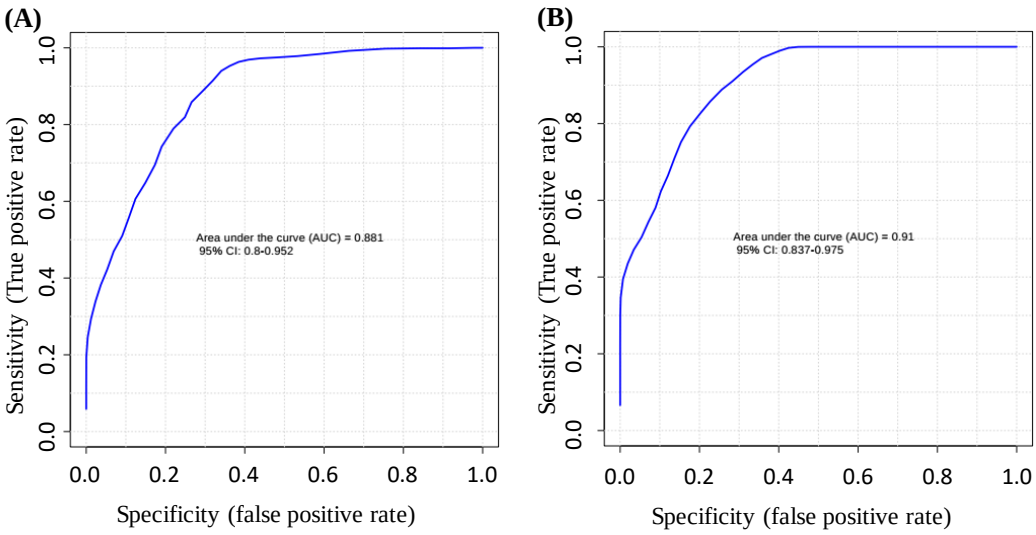

Figure 4.14 ROC curve analysis of microbiome-associated metabolites (A) and all altered metabolites (B) in urine between RA patients and healthy controls.

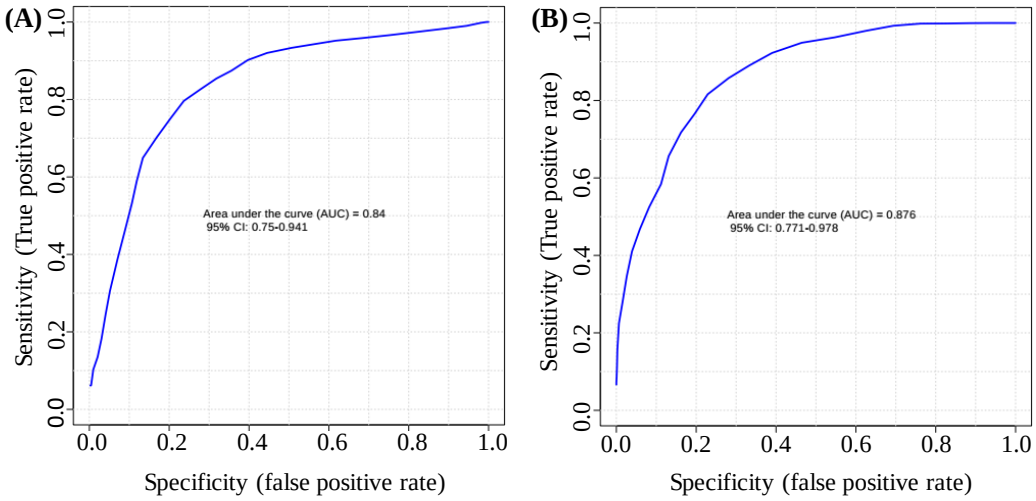

Figure 4.15 ROC curve analysis of (A) tryptophan and phenylalanine-derived metabolites related to microbiome and z(B) all altered metabolites in serum between RA patients and healthy controls.

4.4 Discussion

Identification of specific biomarkers helps to understand the mechanism of disease and differentiating disorders from healthy counterparts. Metabolomics serves as a powerful tool to reveal metabolic perturbations in response to disease. In the study, urinary and serum global metabolomics based on UHPLC-Orbitrap MS and GC-MS showed altered sorts of metabolites were attributed into amine acids metabolism (tryptophan metabolism, valine, leucine and isoleucine biosynthesis), aminoacyl-tRNA biosynthesis and TCA cycle, *etc.* (Figure 4.16). The altered metabolites, especially tryptophan, tryptophan-derived metabolites and branch-chain amino acids were associated with inflammation resulting from arthritis.

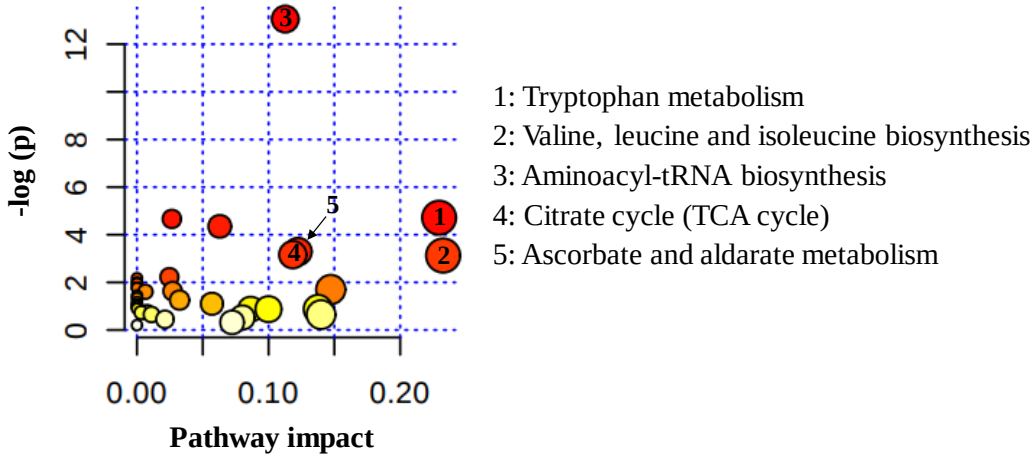

Figure 4.16 Perturbed pathway analysis of urinary and serum altered metabolites of patients with RA.

Tryptophan and phenylalanine metabolism contribute to inflammatory responses and immune activation for a range of physiological processes and biological disorders [210]. Tryptophan as an essential amino acid was mainly catabolized through kynurenine pathway and methoxyindole pathway, and the former pathway approximately accounted for 95% [205]. In the work, we found that decreased tryptophan and increased of kynurenine-derived metabolites (*e.g.* KYN, HKYN, AA) in RA patients were consistent with previous study [102, 204, 211]. Firstly, up-regulation of tryptophan-kynurenine pathway could promote the inflammation by CD4+ cells or dendritic cells through activation of IDO enzyme and neurotoxic N-methyl-D-aspartate (NMDA) agonist (*e.g.* quinolinic acid) and free radical generators [113]. On the one hand, tryptophan-associated metabolites serve inflammatory responses to arthritis disorders. 5-Hydroxyltryptophan crosstalk with NMDA antagonist-kynurenic acid, could partially restore the immune system by activating immune cells, enhancing the production of inflammatory cytokines and nitric oxide in lymphocytes and macrophages [212, 213]. 3-Hydroxy-kynurenine is a derivative of tryptophan and the precursor of kynurenic acid, which could activate the inducible nitric oxide synthase (iNOS) through proinflammatory cytokines (*e.g.* IFN-γ) to impair the cognition and to stimuli arthritis [204, 214]. There were evidences showed that KYN, HKYN and quinolinic acid exerted positively association with inflammation [210]. Under the status of activation of tryptophan pathway with pro-inflammatory stimulation,

down-regulated kynurenic acid may provide insufficient anti-inflammatory feedback to modulate and/or compensate the imbalanced immune responses [215]. On the other hand, IDO activation could inhibit proliferation of natural killer (NK) cells and T cells (CD4+ and CD8+ lymphocytes) [216], and expression of IDO is associated with the severity of animal collagen-induced arthritis [217]. However, the roles of tryptophan metabolites and enzyme are still not clear in pathogenesis of RA. In addition, other metabolites like indole- or phenol-derivatives from tryptophan and phenylalanine contribute to arthritis inflammatory responses. Indoleacrylic acid is converted from tryptophan and produced by commensal *Peptostreptococcus Species*, and its decreased level in the RA sera could suppress the anti-inflammatory capability of intestinal commensals in comparison with healthy controls [203]. Furthermore, indoles produced by commensal microbiota, plays vital roles in pro-and anti-inflammation in intestinal epithelial cells. The indole-derivatives, such as IAA, indoxyl sulfate, HIAA were functioned to increase the expression of anti-inflammatory genes [218]. Importantly, indolepropionic acid (IPA) and *p*-cresol sulfate were formed from tryptophan and tyrosine by huge numbers of anaerobic microorganisms in the human large intestine [219]. IPA is positively associated with level of probiotics in gut microbiome and negatively correlated with inflammation [220]. *p*-Cresol sulfate was reported to be positively associated with mucosal integrity and pro-inflammation [221]. Meanwhile, there are evidences showed that phenylacetic

acid and phenyllactic acid produced from phenylalanine participate into pro-inflammatory responses [222] and anti-inflammatory response by decreasing ROS production as antioxidant [188, 223], respectively. In addition, dopamine up-regulation may promote anti-inflammatory effects on patients with RA through inhibition of Il-6 and IL-8 by overexpression of dopamine receptors [224]. Taken together, the alteration of tryptophan-kynurenine and phenylalanine metabolism affected the imbalance of immune system of RA host by GM-modulation (shown in Figure 4.16).

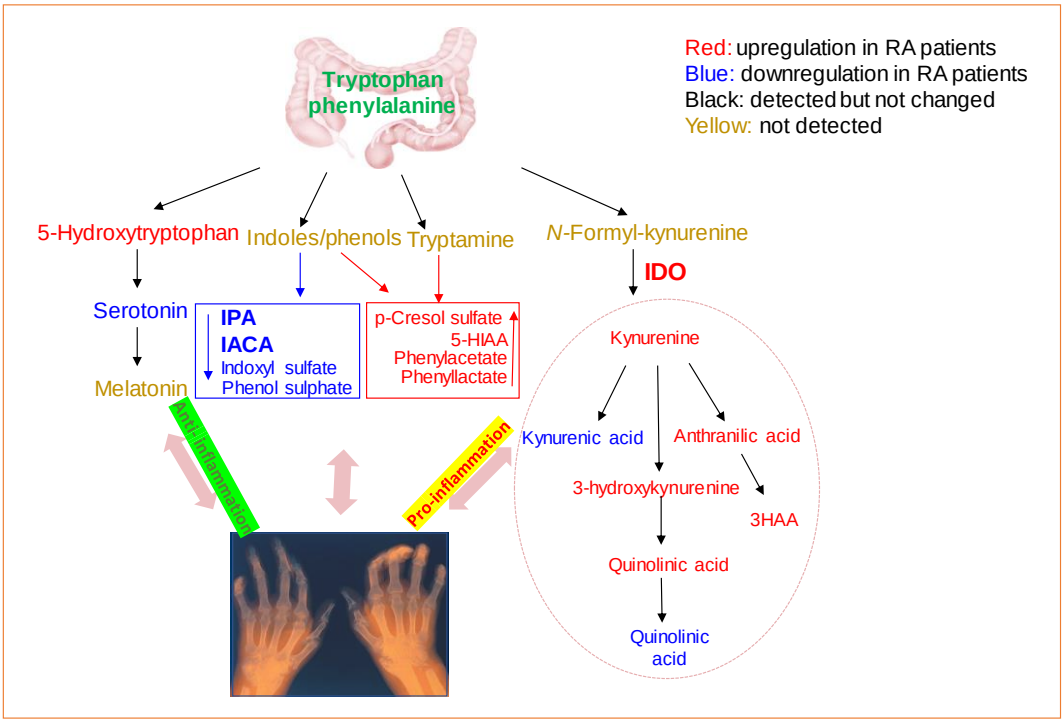

Figure 4.17 Schematic overview of interplay of microbiome-associated tryptophan and phenylalanine metabolites with RA inflammation.

Amino acids are required for many down-stream metabolites biosynthesis, such as protein and neurotransmitter. The deficiency of amino acids could impair immune status by regulating arthritis-associated factors (1) activation of T/B lymphocytes, macrophages and natural killer cells, (2) production of cytokines (IL-6, TNFα, *etc*.) (3) cellular redox state and cell proliferation [18, 225]. Essential amino acids only obtained from diet, are important for formation of cartilage or bone to RA sufferers. In the study, serum EAAs including methionine, tryptophan, threonine, lysine, histidine and BCAAs (valine and isoleucine) are down-regulated in RA patients. Decreased serum serine and increased cystine as the precursor and product of cysteine, respectively, indicated cysteine may be decreased in RA patients. Methionine and cysteine as sulphur-containing amino acid, participate in the function of immune system [226]. As precursors of glutathione (GSH), levels of methionine and cysteine are positively correlated with concentration of GSH [227]. Thus, GSH depletion may influence RA individuals by reducing CD4+ cell number, scavenging free radicals, inhibiting production of IFNγ and impairing lymphocytes proliferation [228, 229]. As reported, BCAAs (valine, leucine and isoleucine) are capable of suppressing skeletal muscle inflammation with the activation of inflammatory factors, such as TNF-α, IL-6 and NF-κB [230], and BCAAs supplementation could attenuate

muscle damage and inflammation during exercise [231]. Furthermore, BCAAs are precursors of SCFAs biosynthesis by bacteria, which are responding to RA inflammation [232, 233]. Down-regulation of urinary and serum histidine may also reduce production of histidine-rich glycoprotein, which could impair the immune response [234]. In short, malfunction of serum amino acids may reflect muscle damage and activation of inflammatory response to arthritis.

Some altered metabolites are associated with ROS production and elimination, which play an important role in the arthritis pathology. For example, disturbed TCA cycle intermediates have been reported in RA patients or animals [19, 99, 172]. In particular, citric acid could help distinguish RA-sufferers from other arthritis-patients or healthy controls [19, 172]. In the study, however, the decrease of citric acid, cis-aconitic acid, and mesaconic acid was different with previous studies [19, 102, 172], which might be caused by different RA sample or species variation [99].

Purine metabolites participate in modulation of inflammatory response to RA [235, 236]. Comparing with healthy controls, uric acid was down-regulated in urine and serum of RA patients. Uric acid, the product of hypoxanthine and xanthine, is functioned to scavenge free radicals as an anti-oxidant [99]. It is noted that RA disorder individuals suffered active oxidative damage with high level of

superoxide anion radical and nitric oxide, *etc.*, which may cause cellular damage, inflammation and/or tissue destruction under arthritis status [237-239]. In addition, uric acid can induce CRP production and inflammatory response in RA patients with cardiovascular complication [240-242]. However, urinary uric acid did not influence inflammatory response in RA patients with leflunomide added to methotrexate treatment [235]. Thus, decreased uric acid might result into the imbalance of reduction of free radicals and inhibition of inflammatory cytokines, but the comprehensive mechanism of uric acid in RA is still needed for further investigation. Meanwhile, significantly decreased urinary purines (hypoxanthine and guanine, FC <0.8, p <0.05) and increased pyrimidine (cytosine, FC=1.98, p <0.01) were observed in RA patients, which are associated with inflammation may induce lower level of uric acid. Moreover, adenosine and its breakdown product inosine along with hypoxanthine were elevated in serum of RA patients, contributing to anti-inflammatory effects through reduced production of proinflammatory cytokines [243, 244]. Increased hypoxanthine is positively associated with grades of knee joint to certain extent [245]. In this study, patients under therapeutic strategies related to purine metabolism (like methotrexate-treatment) were excluded. The findings indicated that purine

metabolism was perturbed owing to immune response, particularly adenosine and inosine may play as potential endogenous immunomodulatory metabolites.

4.5 Chapter summary

In the study, based on platform of LC-MS global metabolomics and targeted metabolomics, we evaluate the metabolites alterations responding to RA without therapeutic strategies and special diet habit by comparing 50 RA patients and 50 healthy controls. Perturbations of metabolism, including tryptophan metabolism, branched chain amino acid (valine, leucine and isoleucine) biosynthesis, aminoacyl-tRNA biosynthesis and citrate cycle were found in patients with RA. According to the alterations of tryptophan and phenylalanine derived metabolites in targeted metabolomics analysis, the results implicated that activation of urinary and serum tryptophan metabolism exert pro-inflammatory effects on RA patients by increasing expression of pro-inflammatory mediators (*e.g.* urinary quinolinic acid and p-cresol sulfate), decreasing anti-inflammatory mediators (*e.g.* urinary kynurenic acid, urinary and serum indoxyl sulfate) and increased IDO expression in patients with RA. For the phenylalanine metabolism, the increased phenylacetic acid and *p*-cresol sulfate have pro-inflammatory effects, while increased phenyllactic acid and decreased phenol sulfate exert anti-inflammatory effects on RA patients. Furthermore, altered purine and energy metabolism, and serum

down-regulated amino acids, particularly valine and isoleucine as BCCAs may be associated with muscle loss, cartilage or chondrocytes damage and activation of arthritis inflammation due to the dysregulation of ROS production and expression of pro-inflammatory cytokines. More interestingly, the results of ROC analysis showed that microbiome derived metabolites, including tryptophan-kynurenine metabolites, indolic and phenolic acids from tryptophan, phenylalanine and tyrosine, amino acids and polyamines, *etc.*, were perturbed responding to RA inflammation, which may provide novel insights into interplay of gut microbiome with RA phenotype.

In conclusion, urinary and serum metabolomics analysis on RA study reveals that activation of tryptophan and phenylalanine metabolism plays a critical role in RA inflammatory responses. In addition, certain serum essential amino acids and conditional amino acids were down-regulated in patients with RA, which may impair immune system by regulating arthritis-associated cells proliferation, cytokine expression and GSH metabolism. Importantly, GM-derived metabolites showed highly association with RA, which may be useful to understand the patho-mechanism of RA in view of metabolome.

Chapter 5 Conclusion and Future Studies

Metabolomics defined as identification and quantification of ‘metabolome’ (small molecule metabolites) is the down-stream discipline in the multi-omics, and it is broadly applied for elucidation of gene function and diagnosis or study of mechanism of human diseases study. Metabolome is easily perturbed by endogenous factors (*i.e.* gene mutation) and exogenous factors (*i.e.*, diet, disease, environmental pollution and microbiome perturbation, *etc.*), which eventually alters phenotype. Because of the diverse physiochemical properties and wide dynamic ranges of small molecule metabolites, a powerful, stable and scalable platform is required for metabolomics study to capture meaningful metabolites in biological samples. Due to advantages of good sensitivity, reproducibility and wide dynamic ranges, MS-based techniques have been employed in metabolomics study on gastrointestinal and arthritis diseases, *i.e.* colorectal cancer, irritable bowel syndrome (IBS), RA and osteoarthritis, *etc*. Previous metabolomics studies on colorectal cancer and RA revealed that several changed metabolites, including but not limited to amino acids, organic acids, lipids and purines, provided potential prospects in diagnostics and therapeutics for diseases.

On basis of MS techniques, we conducted two parts of metabolomics: (1) metabolic effects of SLC25A22 on colorectal cancer cells with *KRAS* mutation and (2) metabolomics study on RA. In the case of metabolic effects of SLC25A22 on *KRAS*-mutant colorectal cancer DLD1 cells, LC-MS-based global metabolic profiles of SLC25A22-silencing CRC

cells and control CRC cells demonstrated that alanine, aspartate and glutamate pathway as well as ammonia metabolism, were significantly changed under the condition of SLC25A22 knockdown. Consequently, targeted metabolomics research on citrate cycle, amino acids and polyamines revealed that knockdown of SLC25A22 induced the down-regulation of TCA cycle intermediates, aspartate-derived amino acids (alanine and serine) and polyamines. In addition, isotope kinetics analysis by using [U-$^{13}C_5$]-glutamine as the isotope tracer on *KRAS*-mutant CRC cells with and without GOT1 blocking indicated that oxaloacetate converted from aspartate by GOT1 played an essential role in cell survival. Furthermore, results from incubation experiment of SLC25A22-knockdown on *KRAS*-mutant CRC cells with polyamine revealed that acetyl-putrescine and acetyl-spermidine could promote CRC cell growth. In conclusion, SLC25A22 is an essential regulator to modulate TCA cycle, aspartate and polyamines biosynthesis, and its overexpression promotes tumor cell growth and survival in metabolic system of *KRAS*-mutant colorectal cells. Additionally, as lipids biosynthesis closely related to TCA cycle, we proposed that lipid metabolism might be altered due to dysfunction of SLC25A22, which requires further investigation. Our findings indicated that SLC25A22 might be a potential promising target for *KRAS*-mutant CRC therapy. However, the metabolic signatures participating in lipid metabolism need for further investigation.

In the part of metabolomics analysis of RA, we have utilized LC-MS and GC-MS platform to comprehensively profile urinary and serum metabolic signatures of RA patients and healthy controls without external stimulus to gut microbiomes (like special daily diet, antibiotics or NASID administration). In the urinary and serum global metabolomics, 32 and 34 metabolites were significantly altered, respectively. The abnormal metabolites responding to RA were mostly attributed to tryptophan metabolism, valine, leucine and isoleucine biosynthesis, aminoacyl-tRNA biosynthesis and citrate cycle. Combining the results of global and targeted metabolomics, most up-regulation tryptophan and phenylalanine derived metabolites, including kynurenine, quinolinic acid, indoles (indolepropionic acid, 5-hydroxyindoleacetic acid) and phenolic acids (phenylacetic acid, phenyllactic acid and *p*-cresol sulfate) indicated activation of tryptophan and phenylalanine metabolism under status of RA, which might exert pro-inflammatory responses. On the other hand, the down-regulation of kynurenic acid, serotonin and dopamine might lead to less prone to exert anti-inflammatory effects. Meanwhile, the overexpression of IDO/TDO has been reported as increase of suppression of host immune response. The down-regulation of serum amino acids is associated with muscle loss, damage of cartilage or chondrocytes in RA patients. Lastly but most importantly, the metabolite alterations (such as tryptophan, phenylalanine derived intermediates, certain amino acids) in RA individuals are associated with gut or intestinal microbiomes. Taken together, RA phenotype is perturbed representing as up-regulation of

tryptophan metabolism, down-regulation of certain amino acids and abnormal energy metabolism or purine biosynthesis. Furthermore, the RA inflammation is closely correlated with alterations of gut microbiome. In the future study, it is necessary to figure out the following concerns in RA status: (1) alteration of more indolic or phenolic acid intermediates by using targeted analysis, (2) variations of critical enzymes apart from IDO/TDO in the tryptophan metabolism based on platform of proteomics, and (3) specific correlation between altered metabolites with changed composition and proportion of gastrointestinal microbiomes based on platform of transcriptomics.

List of References

[1] L. Pauling, A.B. Robinson, R. Teranishi, P. Cary, Quantitative Analysis of Urine Vapor and Breath by Gas-Liquid Partition Chromatography, Proceedings of the National Academy of Sciences, 68 (1971) 2374-2376.

[2] S.G. Oliver, M.K. Winson, D.B. Kell, F. Baganz, Systematic functional analysis of the yeast genome, Trends in Biotechnology, 16 (1998) 373-378.

[3] J.C. Lindon, E. Holmes, J.K. Nicholson, So what's the deal with metabonomics?, Analytical chemistry, 75 (2003) 384a-391a.

[4] J. Barallobre-Barreiro, Y.L. Chung, M. Mayr, Proteomics and metabolomics for mechanistic insights and biomarker discovery in cardiovascular disease, Revista espanola de cardiologia, 66 (2013) 657-661.

[5] J.K. Nicholson, J.C. Lindon, Systems biology: Metabonomics, Nature, 455 (2008) 1054-1056.

[6] O. Fiehn, Metabolomics – the link between genotypes and phenotypes, Plant Molecular Biology, 48 (2002) 155-171.

[7] J.C. Lindon, E. Holmes, M.E. Bollard, E.G. Stanley, J.K. Nicholson, Metabonomics technologies and their applications in physiological monitoring, drug safety assessment and disease diagnosis, Biomarkers, 9 (2004) 1-31.

[8] R. Goodacre, S. Vaidyanathan, W.B. Dunn, G.G. Harrigan, D.B. Kell, Metabolomics by numbers: acquiring and understanding global metabolite data, Trends in Biotechnology, 22 (2004) 245-252.

[9] J.K. Nicholson, I.D. Wilson, Understanding 'Global' Systems Biology: Metabonomics and the Continuum of Metabolism, Nat Rev Drug Discov, 2 (2003) 668-676.

[10] D.B. Kell, Systems biology, metabolic modelling and metabolomics in drug discovery and development, Drug Discovery Today, 11 (2006) 1085-1092.

[11] J.L. Spratlin, N.J. Serkova, S.G. Eckhardt, Clinical applications of metabolomics in oncology: a review, Clin Cancer Res, 15 (2009) 431-440.

[12] T. Kobayashi, S. Nishiumi, A. Ikeda, T. Yoshie, A. Sakai, A. Matsubara, Y. Izumi, H. Tsumura, M. Tsuda, H. Nishisaki, N. Hayashi, S. Kawano, Y. Fujiwara, H. Minami, T. Takenawa, T. Azuma, M. Yoshida, A novel serum metabolomics-based diagnostic approach to pancreatic cancer, Cancer Epidemiol Biomarkers Prev, 22 (2013) 571-579.

[13] I. Bertini, S. Cacciatore, B.V. Jensen, J.V. Schou, J.S. Johansen, M. Kruhoffer, C. Luchinat, D.L. Nielsen, P. Turano, Metabolomic NMR Fingerprinting to Identify and Predict Survival of Patients with Metastatic Colorectal Cancer, Cancer Research, 72 (2011) 356-364.

[14] K. Kim, P. Aronov, S.O. Zakharkin, D. Anderson, B. Perroud, I.M. Thompson, R.H. Weiss, Urine metabolomics analysis for kidney cancer detection and biomarker discovery, Molecular & cellular proteomics, 8 (2009) 558-570.

[15] E.P. Rhee, R.E. Gerszten, Metabolomics and cardiovascular biomarker discovery, Clinical chemistry, 58 (2012) 139-147.

[16] G.D. Lewis, A. Asnani, R.E. Gerszten, Application of metabolomics to cardiovascular biomarker and pathway discovery, Journal of the American College of Cardiology, 52 (2008) 117-123.

[17] D.G. Robertson, Metabonomics in Toxicology: A Review, Toxicological Sciences, 85 (2005) 809-822.

[18] M. He, A.C. Harms, E. van Wijk, M. Wang, R. Berger, S. Koval, T. Hankemeier, J. van der Greef, Role of amino acids in RA studied by metabolomics, International Journal of Rheumatic Diseases, (2017). doi:10.1111/1756-185X.13062.

[19] M. Jiang, T. Chen, H. Feng, Y. Zhang, L. Li, A. Zhao, X. Niu, F. Liang, M. Wang, J. Zhan, C. Lu, X. He, L. Xiao, W. Jia, A. Lu, Serum metabolic signatures of four types of human arthritis, Journal of Proteome Research, 12 (2013) 3769-3779.

[20] M.A. Kamleh, S.G. Snowden, D. Grapov, G.J. Blackburn, D.G. Watson, N. Xu, M. Stahle, C.E. Wheelock, LC-MS Metabolomics of Psoriasis Patients Reveals Disease Severity-Dependent Increases in Circulating Amino Acids That Are Ameliorated by Anti-TNF alpha Treatment, Journal of Proteome Research, 14 (2015) 557-566.

[21] E.J. Want, P. Masson, F. Michopoulos, I.D. Wilson, G. Theodoridis, R.S. Plumb, J. Shockcor, N. Loftus, E. Holmes, J.K. Nicholson, Global metabolic profiling of animal and human tissues via UPLC-MS, Nature protocols, 8 (2013) 17-32.

[22] E.J. Want, I.D. Wilson, H. Gika, G. Theodoridis, R.S. Plumb, J. Shockcor, E. Holmes, J.K. Nicholson, Global metabolic profiling procedures for urine using UPLC-MS, Nature protocols, 5 (2010) 1005-1018.

[23] Z.J. Zhu, A.W. Schultz, J. Wang, C.H. Johnson, S.M. Yannone, G.J. Patti, G. Siuzdak, Liquid chromatography quadrupole time-of-flight mass spectrometry characterization of metabolites guided by the METLIN database, Nature protocols, 8 (2013) 451-460.

[24] C.A. Sellick, R. Hansen, G.M. Stephens, R. Goodacre, A.J. Dickson, Metabolite extraction from suspension-cultured mammalian cells for global metabolite profiling, Nature protocols, 6 (2011) 1241-1249.

[25] S. Bijlsma, I. Bobeldijk, E.R. Verheij, R. Ramaker, S. Kochhar, I.A. Macdonald, B. van Ommen, A.K. Smilde, Large-scale human metabolomics studies: a strategy for data (pre-) processing and validation, Analytical chemistry, 78 (2006) 567-574.

[26] B. Álvarez-Sánchez, F. Priego-Capote, M.D. Luque de Castro, Metabolomics analysis I. Selection of biological samples and practical aspects preceding sample preparation, TrAC Trends in Analytical Chemistry, 29 (2010) 111-119.

[27] D. Vuckovic, Current trends and challenges in sample preparation for global metabolomics using liquid chromatography-mass spectrometry, Analytical and bioanalytical chemistry, 403 (2012) 1523-1548.

[28] P. Yin, A. Peter, H. Franken, X. Zhao, S.S. Neukamm, L. Rosenbaum, M. Lucio, A. Zell, H.U. Haring, G. Xu, R. Lehmann, Preanalytical aspects and sample quality assessment in metabolomics studies of human blood, Clinical chemistry, 59 (2013) 833-845.

[29] W.B. Dunn, D. Broadhurst, P. Begley, E. Zelena, S. Francis-McIntyre, N. Anderson, M. Brown, J.D. Knowles, A. Halsall, J.N. Haselden, A.W. Nicholls, I.D. Wilson, D.B. Kell, R. Goodacre, C. Human Serum Metabolome, Procedures for large-scale metabolic profiling of serum and plasma using gas chromatography and liquid chromatography coupled to mass spectrometry, Nature protocols, 6 (2011) 1060-1083.

[30] O. Beckonert, H.C. Keun, T.M. Ebbels, J. Bundy, E. Holmes, J.C. Lindon, J.K. Nicholson, Metabolic profiling, metabolomic and metabonomic procedures for NMR spectroscopy of urine, plasma, serum and tissue extracts, Nature protocols, 2 (2007) 2692-2703.

[31] G. Paglia, M. Magnusdottir, S. Thorlacius, O.E. Sigurjonsson, S. Guethmundsson, B.O. Palsson, I. Thiele, Intracellular metabolite profiling of platelets: evaluation of extraction processes and chromatographic strategies, Journal of chromatography. B, Analytical technologies in the biomedical and life sciences, 898 (2012) 111-120.

[32] M.A. Lorenz, C.F. Burant, R.T. Kennedy, Reducing time and increasing sensitivity in sample preparation for adherent mammalian cell metabolomics, Analytical chemistry, 83 (2011) 3406-3414.

[33] C.A. Sellick, R. Hansen, A.R. Maqsood, W.B. Dunn, G.M. Stephens, R. Goodacre, A.J. Dickson, Effective Quenching Processes for Physiologically Valid Metabolite Profiling of Suspension Cultured Mammalian Cells, Analytical chemistry, 81 (2009) 174-183.

[34] M. Coen, E. Holmes, J.C. Lindon, J.K. Nicholson, NMR-Based Metabolic Profiling and Metabonomic Approaches to Problems in Molecular Toxicology, Chemical Research in Toxicology, 21 (2008) 9-27.

[35] F.F. Brown, I.D. Campbell, P.W. Kuchel, D.C. Rabenstein, Human erythrocyte metabolism studies by 1H spin echo NMR, FEBS Letters, 82 (1977) 12-16.

[36] B. Mickiewicz, G.E. Duggan, B.W. Winston, C. Doig, P. Kubes, H.J. Vogel, f.t.A.S. Network, Metabolic Profiling of Serum Samples by 1H Nuclear Magnetic Resonance Spectroscopy as a Potential Diagnostic Approach for Septic Shock*, Critical Care Medicine, 42 (2014) 1140-1149.

[37] F. Fauvelle, J. Boccard, F. Cavarec, A. Depaulis, C. Deransart, Assessing Susceptibility to Epilepsy in Three Rat Strains Using Brain Metabolic Profiling Based on HRMAS NMR Spectroscopy and Chemometrics, Journal of Proteome Research, 14 (2015) 2177-2189.

[38] A. Meissner, A.A. van der Plas, N.T. van Dasselaar, A.M. Deelder, J.J. van Hilten, O.A. Mayboroda, 1H-NMR metabolic profiling of cerebrospinal fluid in patients with complex regional pain syndrome–related dystonia, Pain, 155 (2014) 190-196.

[39] A. Miccheli, G. Capuani, F. Marini, A. Tomassini, G. Pratico, S. Ceccarelli, D. Gnani, G. Baviera, A. Alisi, L. Putignani, V. Nobili, Urinary 1H-NMR-based metabolic profiling of children with NAFLD undergoing VSL#3 treatment, International Journal of Obesity, 39 (2015) 1118-1125.

[40] S.P. Putri, S. Yamamoto, H. Tsugawa, E. Fukusaki, Current metabolomics: technological advances, Journal of bioscience and bioengineering, 116 (2013) 9-16.

[41] Z. Lei, D.V. Huhman, L.W. Sumner, Mass spectrometry strategies in metabolomics, The Journal of biological chemistry, 286 (2011) 25435-25442.

[42] J.M. Halket, D. Waterman, A.M. Przyborowska, R.K. Patel, P.D. Fraser, P.M. Bramley, Chemical derivatization and mass spectral libraries in metabolic profiling by GC/MS and LC/MS/MS, Journal of experimental botany, 56 (2005) 219-243.

[43] A.I. Ruiz-Matute, O. Hernandez-Hernandez, S. Rodriguez-Sanchez, M.L. Sanz, I. Martinez-Castro, Derivatization of carbohydrates for GC and GC-MS analyses, Journal of

chromatography B, Analytical technologies in the biomedical and life sciences, 879 (2011) 1226-1240.

[44] V.H. Zaikin, J. M., A handbook of derivatives for mass spectrometry, IM.

[45] E.C. Chan, K.K. Pasikanti, J.K. Nicholson, Global urinary metabolic profiling procedures using gas chromatography-mass spectrometry, Nature protocols, 6 (2011) 1483-1499.

[46] P.Q. Tranchida, F.A. Franchina, P. Dugo, L. Mondello, Comprehensive two-dimensional gas chromatography-mass spectrometry: Recent evolution and current trends, Mass Spectrometry Reviews, 35 (2016) 524-534.

[47] J.H. Winnike, X. Wei, K.J. Knagge, S.D. Colman, S.G. Gregory, X. Zhang, Comparison of GC-MS and GCxGC-MS in the analysis of human serum samples for biomarker discovery, Journal of Proteome Research, 14 (2015) 1810-1817.

[48] P. Arapitsas, A.D. Corte, H. Gika, L. Narduzzi, F. Mattivi, G. Theodoridis, Studying the effect of storage conditions on the metabolite content of red wine using HILIC LC–MS based metabolomics, Food Chemistry, 197 (2016) 1331-1340.

[49] X. Chen, H. Wu, Y. Cao, X. Yao, L. Zhao, T. Wang, Y. Yang, D. Lv, Y. Chai, Y. Cao, Z. Zhu, Ion-pairing chromatography on a porous graphitic carbon column coupled with time-of-flight mass spectrometry for targeted and untargeted profiling of amino acid biomarkers involved in Candida albicans biofilm formation, Molecular bioSystems, 10 (2014) 74-85.

[50] P.D. Rainville, J.L. Simeone, D.S. Root, C.R. Mallet, I.D. Wilson, R.S. Plumb, A method for the direct injection and analysis of small volume human blood spots and plasma extracts containing high concentrations of organic solvents using revered-phase 2D UPLC/MS, The Analyst, 140 (2015) 1921-1931.

[51] J.V.S. Norbert W. Lutz, Ron A. Wevers, Methodologies for metabolomics: experimental strategies and techniques, 88 (2015) 101.

[52] H. Doerfler, D. Lyon, T. Nägele, X. Sun, L. Fragner, F. Hadacek, V. Egelhofer, W. Weckwerth, Granger causality in integrated GC–MS and LC–MS metabolomics data reveals the interface of primary and secondary metabolism, Metabolomics, 9 (2013) 564-574.

[53] P.A. Vorkas, G. Isaac, M.A. Anwar, A.H. Davies, E.J. Want, J.K. Nicholson, E. Holmes, Untargeted UPLC-MS Profiling Pipeline to Expand Tissue Metabolome Coverage: Application to Cardiovascular Disease, Analytical chemistry, 87 (2015) 4184-4193.

[54] P.D. Rainville, G. Theodoridis, R.S. Plumb, I.D. Wilson, Advances in liquid chromatography coupled to mass spectrometry for metabolic phenotyping, TrAC Trends in Analytical Chemistry, 61 (2014) 181-191.

[55] R. Ramautar, G.W. Somsen, G.J. de Jong, CE-MS for metabolomics: developments and applications in the period 2012-2014, Electrophoresis, 36 (2015) 212-224.

[56] W.J. Griffiths, T. Koal, Y. Wang, M. Kohl, D.P. Enot, H.P. Deigner, Targeted metabolomics for biomarker discovery, Angewandte Chemie, 49 (2010) 5426-5445.

[57] J. Xu, Y. Chen, R. Zhang, Y. Song, J. Cao, N. Bi, J. Wang, J. He, J. Bai, L. Dong, L. Wang, Q. Zhan, Z. Abliz, Global and Targeted Metabolomics of Esophageal Squamous Cell Carcinoma Discovers Potential Diagnostic and Therapeutic Biomarkers, Molecular & Cellular Proteomics, 12 (2013) 1306-1318.

[58] A.D. Troise, R. Ferracane, M. Palermo, V. Fogliano, Targeted metabolite profile of food bioactive compounds by Orbitrap high resolution mass spectrometry: The “FancyTiles” approach, Food Research International, 63 (2014) 139-146.

[59] H.G. Gika, I.D. Wilson, G.A. Theodoridis, LC-MS-based holistic metabolic profiling. Problems, limitations, advantages, and future perspectives, Journal of chromatography. B, Analytical technologies in the biomedical and life sciences, 966 (2014) 1-6.

[60] K. Spagou, H. Tsoukali, N. Raikos, H. Gika, I.D. Wilson, G. Theodoridis, Hydrophilic interaction chromatography coupled to MS for metabonomic/metabolomic studies, Journal of separation science, 33 (2010) 716-727.

[61] I.D. Wilson, R. Plumb, J. Granger, H. Major, R. Williams, E.M. Lenz, HPLC-MS-based methods for the study of metabonomics, Journal of chromatography B, Analytical technologies in the biomedical and life sciences, 817 (2005) 67-76.

[62] R. Zhang, D.G. Watson, L. Wang, G.D. Westrop, G.H. Coombs, T. Zhang, Evaluation of mobile phase characteristics on three zwitterionic columns in hydrophilic interaction liquid chromatography mode for liquid chromatography-high resolution mass spectrometry based untargeted metabolite profiling of Leishmania parasites, Journal of chromatography A, 1362 (2014) 168-179.

[63] A. Teleki, A. Sanchez-Kopper, R. Takors, Alkaline conditions in hydrophilic interaction liquid chromatography for intracellular metabolite quantification using tandem mass spectrometry, Analytical biochemistry, 475 (2015) 4-13.

[64] B. Luo, K. Groenke, R. Takors, C. Wandrey, M. Oldiges, Simultaneous determination of multiple intracellular metabolites in glycolysis, pentose phosphate pathway and tricarboxylic acid cycle by liquid chromatography-mass spectrometry, Journal of chromatography A, 1147 (2007) 153-164.

[65] D. McCloskey, J.A. Gangoiti, B.O. Palsson, A.M. Feist, A pH and solvent optimized reverse-phase ion-paring-LC–MS/MS method that leverages multiple scan-types for targeted absolute quantification of intracellular metabolites, Metabolomics, 11 (2015) 1338-1350.

[66] M. Mateos-Vivas, E. Rodriguez-Gonzalo, D. Garcia-Gomez, R. Carabias-Martinez, Hydrophilic interaction chromatography coupled to tandem mass spectrometry in the presence of hydrophilic ion-pairing reagents for the separation of nucleosides and nucleotide mono-, di- and triphosphates, Journal of chromatography A, 1414 (2015) 129-137.

[67] C. Yu, R. Liu, C. Xie, Q. Zhang, Y. Yin, K. Bi, Q. Li, Quantification of free polyamines and their metabolites in biofluids and liver tissue by UHPLC-MS/MS: application to identify the potential biomarkers of hepatocellular carcinoma, Analytical and bioanalytical chemistry, 407 (2015) 6891-6897.

[68] J. Qiu, P.K. Chan, P.V. Bondarenko, Monitoring utilizations of amino acids and vitamins in culture media and Chinese hamster ovary cells by liquid chromatography tandem mass spectrometry, Journal of Pharmaceutical and Biomedical Analysis, 117 (2016) 163-172.

[69] J.E. Oosterink, E.F.G. Naninck, A. Korosi, P.J. Lucassen, J.B. van Goudoever, H. Schierbeek, Accurate measurement of the essential micronutrients methionine, homocysteine, vitamins B6, B12, B9 and their metabolites in plasma, brain and maternal milk of mice using LC/MS ion trap analysis, Journal of Chromatography B, 998–999 (2015) 106-113.

[70] S.U. Bajad, W. Lu, E.H. Kimball, J. Yuan, C. Peterson, J.D. Rabinowitz, Separation and quantitation of water soluble cellular metabolites by hydrophilic interaction chromatography-tandem mass spectrometry, Journal of chromatography A, 1125 (2006) 76-88.

[71] J.D. Rabinowitz, E. Kimball, Acidic acetonitrile for cellular metabolome extraction from Escherichia coli, Analytical chemistry, 79 (2007) 6167-6173.

[72] S. Benito, A. Sanchez, N. Unceta, F. Andrade, L. Aldamiz-Echevarria, M.A. Goicolea, R.J. Barrio, LC-QTOF-MS-based targeted metabolomics of arginine-creatine metabolic pathway-related compounds in plasma: application to identify potential biomarkers in pediatric chronic kidney disease, Analytical and bioanalytical chemistry, (2015).

[73] F. Fei, D.M. Bowdish, B.E. McCarry, Comprehensive and simultaneous coverage of lipid and polar metabolites for endogenous cellular metabolomics using HILIC-TOF-MS, Analytical and bioanalytical chemistry, 406 (2014) 3723-3733.

[74] R. Kaddurah-Daouk, B.S. Kristal, R.M. Weinshilboum, Metabolomics: a global biochemical approach to drug response and disease, Annual review of pharmacology and toxicology, 48 (2008) 653-683.

[75] S. Nishiumi, M. Shinohara, A. Ikeda, T. Yoshie, N. Hatano, S. Kakuyama, S. Mizuno, T. Sanuki, H. Kutsumi, E. Fukusaki, T. Azuma, T. Takenawa, M. Yoshida, Serum

metabolomics as a novel diagnostic approach for pancreatic cancer, Metabolomics, 6 (2010) 518-528.

[76] A. Zhang, H. Sun, X. Wang, Serum metabolomics as a novel diagnostic approach for disease: a systematic review, Analytical and bioanalytical chemistry, 404 (2012) 1239-1245.

[77] S. Nishiumi, T. Kobayashi, A. Ikeda, T. Yoshie, M. Kibi, Y. Izumi, T. Okuno, N. Hayashi, S. Kawano, T. Takenawa, T. Azuma, M. Yoshida, A Novel Serum Metabolomics-Based Diagnostic Approach for Colorectal Cancer, Plos One, 7 (2012) e40459.

[78] A. Floegel, N. Stefan, Z. Yu, K. Mühlenbruch, D. Drogan, H.-G. Joost, A. Fritsche, H.-U. Häring, M. Hrabě de Angelis, A. Peters, M. Roden, C. Prehn, R. Wang-Sattler, T. Illig, M.B. Schulze, J. Adamski, H. Boeing, T. Pischon, Identification of Serum Metabolites Associated With Risk of Type 2 Diabetes Using a Targeted Metabolomic Approach, Diabetes, 62 (2013) 639-648.

[79] M. Mamas, W. Dunn, L. Neyses, R. Goodacre, The role of metabolites and metabolomics in clinically applicable biomarkers of disease, Archieves of Toxicology, 85 (2011) 5-17.

[80] H.R. McMurray, E.R. Sampson, G. Compitello, C. Kinsey, L. Newman, B. Smith, S.R. Chen, L. Klebanov, P. Salzman, A. Yakovlev, H. Land, Synergistic response to oncogenic mutations defines gene class critical to cancer phenotype, Nature, 453 (2008) 1112-1116.

[81] E.C.Y. Chan, P.K. Koh, M. Mal, P.Y. Cheah, K.W. Eu, A. Backshall, R. Cavill, J.K. Nicholson, H.C. Keun, Metabolic Profiling of Human Colorectal Cancer Using High-Resolution Magic Angle Spinning Nuclear Magnetic Resonance (HR-MAS NMR) Spectroscopy and Gas Chromatography Mass Spectrometry (GC/MS), Journal of Proteome Research, 8 (2009) 352-361.

[82] Y. Qiu, G. Cai, M. Su, T. Chen, X. Zheng, Y. Xu, Y. Ni, A. Zhao, L.X. Xu, S. Cai, W. Jia, Serum Metabolite Profiling of Human Colorectal Cancer Using GC−TOFMS and UPLC−QTOFMS, Journal of Proteome Research, 8 (2009) 4844-4850.

[83] Y. Qiu, G. Cai, M. Su, T. Chen, Y. Liu, Y. Xu, Y. Ni, A. Zhao, S. Cai, L.X. Xu, W. Jia, Urinary Metabonomic Study on Colorectal Cancer, Journal of Proteome Research, 9 (2010) 1627-1634.

[84] C. Ludwig, D.G. Ward, A. Martin, M.R. Viant, T. Ismail, P.J. Johnson, M.J. Wakelam, U.L. Gunther, Fast targeted multidimensional NMR metabolomics of colorectal cancer, Magnetic resonance in chemistry, 47 Suppl 1 (2009) S68-73.

[85] A. Hirayama, K. Kami, M. Sugimoto, M. Sugawara, N. Toki, H. Onozuka, T. Kinoshita, N. Saito, A. Ochiai, M. Tomita, H. Esumi, T. Soga, Quantitative metabolome profiling of colon and stomach cancer microenvironment by capillary electrophoresis time-of-flight mass spectrometry, Cancer Research, 69 (2009) 4918-4925.

[86] C. Denkert, J. Budczies, W. Weichert, G. Wohlgemuth, M. Scholz, T. Kind, S. Niesporek, A. Noske, A. Buckendahl, M. Dietel, O. Fiehn, Metabolite profiling of human colon carcinoma – deregulation of TCA cycle and amino acid turnover, Molecular Cancer, 7 (2008) 1-15.

[87] D.I. Benjamin, B.F. Cravatt, D.K. Nomura, Global profiling strategies for mapping dysregulated metabolic pathways in cancer, Cell metabolism, 16 (2012) 565-577.

[88] M.G. Vander Heiden, L.C. Cantley, C.B. Thompson, Understanding the Warburg effect: the metabolic requirements of cell proliferation, Science, 324 (2009) 1029-1033.

[89] J. Zhang, W.S. Ahn, P.A. Gameiro, M.A. Keibler, Z. Zhang, G. Stephanopoulos, 13C isotope-assisted methods for quantifying glutamine metabolism in cancer cells, Methods in enzymology, 542 (2014) 369-389.

[90] D.R. Wise, C.B. Thompson, Glutamine addiction: a new therapeutic target in cancer, Trends in biochemical sciences, 35 (2010) 427-433.

[91] P. Newsholme, J. Procopio, M.M. Lima, T.C. Pithon-Curi, R. Curi, Glutamine and glutamate--their central role in cell metabolism and function, Cell biochemistry and function, 21 (2003) 1-9.

[92] J.R. Cantor, D.M. Sabatini, Cancer cell metabolism: one hallmark, many faces, Cancer discovery, 2 (2012) 881-898.

[93] L. Klareskog, A.I. Catrina, S. Paget, RA, The Lancet, 373 (2009) 659-672.

[94] G.S. Firestein, Evolving concepts of RA, Nature, 423 (2003) 356-361.

[95] Y. Alamanos, A.A. Drosos, Epidemiology of adult RA, Autoimmunity Reviews, 4 (2005) 130-136.

[96] R.F. van Vollenhoven, Sex differences in RA: more than meets the eye, BMC Medicine, 7 (2009) 12-15.

[97] I.B. McInnes, G. Schett, Cytokines in the pathogenesis of RA, Nature Reviews Immunology, 7 (2007) 429-442.

[98] V. Majithia, S.A. Geraci, RA: diagnosis and management, American Journal of Medicine**,** 120 (2007) 936-939.

[99] H.W. Zhang, P. Fu, B.L. Ke, S.P. Wang, M. Li, L. Han, C.C. Peng, W.D. Zhang, R.H. Liu, Metabolomic analysis of biochemical changes in the plasma and urine of collagen-induced arthritis in rats after treatment with Huang-Lian-Jie-Du-Tang, Journal of Ethnopharmacology, 154 (2014) 55-64.

[100] Y. Qi, S. Li, Z. Pi, F. Song, N. Lin, S. Liu, Z. Liu, Metabonomic study of Wu-tou decoction in adjuvant-induced arthritis rat using ultra-performance liquid chromatography coupled with quadrupole time-of-flight mass spectrometry, Journal of chromatography. B, Analytical technologies in the biomedical and life sciences, 953-954 (2014) 11-19.

[101] M.S. Paller, J.R. Hoidal, T.F. Ferris, Oxygen free radicals in ischemic acute renal failure in the rat, Journal of Clinical Investigation, 74 (1984) 1156-1164.

[102] R.C. Yue, L. Zhao, Y.H. Hu, P. Jiang, S.P. Wang, L. Xiang, W.C. Liu, W.D. Zhang, R.H. Liu, Rapid-resolution liquid chromatography TOF-MS for urine metabolomic analysis of collagen-induced arthritis in rats and its applications, Journal of Ethnopharmacology, 145 (2013) 465-475.

[103] Z. Tatar, C. Migne, M. Petera, P. Gaudin, T. Lequerre, H. Marotte, J. Tebib, E.P. Guillot, M. Soubrier, Variations in the metabolome in response to disease activity of RA, BMC Musculoskel Disorders, 17 (2016).

[104] F. Bäckhed, R.E. Ley, J.L. Sonnenburg, D.A. Peterson, J.I. Gordon, Host-Bacterial Mutualism in the Human Intestine, Science, 307 (2005) 1915-1920.

[105] J.U. Scher, S.B. Abramson, The microbiome and RA, Nature Review Rheumatology, 7 (2011) 569-578.

[106]A.V. Chervonsky, Influence of microbial environment on autoimmunity, Nature immunology, 11 (2010) 28-35.

[107] J.M. Kinross, A.W. Darzi, J.K. Nicholson, Gut microbiome-host interactions in health and disease, Genome Medicine, 3 (2011) 14.

[108] S.B. Brusca, S.B. Abramson, J.U. Scher, Microbiome and mucosal inflammation as extra-articular triggers for RA and autoimmunity, Curr Opin Rheumatol, 26 (2014) 101-107.

[109] X. Liu, B. Zeng, J. Zhang, W. Li, F. Mou, H. Wang, Q. Zou, B. Zhong, L. Wu, H. Wei, Y. Fang, Role of the Gut Microbiome in Modulating Arthritis Progression in Mice, Scientific Reports, 6 (2016) 30594.

[110] J. Vaahtovuo, E. Munukka, M. Korkeamaki, R. Luukkainen, P. Toivanen, Fecal microbiota in early RA, Journal of Rheumatology, 35 (2008) 1500-1505.

[111] X. Zhang, D. Zhang, H. Jia, Q. Feng, D. Wang, D. Liang, X. Wu, J. Li, L. Tang, Y. Li, Z. Lan, B. Chen, Y. Li, H. Zhong, H. Xie, Z. Jie, W. Chen, S. Tang, X. Xu, X. Wang, X. Cai, S. Liu, Y. Xia, J. Li, X. Qiao, J.Y. Al-Aama, H. Chen, L. Wang, Q.-j. Wu, F. Zhang, W. Zheng, Y. Li, M. Zhang, G. Luo, W. Xue, L. Xiao, J. Li, W. Chen, X. Xu, Y. Yin, H. Yang, J.

Wang, K. Kristiansen, L. Liu, T. Li, Q. Huang, Y. Li, J. Wang, The oral and gut microbiomes are perturbed in RA and partly normalized after treatment, Nature Medicine, 21 (2015) 895-905.

[112] J.K. Nicholson, E. Holmes, J. Kinross, R. Burcelin, G. Gibson, W. Jia, S. Pettersson, Host-Gut Microbiota Metabolic Interactions, Science, 336 (2012) 1262-1267.

[113] K. Schroecksnadel, S. Kaser, M. Ledochowski, G. Neurauter, E. Mur, M. Herold, D. Fuchs, Increased degradation of tryptophan in blood of patients with RA, Journal Rheumatology, 30 (2003) 1935-1939.

[114] J. Ferlay, I. Soerjomataram, R. Dikshit, S. Eser, C. Mathers, M. Rebelo, D.M. Parkin, D. Forman, F. Bray, Cancer incidence and mortality worldwide: Sources, methods and major patterns in GLOBOCAN 2012, International Journal of Cancer, 136 (2015) E359-E386.

[115] C. Tan, X. Du, KRAS mutation testing in metastatic colorectal cancer, World Journal of Gastroenterology, 18 (2012) 5171-5180.

[116] J.L. Bos, ras oncogenes in human cancer: a review, Cancer Research, 49 (1989) 4682-4689.

[117] G. Hutchins, K. Southward, K. Handley, L. Magill, C. Beaumont, J. Stahlschmidt, S. Richman, P. Chambers, M. Seymour, D. Kerr, R. Gray, P. Quirke, Value of mismatch repair, KRAS, and BRAF mutations in predicting recurrence and benefits from chemotherapy in colorectal cancer, Journal of Clinical Oncology, 29 (2011) 1261-1270.

[118] Q. Wen, P.D. Dunne, P.G. O'Reilly, G. Li, A.J. Bjourson, D.G. McArt, P.W. Hamilton, S.-D. Zhang, KRAS mutant colorectal cancer gene signatures identified angiotensin II receptor blockers as potential therapies, Oncotarget, 8 (2017) 3206-3225.

[119] H.C. Hsu, T.K. Thiam, Y.J. Lu, C.Y. Yeh, W.S. Tsai, J.F. You, H.Y. Hung, C.N. Tsai, A. Hsu, H.C. Chen, S.J. Chen, T.S. Yang, Mutations of KRAS/NRAS/BRAF predict cetuximab resistance in metastatic colorectal cancer patients, Oncotarget, 7 (2016) 22257-22270.

[120] H. Xie, Y. Hou, J. Cheng, M.S. Openkova, B. Xia, W. Wang, A. Li, K. Yang, J. Li, H. Xu, C. Yang, L. Ma, Z. Li, X. Fan, K. Li, G. Lou, Metabolic profiling and novel plasma biomarkers for predicting survival in epithelial ovarian cancer, Oncotarget, 8 (2017) 32134-32146.

[121] C.C. Wong, Y. Qian, X. Li, J. Xu, W. Kang, J.H. Tong, K.-F. To, Y. Jin, W. Li, H. Chen, M.Y.Y. Go, J.-L. Wu, K.W. Cheng, S.S.M. Ng, J.J.Y. Sung, Z. Cai, J. Yu, SLC25A22 Promotes Proliferation and Survival of Colorectal Cancer Cells With KRAS Mutations, and Xenograft Tumor Progression in Mice, via Intracellular Synthesis of Aspartate, Gastroenterology, (2016).

[122] A. Poduri, E.L. Heinzen, V. Chitsazzadeh, F.M. Lasorsa, P.C. Elhosary, C.M. LaCoursiere, E. Martin, C.J. Yuskaitis, R.S. Hill, K.D. Atabay, B. Barry, J.N. Partlow, F.A. Bashiri, R.M. Zeidan, S.A. Elmalik, M.M.U. Kabiraj, S. Kothare, T. Stödberg, A. McTague, M.A. Kurian, I.E. Scheffer, A.J. Barkovich, F. Palmieri, M.A. Salih, C.A. Walsh, SLC25A22 is a novel gene for migrating partial seizures in infancy, Annals of neurology, 74 (2013) 873-882.

[123] F. Molinari, A. Kaminska, G. Fiermonte, N. Boddaert, A. Raas-Rothschild, P. Plouin, L. Palmieri, F. Brunelle, F. Palmieri, O. Dulac, A. Munnich, L. Colleaux, Mutations in the mitochondrial glutamate carrier SLC25A22 in neonatal epileptic encephalopathy with suppression bursts, Clinical genetics, 76 (2009) 188-194.

[124] D.S. Wishart, Emerging applications of metabolomics in drug discovery and precision medicine, Nature Review Drug Discovery, 15 (2016) 473-484.

[125] R.H. Weiss, K. Kim, Metabolomics in the study of kidney diseases, Nature reviews. Nephrology, 8 (2011) 22-33.

[126] O.A. Ulanovskaya, A.M. Zuhl, B.F. Cravatt, NNMT promotes epigenetic remodeling in cancer by creating a metabolic methylation sink, Nature Chemical Biology, 9 (2013) 300-306.

[127] Caroline H. Johnson, Christine M. Dejea, D. Edler, Linh T. Hoang, Antonio F. Santidrian, Brunhilde H. Felding, J. Ivanisevic, K. Cho, Elizabeth C. Wick, Elizabeth M. Hechenbleikner, W. Uritboonthai, L. Goetz, Robert A. Casero, Drew M. Pardoll, James R. White, Gary J. Patti, Cynthia L. Sears, G. Siuzdak, Metabolism Links Bacterial Biofilms and Colon Carcinogenesis, Cell metabolism, 21 (2015) 891-897.

[128] G.J. Patti, O. Yanes, G. Siuzdak, Metabolomics: the apogee of the omics trilogy, Nature reviews. Molecular cell biology, 13 (2012) 263-269.

[129] C.H. Johnson, J. Ivanisevic, G. Siuzdak, Metabolomics: beyond biomarkers and towards mechanisms, Nature reviews. Molecular cell biology, 17 (2016) 451-459.

[130] W.B. Dunn, D. Broadhurst, P. Begley, E. Zelena, S. Francis-McIntyre, N. Anderson, M. Brown, J.D. Knowles, A. Halsall, J.N. Haselden, A.W. Nicholls, I.D. Wilson, D.B. Kell, R. Goodacre, Procedures for large-scale metabolic profiling of serum and plasma using gas chromatography and liquid chromatography coupled to mass spectrometry, Nature Protocols, 6 (2011) 1060-1083.

[131] C.A. Smith, E.J. Want, G. O'Maille, R. Abagyan, G. Siuzdak, XCMS: Processing Mass Spectrometry Data for Metabolite Profiling Using Nonlinear Peak Alignment, Matching, and Identification, Analytical chemistry, 78 (2006) 779-787.

[132] S. Bijlsma, I. Bobeldijk, E.R. Verheij, R. Ramaker, S. Kochhar, I.A. Macdonald, B. van Ommen, A.K. Smilde, Large-Scale Human Metabolomics Studies: A Strategy for Data (Pre-) Processing and Validation, Analytical chemistry, 78 (2006) 567-574.

[133] L. Liu, M. Wang, X. Yang, M. Bi, L. Na, Y. Niu, Y. Li, C. Sun, Fasting serum lipid and dehydroepiandrosterone sulfate as important metabolites for detecting isolated postchallenge diabetes: serum metabolomics via ultra-high-performance LC-MS, Clinical chemistry, 59 (2013) 1338-1348.

[134] J. Xia, D.S. Wishart, Using MetaboAnalyst 3.0 for Comprehensive Metabolomics Data Analysis, Current protocols in bioinformatics, 55 (2016) 14 10 11-14 10 91.

[135] X. Li, C.C. Wong, Z. Tang, J. Wu, S. Li, Y. Qian, J. Xu, Z. Yang, Y. Shen, J. Yu, Z. Cai, Determination of amino acids in colon cancer cells by using UHPLC-MS/MS and [U-13C5]-glutamine as the isotope tracer, Talanta, 162 (2017) 285-292.

[136] L. Dang, D.W. White, S. Gross, B.D. Bennett, M.A. Bittinger, E.M. Driggers, V.R. Fantin, H.G. Jang, S. Jin, M.C. Keenan, K.M. Marks, R.M. Prins, P.S. Ward, K.E. Yen, L.M. Liau, J.D. Rabinowitz, L.C. Cantley, C.B. Thompson, M.G. Vander Heiden, S.M. Su, Cancer-associated IDH1 mutations produce 2-hydroxyglutarate, Nature, 462 (2009) 739-744.

[137] J.F. Xiao, B. Zhou, H.W. Ressom, Metabolite identification and quantitation in LC-MS/MS-based metabolomics, Trends in Analytical Chemistry, 32 (2012) 1-14.

[138] M. Yuan, S.B. Breitkopf, X. Yang, J.M. Asara, A positive/negative ion-switching, targeted mass spectrometry-based metabolomics platform for bodily fluids, cells, and fresh and fixed tissue, Nature protocols, 7 (2012) 872-881.

[139] C. Denkert, J. Budczies, W. Weichert, G. Wohlgemuth, M. Scholz, T. Kind, S. Niesporek, A. Noske, A. Buckendahl, M. Dietel, O. Fiehn, Metabolite profiling of human colon carcinoma – deregulation of TCA cycle and amino acid turnover, Molecular Cancer, 7 (2008) 72.

[140] C.M. Sousa, D.E. Biancur, X. Wang, C.J. Halbrook, M.H. Sherman, L. Zhang, D. Kremer, R.F. Hwang, A.K. Witkiewicz, H. Ying, J.M. Asara, R.M. Evans, L.C. Cantley, C.A. Lyssiotis, A.C. Kimmelman, Pancreatic stellate cells support tumour metabolism through autophagic alanine secretion, Nature, 536 (2016) 479-483.

[141] K. Birsoy, T. Wang, W.W. Chen, E. Freinkman, M. Abu-Remaileh, D.M. Sabatini, An Essential Role of the Mitochondrial Electron Transport Chain in Cell Proliferation Is to Enable Aspartate Synthesis, Cell, 162 (2015) 540-551.

[142] A.S. Krall, S. Xu, T.G. Graeber, D. Braas, H.R. Christofk, Asparagine promotes cancer cell proliferation through use as an amino acid exchange factor, Nature communications, 7 (2016) 11457.

[143] K. Toda, K. Kawada, M. Iwamoto, S. Inamoto, T. Sasazuki, S. Shirasawa, S. Hasegawa, Y. Sakai, Metabolic Alterations Caused by KRAS Mutations in Colorectal Cancer Contribute to Cell Adaptation to Glutamine Depletion by Upregulation of Asparagine Synthetase, Neoplasia, 18 (2016) 654-665.

[144] C. Jose, E. Hébert-Chatelain, N. Bellance, A. Larendra, M. Su, K. Nouette-Gaulain, R. Rossignol, AICAR inhibits cancer cell growth and triggers cell-type distinct effects on OXPHOS biogenesis, oxidative stress and Akt activation, Biochimica et Biophysica Acta (BBA) - Bioenergetics, 1807 (2011) 707-718.

[145] F.V. Din, A. Valanciute, V.P. Houde, D. Zibrova, K.A. Green, K. Sakamoto, D.R. Alessi, M.G. Dunlop, Aspirin inhibits mTOR signaling, activates AMP-activated protein kinase, and induces autophagy in colorectal cancer cells, Gastroenterology, 142 (2012) 1504-1515 e1503.

[146] L. Jin, G.N. Alesi, S. Kang, Glutaminolysis as a target for cancer therapy, Oncogene, 35 (2016) 3619-3625.

[147] A.J. Vargas, E.L. Ashbeck, B.C. Wertheim, R.B. Wallace, M.L. Neuhouser, C.A. Thomson, P.A. Thompson, Dietary polyamine intake and colorectal cancer risk in postmenopausal women, The American Journal of Clinical Nutrition, 102 (2015) 411-419.

[148] E.W. Gerner, F.L. Meyskens, Jr., Polyamines and cancer: old molecules, new understanding, Nature reviews Cancer, 4 (2004) 781-792.

[149] B. Buszewski, S. Noga, Hydrophilic interaction liquid chromatography (HILIC)—a powerful separation technique, Analytical and bioanalytical chemistry, 402 (2012) 231-247.

[150] N. Sriboonvorakul, N. Leepipatpiboon, A.M. Dondorp, T. Pouplin, N.J. White, J. Tarning, N. Lindegardh, Liquid chromatographic-mass spectrometric method for simultaneous determination of small organic acids potentially contributing to acidosis in severe malaria, Journal of chromatography B, Analytical technologies in the biomedical and life sciences, 941 (2013) 116-122.

[151] Z.T. How, F. Busetti, K.L. Linge, I. Kristiana, C.A. Joll, J.W. Charrois, Analysis of free amino acids in natural waters by liquid chromatography-tandem mass spectrometry, Journal of chromatography A, 1370 (2014) 135-146.

[152] D.W. Johnson, Free amino acid quantification by LC-MS/MS using derivatization generated isotope-labelled standards, Journal of chromatography. B, Analytical technologies in the biomedical and life sciences, 879 (2011) 1345-1352.

[153] D. Daye, K.E. Wellen, Metabolic reprogramming in cancer: unraveling the role of glutamine in tumorigenesis, Seminars in cell & developmental biology, 23 (2012) 362-369.

[154] G. Wu, Urea synthesis in enterocytes of developing pigs, Biochemical Journal, 312 (1995) 717-723.

[155] S.M. Morris, Jr., Regulation of enzymes of the urea cycle and arginine metabolism, Annual review of nutrition, 22 (2002) 87-105.

[156] L.B. Sullivan, D.Y. Gui, A.M. Hosios, L.N. Bush, E. Freinkman, M.G. Vander Heiden, Supporting Aspartate Biosynthesis Is an Essential Function of Respiration in Proliferating Cells, Cell, 162 (2015) 552-563.

[157] J. Son, C.A. Lyssiotis, H. Ying, X. Wang, S. Hua, M. Ligorio, R.M. Perera, C.R. Ferrone, E. Mullarky, N. Shyh-Chang, Y. Kang, J.B. Fleming, N. Bardeesy, J.M. Asara, M.C. Haigis, R.A. DePinho, L.C. Cantley, A.C. Kimmelman, Glutamine supports pancreatic cancer growth through a KRAS-regulated metabolic pathway, Nature, 496 (2013) 101-105.

[158] K. Soda, The mechanisms by which polyamines accelerate tumor spread, Journal of Experimental & Clinical Cancer Research, 30 (2011) 95.

[159] A.C. Goodwin, C.E.D. Shields, S. Wu, D.L. Huso, X. Wu, T.R. Murray-Stewart, A. Hacker-Prietz, S. Rabizadeh, P.M. Woster, C.L. Sears, R.A. Casero, Polyamine catabolism contributes to enterotoxigenic Bacteroides fragilis-induced colon tumorigenesis, Proceedings of the National Academy of Sciences, 108 (2011) 15354-15359.

[160] C. Wang, P. Ruan, Y. Zhao, X. Li, J. Wang, X. Wu, T. Liu, S. Wang, J. Hou, W. Li, Q. Li, J. Li, F. Dai, D. Fang, C. Wang, S. Xie, Spermidine/spermine N(1)-acetyltransferase regulates cell growth and metastasis via AKT/β-catenin signaling pathways in hepatocellular and colorectal carcinoma cells, Oncotarget, 8 (2017) 1092-1109.

[161] M. Cross, E. Smith, D. Hoy, L. Carmona, F. Wolfe, T. Vos, B. Williams, S. Gabriel, M. Lassere, N. Johns, R. Buchbinder, A. Woolf, L. March, The global burden of RA: estimates from the global burden of disease 2010 study, Annals of Rheumatic Diseases, 73 (2014) 1316-1322.

[162] S. Bhattacharyya, S.M. Helfgott, Neurologic complications of systemic lupus erythematosus, sjogren syndrome, and RA, Seminars in neurology, 34 (2014) 425-436.

[163] D. Assayag, J.S. Lee, T.E. King, Jr., RA associated interstitial lung disease: a review, Medicina, 74 (2014) 158-165.

[164] A. Young, G. Koduri, Extra-articular manifestations and complications of RA, Best Practice & Research Clinical Rheumatology, 21 (2007) 907-927.

[165] H. Visser, Early diagnosis of RA, Best Practice & Research Clinical Rheumatology, 19 (2005) 55-72.

[166] J.K. Nicholson, J.C. Lindon, Metabonomics, Nature, 455 (2008) 1054.

[167] J.K. Nicholson, E. Holmes, I.D. Wilson, Gut microorganisms, mammalian metabolism and personalized health care, Nature reviews. Microbiology, 3 (2005) 431-438.

[168] R. Madsen, T. Lundstedt, J. Trygg, Chemometrics in metabolomics--a review in human disease diagnosis, Analytica Chimica Acta, 659 (2010) 23-33.

[169] R. Priori, R. Scrivo, J. Brandt, M. Valerio, L. Casadei, G. Valesini, C. Manetti, Metabolomics in rheumatic diseases: The potential of an emerging methodology for improved patient diagnosis, prognosis, and treatment efficacy, Autoimmunity Reviews, 12 (2013) 1022-1030.

[170] G.A. Theodoridis, H.G. Gika, E.J. Want, I.D. Wilson, Liquid chromatography-mass spectrometry based global metabolite profiling: a review, Analytica Chimica Acta, 711 (2012) 7-16.

[171] R.K. Madsen, T. Lundstedt, J. Gabrielsson, C.J. Sennbro, G.M. Alenius, T. Moritz, S. Rantapaa-Dahlqvist, J. Trygg, Diagnostic properties of metabolic perturbations in RA, Arthritis Research & Therapy, 13 (2011) R19.

[172] S. Kim, J. Hwang, J. Xuan, Y.H. Jung, H.S. Cha, K.H. Kim, Global Metabolite Profiling of Synovial Fluid for the Specific Diagnosis of RA from Other Inflammatory Arthritis, Plos One, 9 (2014).

[173] N. Kamada, S.U. Seo, G.Y. Chen, G. Nunez, Role of the gut microbiota in immunity and inflammatory disease, Nature Review Immunology, 13 (2013) 321-335.

[174] M.E. Sandberg, C. Bengtsson, L. Klareskog, L. Alfredsson, S. Saevarsdottir, Recent infections are associated with decreased risk of RA: a population-based case-control study, Annal Rheumatic Diseases, 74 (2015) 904-907.

[175] F.C. Arnett, S.M. Edworthy, D.A. Bloch, D.J. McShane, J.F. Fries, N.S. Cooper, L.A. Healey, S.R. Kaplan, M.H. Liang, H.S. Luthra, T.A. Medsger, D.M. Mitchell, D.H. Neustadt, R.S. Pinals, J.G. Schaller, J.T. Sharp, R.L. Wilder, G.G. Hunder, The american rheumatism association 1987 revised criteria for the classification of RA, Arthritis & Rheumatism, 31 (1988) 315-324.

[176] X. Li, C.C. Wong, Z. Tang, J. Wu, S. Li, Y. Qian, J. Xu, Z. Yang, Y. Shen, J. Yu, Z. Cai, Determination of amino acids in colon cancer cells by using UHPLC-MS/MS and [U-(13)C5]-glutamine as the isotope tracer, Talanta, 162 (2017) 285-292.

[177] H. Luan, L.F. Liu, N. Meng, Z. Tang, K.K. Chua, L.L. Chen, J.X. Song, V.C. Mok, L.X. Xie, M. Li, Z. Cai, LC-MS-based urinary metabolite signatures in idiopathic Parkinson's disease, Journal of Proteome Research, 14 (2015) 467-478.

[178] H. Luan, L.F. Liu, Z. Tang, M. Zhang, K.K. Chua, J.X. Song, V.C. Mok, M. Li, Z. Cai, Comprehensive urinary metabolomic profiling and identification of potential noninvasive marker for idiopathic Parkinson's disease, Scitific Reports, 5 (2015) 13888.

[179] J.Y. Hsu, J.F. Hsu, Y.R. Chen, C.L. Shih, Y.S. Hsu, Y.J. Chen, S.H. Tsai, P.C. Liao, Urinary exposure marker discovery for toxicants using ultra-high pressure liquid chromatography coupled with Orbitrap high resolution mass spectrometry and three untargeted metabolomics approaches, Analytica Chimica Acta, 939 (2016) 73-83.

[180] X. Zhao, J. Chen, L. Ye, G. Xu, Serum metabolomics study of the acute graft rejection in human renal transplantation based on liquid chromatography-mass spectrometry, Journal of Proteome Research, 13 (2014) 2659-2667.

[181] J. Xia, D.S. Wishart, Using MetaboAnalyst 3.0 for Comprehensive Metabolomics Data Analysis, Current protocols in bioinformatics, 55 (2002) 14.10.1-14.10.91.

[182] L. Xiang, H. Zhang, J. Wei, X.Y. Tian, H. Luan, S. Li, H. Zhao, G. Cao, A.C.K. Chung, C. Yang, Y. Huang, Z. Cai, Metabolomics studies on db/db diabetic mice in skeletal muscle reveal effective clearance of overloaded intermediates by exercise, Analytica Chimica Acta, ××× (2017) 1-10.

[183] J. Zeng, P. Yin, Y. Tan, L. Dong, C. Hu, Q. Huang, X. Lu, H. Wang, G. Xu, Metabolomics study of hepatocellular carcinoma: discovery and validation of serum potential biomarkers by using capillary electrophoresis-mass spectrometry, Journal of Proteome Research, 13 (2014) 3420-3431.

[184] H.G. Gika, G.A. Theodoridis, J.E. Wingate, I.D. Wilson, Within-Day Reproducibility of an HPLC−MS-Based Method for Metabonomic Analysis: Application to Human Urine, Journal of Proteome Research, 6 (2007) 3291-3303.

[185] M.N. Triba, L. Le Moyec, R. Amathieu, C. Goossens, N. Bouchemal, P. Nahon, D.N. Rutledge, P. Savarin, PLS/OPLS models in metabolomics: the impact of permutation of

dataset rows on the K-fold cross-validation quality parameters, Molecular bioSystems, 11 (2015) 13-19.

[186] B. Tan, B. Huang, J. Wang, G.P. Guang, C.B. Yang, Y. Yin, 408 Aromatic amino acids alleviate intestinal inflammation in piglets through calcium-sensing receptor activation, Journal of Animal Science, 95 (2017) 201-202.

[187] S. Mateen, S. Moin, A.Q. Khan, A. Zafar, N. Fatima, Increased Reactive Oxygen Species Formation and Oxidative Stress in RA, PLoS One, 11 (2016) e0152925.

[188] N. Beloborodova, I. Bairamov, A. Olenin, V. Shubina, V. Teplova, N. Fedotcheva, Effect of phenolic acids of microbial origin on production of reactive oxygen species in mitochondria and neutrophils, Journal of Biomedical Science, 19 (2012) 89.

[189] P.G. Anantharaju, P.C. Gowda, M.G. Vimalambike, S.V. Madhunapantula, An overview on the role of dietary phenolics for the treatment of cancers, Nutrition Journal, 15 (2016) 99.

[190] A. Mirshafiey, M. Mohsenzadegan, The role of reactive oxygen species in immunopathogenesis of RA, Iranian journal of allergy, asthma and immunology, 7 (2008) 195-202.

[191] S. Dasgupta, Y. Zhou, M. Jana, N.L. Banik, K. Pahan, Sodium phenylacetate inhibits adoptive transfer of experimental allergic encephalomyelitis in SJL/J mice at multiple steps, Journal of Immunology, 170 (2003) 3874-3882.

[192] C.A. Hitchon, H.S. El-Gabalawy, T. Bezabeh, Characterization of synovial tissue from arthritis patients: a proton magnetic resonance spectroscopic investigation, Rheumatology International, 29 (2009) 1205-1211.

[193] H. Wen, H.J. Yang, Y.J. An, J.M. Kim, D.H. Lee, X. Jin, S.W. Park, K.J. Min, S. Park, Enhanced phase II detoxification contributes to beneficial effects of dietary restriction as revealed by multi-platform metabolomics studies, Molecular & cellular proteomics, 12 (2013) 575-586.

[194] D.B. Njoku, Drug-induced hepatotoxicity: metabolic, genetic and immunological basis, International journal of molecular sciences, 15 (2014) 6990-7003.

[195] V. Lo Cascio, F. Bertoldo, G. Gambaro, E. Gasperi, F. Furlan, F. Colapietro, C. Lo Cascio, M. Campagnola, Urinary galactosyl-hydroxylysine in postmenopausal osteoporotic women: A potential marker of bone fragility, Journal of bone and mineral research, 14 (1999) 1420-1424.

[196] A.W. Al-Dehaimi, A. Blumsohn, R. Eastell, Serum galactosyl hydroxylysine as a biochemical marker of bone resorption, Clinical chemistry, 45 (1999) 676-681.

[197] K.Y. Kang, S.H. Lee, S.M. Jung, S.H. Park, B.H. Jung, J.H. Ju, Downregulation of Tryptophan-related Metabolomic Profile in RA Synovial Fluid, Journal of Rheumatology, 42 (2015) 2003-2011.

[198] F. Valerio, P. Lavermicocca, M. Pascale, A. Visconti, Production of phenyllactic acid by lactic acid bacteria: an approach to the selection of strains contributing to food quality and preservation, FEMS microbiology letters, 233 (2004) 289-295.

[199] K. Peter, M. Rehli, K. Singer, K. Renner-Sattler, M. Kreutz, Lactic acid delays the inflammatory response of human monocytes, Biochemical and biophysical research communications, 457 (2015) 412-418.

[200] X.Y. Yang, K.D. Zheng, K. Lin, G.F. Zheng, H. Zou, J.M. Wang, Y.Y. Lin, C.M. Chuka, R.S. Ge, W.T. Zhai, J.G. Wang, Energy Metabolism Disorder as a Contributing Factor of RA: A Comparative Proteomic and Metabolomic Study, Plos One, 10 (2015).

[201] C.F. Labuschagne, N.J. van den Broek, G.M. Mackay, K.H. Vousden, O.D. Maddocks, Serine, but not glycine, supports one-carbon metabolism and proliferation of cancer cells, Cell reports, 7 (2014) 1248-1258.

[202] F. Moroni, A. Cozzi, M. Sili, G. Mannaioni, Kynurenic acid: a metabolite with multiple actions and multiple targets in brain and periphery, Journal of neural transmission, 119 (2012) 133-139.

[203] A. Berstad, J. Raa, J. Valeur, Tryptophan: 'essential' for the pathogenesis of irritable bowel syndrome?, Scandinavian journal of gastroenterology, 49 (2014) 1493-1498.

[204] K. Schroecksnadel, S. Kaser, M. Ledochowski, G. Neurauter, E. Mur, M. Herold, D. Fuchs, Increased degradation of tryptophan in blood of patients with RA, The Journal of Rheumatology, 30 (2003) 1935-1939.

[205] D. Keszthelyi, F.J. Troost, A.A. Masclee, Understanding the role of tryptophan and serotonin metabolism in gastrointestinal function, Neurogastroenterology and motility : the official journal of the European Gastrointestinal Motility Society, 21 (2009) 1239-1249.

[206] E.P. Neis, C.H. Dejong, S.S. Rensen, The role of microbial amino acid metabolism in host metabolism, Nutrients, 7 (2015) 2930-2946.

[207] Z. Dai, Z. Wu, S. Hang, W. Zhu, G. Wu, Amino acid metabolism in intestinal bacteria and its potential implications for mammalian reproduction, Molecular human reproduction, 21 (2015) 389-409.

[208] M.M. Unger, J. Spiegel, K.U. Dillmann, D. Grundmann, H. Philippeit, J. Burmann, K. Fassbender, A. Schwiertz, K.H. Schafer, Short chain fatty acids and gut microbiota differ between patients with Parkinson's disease and age-matched controls, Parkinsonism & related disorders, 32 (2016) 66-72.

[209] J. Tan, C. McKenzie, M. Potamitis, A.N. Thorburn, C.R. Mackay, L. Macia, The role of short-chain fatty acids in health and disease, Advances in immunology, 121 (2014) 91-119.

[210] Q. Wang, D. Liu, P. Song, M.H. Zou, Tryptophan-kynurenine pathway is dysregulated in inflammation, and immune activation, Frontiers in bioscience, 20 (2015) 1116-1143.

[211] L. Kolodziej, An exploratory study of the interplay between decreased concentration of tryptophan, accumulation of kynurenines, and inflammatory arthritis, IUBMB Life, 64 (2012) 983-987.

[212] A. Sulli, G.J. Maestroni, B. Villaggio, E. Hertens, C. Craviotto, C. Pizzorni, M. Briata, B. Seriolo, M. Cutolo, Melatonin serum levels in RA, Annals of the New York Academy of Sciences, 966 (2002) 276-283.

[213] C.M. Forrest, G.M. Mackay, N. Stoy, T.W. Stone, L.G. Darlington, Inflammatory status and kynurenine metabolism in RA treated with melatonin, British Journal of Clinical Pharmacology, 64 (2007) 517-526.

[214] G.F. Oxenkrug, Genetic and hormonal regulation of tryptophan kynurenine metabolism: implications for vascular cognitive impairment, major depressive disorder, and aging, Annals of the New York Academy of Sciences, 1122 (2007) 35-49.

[215] Y. Mandi, L. Vecsei, The kynurenine system and immunoregulation, Journal of neural transmission, 119 (2012) 197-209.

[216] G. Frumento, R. Rotondo, M. Tonetti, G. Damonte, U. Benatti, G.B. Ferrara, Tryptophan-derived Catabolites Are Responsible for Inhibition of T and Natural Killer Cell Proliferation Induced by Indoleamine 2,3-Dioxygenase, The Journal of Experimental Medicine, 196 (2002) 459-468.

[217] R.O. Williams, Exploitation of the IDO Pathway in the Therapy of RA, International journal of tryptophan research, 6 (2013) 67-73.

[218] J.K. Nicholson, E. Holmes, J. Kinross, R. Burcelin, G. Gibson, W. Jia, S. Pettersson, Host-Gut Microbiota Metabolic Interactions, Science, 336 (2012) 1262.

[219] E.A. Smith, G.T. Macfarlane, Formation of Phenolic and Indolic Compounds by Anaerobic Bacteria in the Human Large Intestine, Microbial Ecology, 33 (1997) 180-188.

[220] A. Abildgaard, B. Elfving, M. Hokland, G. Wegener, S. Lund, Probiotic treatment reduces depressive-like behaviour in rats independently of diet, Psychoneuroendocrinology, 79 (2017) 40-48.

[221] D. Weber, P.J. Oefner, A. Hiergeist, J. Koestler, A. Gessner, M. Weber, J. Hahn, D. Wolff, F. Stammler, R. Spang, W. Herr, K. Dettmer, E. Holler, Low urinary indoxyl sulfate

levels early after transplantation reflect a disrupted microbiome and are associated with poor outcome, Blood, 126 (2015) 1723-1728.

[222] G. Cohen, J. Raupachova, W.H. Horl, The uraemic toxin phenylacetic acid contributes to inflammation by priming polymorphonuclear leucocytes, Nephrology, dialysis, transplantation : official publication of the European Dialysis and Transplant Association - European Renal Association, 28 (2013) 421-429.

[223] J.P. Wang, J.S. Yoo, J.H. Lee, H.D. Jang, H.J. Kim, S.O. Shin, S.I. Seong, I.H. Kim, Effects of phenyllactic acid on growth performance, nutrient digestibility, microbial shedding, and blood profile in pigs, Journal of Animal Science, 87 (2009) 3235-3243.

[224] S. Capellino, M. Cosentino, A. Luini, R. Bombelli, T. Lowin, M. Cutolo, F. Marino, R.H. Straub, Increased expression of dopamine receptors in synovial fibroblasts from patients with RA: inhibitory effects of dopamine on interleukin-8 and interleukin-6, Arthritis & rheumatology, 66 (2014) 2685-2693.

[225] P. Li, Y.L. Yin, D. Li, S.W. Kim, G. Wu, Amino acids and immune function, The British Journal of Nutrition, 98 (2007) 237-252.

[226] R.F. Grimble, The effects of sulfur amino acid intake on immune function in humans, The Journal of nutrition, 136 (2006) 1660s-1665s.

[227] T. Malmezat, D. Breuille, C. Pouyet, C. Buffiere, P. Denis, P.P. Mirand, C. Obled, Methionine transsulfuration is increased during sepsis in rats, American journal of physiology. Endocrinology and metabolism, 279 (2000) E1391-1397.

[228] R.F. Grimble, The Effects of Sulfur Amino Acid Intake on Immune Function in Humans, The Journal of nutrition, 136 (2006) 1660S-1665S.

[229] Frontmatter, Glutathione and Sulfur Amino Acids in Human Health and Disease. Wiley.

[230] H. Nicastro, C.R. da Luz, D.F. Chaves, L.R. Bechara, V.A. Voltarelli, M.M. Rogero, A.H. Lancha, Jr., Does Branched-Chain Amino Acids Supplementation Modulate Skeletal

Muscle Remodeling through Inflammation Modulation? Possible Mechanisms of Action, Journal of nutrition and metabolism, 2012 (2012) 136937.

[231] K. Matsumoto, T. Koba, K. Hamada, M. Sakurai, T. Higuchi, H. Miyata, Branched-chain amino acid supplementation attenuates muscle soreness, muscle damage and inflammation during an intensive training program, The Journal of sports medicine and physical fitness, 49 (2009) 424-431.

[232] A.M. Davila, F. Blachier, M. Gotteland, M. Andriamihaja, P.H. Benetti, Y. Sanz, D. Tome, Intestinal luminal nitrogen metabolism: role of the gut microbiota and consequences for the host, Pharmacological research, 68 (2013) 95-107.

[233] A. Abendroth, A. Michalsen, R. Ludtke, A. Ruffer, F. Musial, G.J. Dobos, J. Langhorst, Changes of Intestinal Microflora in Patients with RA during Fasting or a Mediterranean Diet, Forschende Komplementarmedizin (2006), 17 (2010) 307-313.

[234] A.L. Jones, M.D. Hulett, C.R. Parish, Histidine-rich glycoprotein: A novel adaptor protein in plasma that modulates the immune, vascular and coagulation systems, Immunology and cell biology, 83 (2005) 106-118.

[235] J.Y. Choe, S.K. Kim, Association between serum uric acid and inflammation in RA: perspective on lowering serum uric acid of leflunomide, Clinica Chimica Acta, 438 (2015) 29-34.

[236] K. Varani, M. Padovan, M. Govoni, F. Vincenzi, F. Trotta, P.A. Borea, The role of adenosine receptors in RA, Autoimmunity Reviews, 10 (2010) 61-64.

[237] R.A. Greenwald, Oxygen radicals, inflammation, and arthritis: pathophysiological considerations and implications for treatment, Semin Arthritis Rheum, 20 (1991) 219-240.

[238] M. Veselinovic, N. Barudzic, M. Vuletic, V. Zivkovic, A. Tomic-Lucic, D. Djuric, V. Jakovljevic, Oxidative stress in RA patients: relationship to diseases activity, Molecular and cellular biochemistry, 391 (2014) 225-232.

[239] S. Datta, S. Kundu, P. Ghosh, S. De, A. Ghosh, M. Chatterjee, Correlation of oxidant status with oxidative tissue damage in patients with RA, Clin Rheumatol, 33 (2014) 1557-1564.

[240] D.H. Kang, S.K. Park, I.K. Lee, R.J. Johnson, Uric acid-induced C-reactive protein expression: implication on cell proliferation and nitric oxide production of human vascular cells, Journal of the American Society of Nephrology, 16 (2005) 3553-3562.

[241] D. Daoussis, G.D. Kitas, Uric acid and cardiovascular risk in RA, Rheumatology, 50 (2011) 1354-1355.

[242] D.P. Chen, C.K. Wong, L.S. Tam, E.K. Li, C.W. Lam, Activation of human fibroblast-like synoviocytes by uric acid crystals in RA, Cellular & molecular immunology, 8 (2011) 469-478.

[243] G. Hasko, D.G. Kuhel, Z.H. Nemeth, J.G. Mabley, R.F. Stachlewitz, L. Virag, Z. Lohinai, G.J. Southan, A.L. Salzman, C. Szabo, Inosine inhibits inflammatory cytokine production by a posttranscriptional mechanism and protects against endotoxin-induced shock, Journal of Immunology, 164 (2000) 1013-1019.

[244] E.S. Chan, P. Fernandez, B.N. Cronstein, Adenosine in inflammatory joint diseases, Purinergic signalling, 3 (2007) 145-152.

[245] Y. Nakanishi, H. Yamanaka, M. Hakoda, S. Nakazawa, S. Saito, M. Hara, N. Kamatani, S. Kashiwazaki, Association between hypoxanthine concentration in synovial fluid and joint destruction in patients with RA, Japanese Journal of Rheumatology, 8 (1998) 59-67.

CURRICULUM VITAE

Academic qualifications of the thesis author, Ms. LI Xiaona:

- Received the degree of Bachelor of Pharmacy from Shanxi University, July 2009.

- Received the degree of Master of Pharmaceutical Analysis from Peking University, July 2012.

July 2018

Outcome of the thesis work

I. Publications

1. **Li X**, Wong CC, Cai Z*, *et al*. Determination of amino acids in colon cancer cells by using UHPLC-MS/MS and [U-$^{13}C_5$]-glutamine as the isotope tracer. Talanta. 2017, 1 (162): 285-292

2. **Li X**, Wong CC*, Cai Z*, *et al.* LC-MS-based metabolomics revealed SLC25A22 as an essential regulator of aspartate-derived amino acids and polyamines in *KRAS*-mutant colorectal cancer. Oncotarget. 2017, 8(60): 101333–101344

3. Wong CC, Qian Y, **Li X**, et al. SLC25A22 Promotes Proliferation and Survival of Colorectal Cancer Cells With KRAS Mutations and Xenograft Tumor Progression in Mice via Intracellular Synthesis of Aspartate. Gastroenterology. 2016, 151 (5): 945-960.e6

4. Li X, Wu X, Lu A*, Cai Z*, *et al*. LC-MS-based urinary metabolic signatures of RA patients. Analytica Chimica Acta. (Ready to submit)

5. Li X, Wu X, Lu A*, Cai Z*, *et al*. Mass spectrometry-based serum metabolomics study of RA. (Preparing)

6. Li X, Wu X, Lu A*, Cai Z*, *et al*. Correlation of fecal metabolic signatures with gut microbiome alteration of RA. (Preparing)

II. Conference and symposium presentations

1. 65th ASMS Conference on Mass Spectrometry and Allied Topics. Indianapolis, US.

Date: 4-8, June 2017

Title of poster presentation: LC-MS-based metabolomics revealed SLC25A22 as an essential regulator in aspartate-derived amino acids and polyamines in KRAS-mutant colorectal cancer

2. 13th annual meeting of metabolomics. Brisbane, Australia.

Date: 26-29, June 2017

Title of oral presentation: LC-MS-based metabolomics revealed SLC25A22 as an essential regulator of tricarboxylic acid (TCA) cycle, aspartate-derived amino acids and polyamines in *KRAS*-mutant colorectal cancer.

Award: Travel award & Student Prize

Honors, awards and fellowships

Prof. Jerry W. Barrett Scholarship, Hong Kong Baptist University, 2017